REPUBLIQUE DU CAMEROUN
Paix – Travail – Patrie

REPUBLIC OF CAMEROON
Peace – Work – Fatherland

Department of Civil, Architectural and Environmental Engineering University of Padua

ICEA

Department of Civil Engineering

Department of Civil, Architectural and Environmental Engineering

IMPERFECTION TOLERANCES DURING THE ERECTION OF STEEL PLATE GIRDERS AND GEOMETRICAL NONLINEARITIES

A thesis submitted in partial fulfilment of the requirements for the degree of

Master of Engineering (MEng) in Civil Engineering

Curriculum: Structures

Presented by:

SONNA DONKO Maël

Student number: **15TP20961**

Supervised by:

Prof. Eng. Carmelo MAJORANA

Co-supervised by:

Dr. Eng. Emanuele MAJORANA

Dr. Eng. Guillaume Hervé POH'SIE

Academic Year : 2019/2020

REPUBLIQUE DU CAMEROUN
Paix – Travail – Patrie

REPUBLIC OF CAMEROON
Peace – Work – Fatherland

Department of Civil,
Architectural and
Environmental
Engineering
University of Padua

Department of Civil Engineering

Department of Civil, Architectural and
Environmental Engineering

IMPERFECTION TOLERANCES DURING THE ERECTION OF STEEL PLATE GIRDERS AND GEOMETRICAL NONLINEARITIES

A thesis submitted in partial fulfilment of the requirements for the degree of

Master of Engineering (MEng) in Civil Engineering

Curriculum: Structures

Presented by:

SONNA DONKO Maël

Student number: **15TP20961**

Supervised by:

Prof. Eng. Carmelo MAJORANA

Co-supervised by:

Dr. Eng. Emanuele MAJORANA

Dr. Eng. Guillaume Hervé POH'SIE

Academic Year : 2019/2020

DEDICATION

I dedicate this thesis

to the

SONNA family

who offered unconditional love, invaluable educational facilities, guidance and support

throughout this journey.

Thank you so much.

Imperfection tolerances during the erection of steel plate girders and geometrical nonlinearities
Master of Engineering defended by SONNA DONKO Maël
NASPW Yaoundé 2019/2020

i

ACKNOWLEDGEMENTS

Imperfection tolerances during the erection of steel plate girders and geometrical nonlinearities
Master of Engineering defended by SONNA DONKO Maël
NASPW Yaoundé 2019/2020

ii

GLOSSARY

LIST OF ABBREVIATIONS

3D	3-dimension
Abaqus/CAE	Complete Abaqus Environment
AWS	American Welding Society
BC	Boundary Condition
BOF	Basic Oxygen Furnace
BS	British Standard
CAE	Computer-Aided Engineering
EAF	Electric Arc Furnace
EC3-1-5	Eurocode 3 part 1-5 (EN 1993-1-5)
EN	European Standard
EP	End Plate
FE	Finite Element
FEA	Finite Element Analysis
FEM	Finite Element Method
GMNA	Geometrically and Materially Nonlinear Analysis
GMNIA	Geometrically and Materially Nonlinear Analysis with Imperfections included
GNA	Geometrically Nonlinear elastic Analysis
GNIA	Geometrically Nonlinear elastic Analysis with Imperfections included
IABSE	International Association for Bridge and Structural Engineering
LPF	Load Proportionality Factor
MNA	Materially Nonlinear Analysis
N.A.	Neutral Axis
S4R	4-node quadrilateral Shell element with Reduced integration
TP	Test Plate
ULS	Ultimate Limit State

Imperfection tolerances during the erection of steel plate girders and geometrical nonlinearities
Master of Civil Engineering defended by SONNA DONKO Maël
NASPW Yaoundé 2019/2020
iii

LIST OF SYMBOLS

a	Length of the plate, parallel to the applied load
a_{mn}	Double trigonometric Fourier series parameter
A	Cross-sectional area of the section
A_{eff}	Cross-sectional area of the reduced effective section
b or D	Width of the plate, perpendicular to the applied load
b_{e1}	Effective width of the more compressed part
b_{e2}	Effective width of the less compressed part
b_{eff}	Effective width
D	Plate flexural rigidity
e	Eccentricity of the resultant axial force from the centroid of the section
E	Elastic modulus
f_u	Ultimate strength of the plate
$f_{u,Ana}$	Analytical value of the ultimate strength
$f_{u,EC3}$	EC3-1-5 value of the ultimate strength
$f_{u,FE}$	Finite element value of the ultimate strength
f_y	Yield strength
F	Stress variation in the plate
G	Shear modulus
I	Second moment of area of the section
I_{eff}	Second moment of area of the reduced effective ection
Imp_i	i^{th} initial imperfection amplitude
k	Initial imperfection amplitude parameter
k_{cr}	Critical or buckling load coefficient
$[K_e]$	Linear elastic stiffness matrix
$[K_g]$	Geometric stiffness matrix
$[K_m]$	Plastic reduction matrix

Imperfection tolerances during the erection of steel plate girders and geometrical nonlinearities
Master of Civil Engineering defended by SONNA DONKO Maël
NASPW Yaoundé 2019/2020

iv

m	Number of sinus half-waves over the length of the plate
n	Number of sinus half-waves over the width of the plate
N	Resultant axial force
N_{cr}	Axial critical force per unit length in the loading direction
N_x	Axial force per unit length in the loading direction
N_y	Axial force per unit length perpendicular to the loading direction
N_{xy}	Diagonal axial force
P	Load
R	Correlation coefficient of multiple determination
R^2	Squared correlation coefficient of multiple determination
S	Mesh size
t	Thickness of plate
T_i	i^{th} trial
T	External work done
U	Internal work done
v	Vertical deflection
w	Out-of-plane deflection at any point on the plate
w_0	Initial deflection (or imperfection) system in the plate
$y_{\Delta A}$	Position of the gap's centroid
$y_{eff,G}$	Position of the centroid of the effective cross-section
$y_{eff,sup}$	Position of the upper fibre from the centroid of the effective cross-section
y_{sup}	Position of the upper fibre of the cross-section

Imperfection tolerances during the erection of steel plate girders and geometrical nonlinearities
Master of Civil Engineering defended by SONNA DONKO Maël
NASPW Yaoundé 2019/2020

v

α	Aspect ratio
β	Slenderness ratio
β_{cr}	Critical slenderness ratio
δ or Imp	Initial imperfection amplitude
Δ	Displacement
Δf_u	Deviation in the ultimate strength
Δl	Arc-length
$\Delta\sigma_{cr}$	Deviation of critical stress value
λ	Load coefficient
λ_1	Fundamental or first eigenvalue
$\bar{\lambda}_p$	Slenderness ratio
ν	Poisson's ratio
ψ	Stress ratio
ρ	Width reduction factor
σ_1	Larger compressive stress
σ_2	Smaller compressive stress
σ_c	Maximum compressive stress
σ_{cr}	Critical or buckling stress
$\sigma_{cr,Ana}$	Analytical value of the critical stress
$\sigma_{cr.EC3}$	EC3-1-5 value of the critical stress
$\sigma_{cr,FE}$	Finite element value of the critical stress
σ_t	Maximum tensile stress

Imperfection tolerances during the erection of steel plate girders and geometrical nonlinearities
Master of Civil Engineering defended by SONNA DONKO Maël
NASPW Yaoundé 2019/2020

vi

ABSTRACT

This work aims to prove that the strict initial imperfection tolerance limits proposed by the American AWS D1.1/D1.1M and the European EN 1090-2 codes could be relaxed for the webs of the most encountered steel I-plate girders subjected to local bend-buckling during their erection phase. To achieve this, a parametric study was done involving 36 perfect webs and 612 imperfect webs with varying aspect ratio, slenderness ratio, initial imperfection amplitude and stress ratio using Abaqus/CAE by Finite Element (FE) linear buckling analyses then FE geometrically and materially nonlinear analyses with imperfections included (GMNIA). After investigating the results, the equation to determine the ultimate strength of web plates as a function of initial imperfection amplitude and that used to determine the tolerance limit from the web's slenderness ratio and stress ratio were derived. The results obtained prove that the ultimate strength given by EC3-1-5 is overestimated with values up to 24.91% more than the FE results. For monosymmetric I-plate girders during erection, the derived equations show that EN 1090-2 and AWS D1.1/D1.1M tolerance limits can be relaxed to around 40% and 80% in less slender webs and close to 60% and 200% in more slender webs respectively. These results are significant, thus they will be highly welcomed by fabricators and erectors as they will help to avoid costly web straightening operations and ease on-site evaluation of imperfect webs of I-plate girders. To designers and researchers, the proposed well-calibrated boundary conditions and mesh density will ease their works on similar FE modelling.

Keywords: plate girder, GMNIA, initial imperfection, ultimate strength, erection.

Imperfection tolerances during the erection of steel plate girders and geometrical nonlinearities
Master of Civil Engineering defended by SONNA DONKO Maël
NASPW Yaoundé 2019/2020

vii

RESUME

L'objectif de ce travail est de prouver que les limites strictes de tolérance aux imperfections initiales proposées par les codes américains AWS D1.1/D1.1M et européens EN 1090-2 peuvent être assouplies pour les âmes des poutres en acier reconstituées soudées les plus courantes et soumises à des flexions locales pendant leur phase de montage. Pour ce faire, une étude paramétrique a été réalisée en impliquant 36 âmes parfaites et 612 âmes imparfaites dont le rapport d'aspect, le rapport d'élancement, l'amplitude de l'imperfection initiale et le rapport de contrainte varient, à l'aide d'Abaqus/CAE, par des analyses de voilement linéaire par éléments finis (FE), puis des analyses FE non linéaires géométriques et matérielles avec imperfections incluses (GMNIA). Après étude des résultats, l'équation permettant de déterminer la résistance ultime des plaques d'âme et celle utilisée pour déterminer la limite de tolérance ont été dérivées. Les résultats obtenus prouvent que la résistance ultime donnée par l'EC3-1-5 est surestimée avec des valeurs jusqu'à 24,91% supérieures aux résultats FE. Pour les poutres en I monosymétriques pendant leur montage, les équations dérivées montrent que les limites de tolérance de l'EN 1090-2 et de l'AWS D1.1/D1.1M peuvent être assouplies à environ 40% et 80% pour les âmes moins élancées et à près de 60% et 200% pour les âmes plus élancées respectivement. Ces résultats sont significatifs et seront donc très appréciés par les fabricants et les monteurs, car ils permettront d'éviter les opérations coûteuses de redressement des âmes et faciliteront l'évaluation sur site des âmes imparfaites des poutres en acier. Pour les concepteurs et les chercheurs, les conditions aux limites et la densité de maillage proposées faciliteront leurs travaux sur des modélisations FE similaires.

Mots-clés : poutres en acier reconstituées soudées, GMNIA, imperfection initiale, résistance ultime, érection.

Imperfection tolerances during the erection of steel plate girders and geometrical nonlinearities
Master of Civil Engineering defended by SONNA DONKO Maël
NASPW Yaoundé 2019/2020

viii

LIST OF FIGURES

Imperfection tolerances during the erection of steel plate girders and geometrical nonlinearities
Master of Civil Engineering defended by SONNA DONKO Maël
NASPW Yaoundé 2019/2020

ix

Imperfection tolerances during the erection of steel plate girders and geometrical nonlinearities
Master of Civil Engineering defended by SONNA DONKO Maël
NASPW Yaoundé 2019/2020

x

Imperfection tolerances during the erection of steel plate girders and geometrical nonlinearities
Master of Civil Engineering defended by SONNA DONKO Maël
NASPW Yaoundé 2019/2020

xi

LIST OF TABLES

Imperfection tolerances during the erection of steel plate girders and geometrical nonlinearities
Master of Civil Engineering defended by SONNA DONKO Maël
NASPW Yaoundé 2019/2020

xii

Imperfection tolerances during the erection of steel plate girders and geometrical nonlinearities
Master of Civil Engineering defended by SONNA DONKO Maël
NASPW Yaoundé 2019/2020

xiii

TABLE OF CONTENTS

Imperfection tolerances during the erection of steel plate girders and geometrical nonlinearities
Master of Civil Engineering defended by SONNA DONKO Maël
NASPW Yaoundé 2019/2020

xiv

Imperfection tolerances during the erection of steel plate girders and geometrical nonlinearities
Master of Civil Engineering defended by SONNA DONKO Maël
NASPW Yaoundé 2019/2020

xv

Imperfection tolerances during the erection of steel plate girders and geometrical nonlinearities
Master of Civil Engineering defended by SONNA DONKO Maël
NASPW Yaoundé 2019/2020

xvi

GENERAL INTRODUCTION

Steel plates are widely used in many engineering fields for the construction of crane girders, ships, aerospace, offshore, gas and liquid containment structures. In bridge engineering, the use of slender steel plates is common for plate girders capable of carrying higher loads over long spans. During a bridge's incremental launching process, the girder is pulled from one bridge pier to another generating large bending moments due to the self-weight of the girder and the launching equipment. If special attention is not taken, instability of the slender web may occur after exhausting its post-buckling reserve strength. Plate girders subjected to the random nature of out-of-plane geometric imperfections of the web could reduce its post-buckling strength, rendering it more unstable.

In the 1970s, several girder bridges collapsed due to considerably high initial imperfections, thus, rules like the Merrison's rules were drafted to provide imperfection tolerances, but were found to be in many cases strict for the fabricators and resulted in too high total cost of the structure. The International Association for Bridges and Structural Engineering (IABSE) Task group on Tolerances in Steel Plated Structures (Massonet, 1980) was then created to set realistic and easy to control tolerances. From then, a large amount of research was done to find a correlation between imperfections and post-buckling (ultimate) strength, thus finding imperfection tolerance limits that correspond to an acceptable drop in strength. Rangelov (1992) and Sadovský (1996) proposed strength-based formulations of fabrication tolerances that were used in codes. In the last 2 decades, with a boom in finite element (FE) approaches, Maiorana (2009) concluded that imperfection amplitudes below the codes' tolerance have minimum influence on the ultimate strength of webs subjected to patch loading. Through experimental and FE tests, Kala (2010) showed that it is not indispensable to abide by the stringent web tolerances, and that imperfect webs of plate girders can be used without being straightened. Finally, while studying shear on web plates, Ghadami (2019) derived an ultimate shear strength reduction factor as a function of initial imperfection and thus suggested a maximum permissible construction tolerance.

An easily applicable equation to determine the ultimate strength of webs subjected to direct stresses which is a function of initial imperfection amplitude has not been found in the literature. Also, the assessment, through an equation, of acceptable imperfection tolerances for

Imperfection tolerances during the erection of steel plate girders and geometrical nonlinearities
Master of Civil Engineering defended by SONNA DONKO Maël
NASPW Yaoundé 2019/2020

1

webs of monosymmetric plate girders, in a manner to relax strict and costly tolerance limits, has not yet been reported in the literature.

As such, this study aims to evaluate the ultimate strength formulation proposed by the European standard, determine the effects of plate girder's real-life geometrical parameters on its ultimate strength, investigate possible tolerance limit relaxation, which will be highly welcomed by fabricators-erectors and identify trends then use regression analysis to derive both ultimate strength and tolerance limit equations. To do this, the necessary theoretical background and concepts that underneath this work is explained in the first chapter, then the second chapter describes the methodology used to verify the FE modelling procedure applied in Abaqus/CAE and the rigorous methodology used to perform parametric analytical and nonlinear FE analyses, this chapter also provides criteria for method comparison and gives the methodology used for regression analysis. Chapter 3 proves the validity of the FE modelling procedure used for the analyses and chapter 4 presents the parametric study results of the 36 perfect and 612 imperfect webs studied, compares the FE and the analytical results, then presents both the proposed ultimate strength and tolerance limit equations gotten through regression analyses.

Imperfection tolerances during the erection of steel plate girders and geometrical nonlinearities
Master of Civil Engineering defended by SONNA DONKO Maël
NASPW Yaoundé 2019/2020

2

CHAPTER 1. LITERATURE REVIEW

Introduction

Steel, an alloy of iron and carbon, is widely used in bridge engineering in the form of welded slender I-plate girders. These plate girders are usually covered by a concrete slab which makes the composite cross-section highly resistant to bending solicitations during its service life. Nonetheless, during the plate girder's erection phase, the concrete is not present and the girder is left to resist bending on its own, thus, making it vulnerable to web-bend buckling due to its slender nature. Also, these plate girders usually experience inherent and unavoidable imperfections which makes the structure exhibit significant nonlinear behaviours rendering it more susceptible to buckling and a possible nonlinear post-buckling response. This chapter is meant for a thorough explanation of the theory underneath these concepts to ease the understanding of subsequent works. As such, the chapter starts by discussing the origin of steel right up to its application in bridge engineering passing through its properties. The next part discusses the structure of a plate girder, an erection methodology, its cross-section classification and its behaviour from the pre-critical to the post-critical phase passing through the buckling state under direct but also shear stresses. Then comes the section on imperfections to help understand the dimensional variations in plate girders and the types of tolerances that exist. Nonlinearities and their methods of analysis are detailed, at the end of this chapter, to help approach the nonlinear behaviours caused by imperfections in the web of plate girders and defined mathematically by the Föppl-von Kármán-Marguerre differential equations.

1.1. Steel

Steel is an alloy of iron and carbon, with a maximum of 1.5% carbon content. The carbon occurs in the form of cementite (Fe_3C) and other elements like silicon, sulphur, phosphorus and manganese are also present to provide specific and desired properties to the steel. It is important to start by giving a general overview of steel as it is the material that composes the plate girders under study. As such, this section provides a brief history of the evolution of steel from iron, its manufacturing techniques, encountered typologies, intrinsic properties, gives its application in engineering and ends with its defects, causes and treatment techniques.

Imperfection tolerances during the erection of steel plate girders and geometrical nonlinearities
Master of Civil Engineering defended by SONNA DONKO Maël
NASPW Yaoundé 2019/2020

3

1.1.1. History of steel

The earliest use of iron, the chief component of steel, was for small tools, in approximately 4000 B.C. In the latter part of the eighteenth century and the early nineteenth century, cast iron and wrought iron, an evolved form of steel, were used in various types of bridges. Steel, an alloy of primarily iron and carbon, with fewer impurities and less carbon than cast iron, was first used in heavy construction in the nineteenth century. Then, with the advent of the Bessemer converter in 1855, steel began to displace wrought iron and cast iron in construction (T. Segui, 2013).

1.1.2. Steel manufacturing techniques

The main raw materials used in the large-scale production of steel are mined iron ore (haematite and magnetite), coal from raw coke, fluxing materials, refractory materials and specific alloys.

When iron ore is heated at about 2,000°C and it melts, it contains too much carbon to provide the desirable properties for steel. Iron ore pellets, products of the first process, are remelted and processed to reduce the amount of carbon, then additional elements are added and the desired steel is produced.

Modern steel is made from pig iron using either the basic oxygen furnace (BOF) or an electric arc furnace (EAF). About 40% of steel is made using the BOF process in which pure oxygen is blown into melted iron, reducing the amounts of carbon, manganese, silicon, and phosphorus then fluxes are added to further reduce levels of sulphur and phosphorus. On the other hand, the EAF process is used to make about 60% of steel using nearly entirely recycled scrap steel sent into the furnace and heated by an electric arc. Industrial electric arc furnace temperatures can reach 1800 °C.

1.1.3. Steel typologies

Steel can be separated into low alloy and high alloy steel. More so, it can be further distinguished into low alloy with varying carbon contents, tool steel and stainless steel.

Imperfection tolerances during the erection of steel plate girders and geometrical nonlinearities
Master of Civil Engineering defended by SONNA DONKO Maël
NASPW Yaoundé 2019/2020

4

1.1.3.1. Plain carbon (low alloy) steel

Plain carbon steel is an alloy of iron and carbon with carbon content ranging from 0.15% to 1.5% with no more than 0.5% of silicon and 1.5% of manganese. They are divided into three types:

- Low-carbon or mild steel, 0.15% to 0.45% carbon
- Medium-carbon steel, 0.45% to 0.8% carbon
- High-carbon steel, 0.8% to 1.5% carbon

1.1.3.2. Tool steel

Tool steel is a variety of steel with a carbon content between 0.7% and 1.5%. They are adequate to be made into tools due to their distinctive hardness, abrasion resistance, their ability to hold a cutting edge, and/or their resistance to deformation at elevated temperatures. Also, tool steel with higher ratios of vanadium is more resistant to corrosion.

1.1.3.3. Stainless steel

Stainless steel differs from carbon steel by the high amount of chromium present. With about 18% of chromium, stainless steel does not readily corrode, rust or stain with water as ordinary steel does. Despite the name, it is not fully stain-proof, most notably under low-oxygen, high-salinity, or poor circulation environments. They are used where both the properties of steel and corrosion resistance are required.

1.1.4. Properties of steel

1.1.4.1. Physical properties

The amount of steel variation does not look significant, because carbon never makes up more than 1.5% of steel. Thus, most steels have a density of about 7,850 kg/m^3, making them 7.85 times denser than water. Also, their melting point of 1,510°C is higher than that of most metals and their coefficient of linear expansion, at 20°C, of 11.1μm/m°C makes them more resistant to changing size with changes in temperature than the likes of copper (16.7), tin (21.4) and lead (29.1).

1.1.4.2. Chemical properties

Steel is an extremely versatile material available in a very wide range of properties and chemical compositions to suit every field of technology (Gorenc et al., 2012). Carbon makes steel harder than pure iron due to the carbon atoms which makes it more difficult for dislocations in the iron crystal lattice to slide past each other. Also, steel contains additional

Imperfection tolerances during the erection of steel plate girders and geometrical nonlinearities
Master of Civil Engineering defended by SONNA DONKO Maël
NASPW Yaoundé 2019/2020

5

elements, either as impurities or added to provide desirable properties. Most steel contains manganese, phosphorus, sulphur, silicon, and trace amounts of aluminium, oxygen, and nitrogen.

Intentionally addition of nickel, chromium, manganese, titanium, molybdenum, boron, niobium and other metals influence the hardness, ductility and strength of steel.

11% or more chromium addition provides corrosion resistance which yields stainless steel. Also, corrosion resistance can be provided by galvanizing carbon steel through electroplating or hot-dipping in zinc.

1.1.4.3. Mechanical properties of steel

Steel's mechanical properties are obtained through a combination of chemical composition, heat treatment and manufacturing processes. The main constituent of steel is iron, but the addition of very small quantities of other elements can have a significant effect on the properties of the steel. The strength of steel can be increased by the addition of alloys such as manganese, niobium and vanadium. The addition of these alloys can also greatly affect other properties, such as ductility, toughness and weldability (Steel Construction, 2015).

Thus, the main mechanical properties of steel are:

- strength
- toughness
- ductility
- weldability
- durability

Other mechanical properties of steel are found from observations and by plotting the stress versus strain diagrams from data obtained after tensile tests. Figure 1.1 depicts the typical stress-strain diagrams for mild steel and low-alloy steel.

Imperfection tolerances during the erection of steel plate girders and geometrical nonlinearities
Master of Civil Engineering defended by SONNA DONKO Maël
NASPW Yaoundé 2019/2020
6
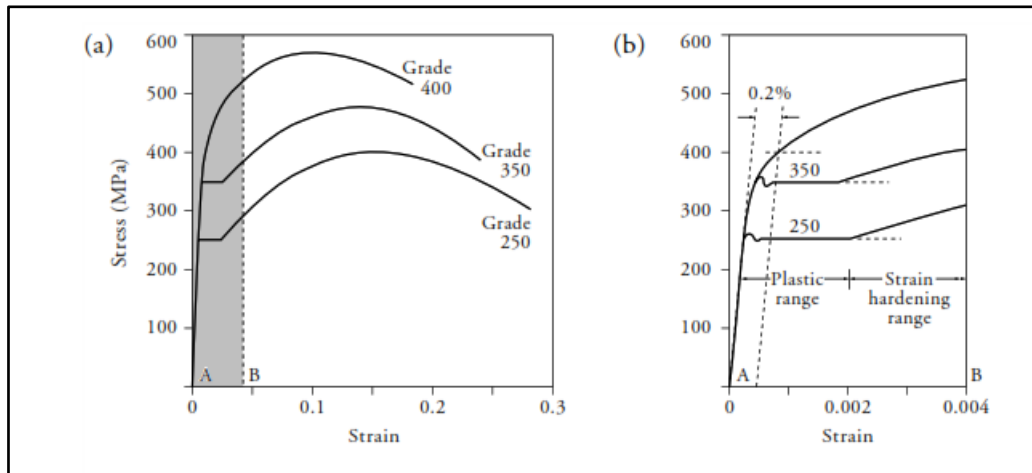
(a) Complete stress vs strain diagram

(b) Enlarged portion of the diagram (a) in region A-B

Figure 1.1. Typical stress-strain diagrams of steel (Gorenc et al., 2012)

These other mechanical properties usually take the values of:

- modulus of elasticity, $E = 206,000 \frac{N}{mm^2}$ (range of 190,000 to 210,000 N/mm^2)

- Poisson's ratio, $\nu = 0.3$

- shear modulus, often taken as $81,000 \, N/mm^2$ but calculated using equation (1.1).

$$G = \frac{E}{2(1 + \nu)} N/mm^2 \qquad (1.1)$$

1.1.5. Applications of steel

Steel is a versatile and effective material able to carry loads in tension, compression and shear. Its high strength-to-weight ratio implies a minimum structural weight of superstructures and thus minimises the cost of substructures. Also, steel's low self-weight positively impacts the cost of transporting and handling its components.

Thus, steel is used as beams, steel frames, columns, bars, plate girders in warehouses, aircraft hangers, bridges, residential and commercial buildings so as to provide economic solutions to the demands of safety, shallow construction depth, rapid construction, and minimal maintenance and flexibility in future use. Steel structures are also widely used in the mining, transportation, ship and aeronautics sectors. Steel scores well on all the sustainability measures

Imperfection tolerances during the erection of steel plate girders and geometrical nonlinearities
Master of Civil Engineering defended by SONNA DONKO Maël
NASPW Yaoundé 2019/2020

7

and offers a broad range of benefits addressing the economic, environmental, and social priorities of sustainability.

In the world, the first structural steel railroad bridge was the Eads bridge, constructed in 1874 in St. Louis, Missouri. In Cameroon, the first major bridge was built by the Germans in 1911. Figure 1.2 shows this arch bridge built over the Sanaga River and simultaneously as a highway, railway, and pedestrian bridge.

Figure 1.2. German arch bridge over River Sanaga, Cameroon (Radio Museum, 2016)

1.1.6. Defects, causes and treatments of steel

In this section, the main defects encountered in steel, its causes and treatment techniques are briefly discussed.

1.1.6.1. Corrosion

Steel is usually very susceptible to corrosion in outdoor atmospheres due to its oxidation in the air to produce metal oxides, rust.

To prevent corrosion, steel needs to be adequately protected by the application of an appropriate barrier, on its surface, from the atmosphere. This barrier protects the steel and prolongs its life span. Common surface barriers include dry abrasive blasting, coal coatings and paints.

1.1.6.2. Fire susceptibility

Although steel is incombustible, it is highly susceptible to high temperatures during a fire, causing a loss in its resistance.

To prevent its loss in strength during a fire, steel needs to be protected with fireproof coatings such as expanded mineral coatings, concrete and intumescent materials.

Imperfection tolerances during the erection of steel plate girders and geometrical nonlinearities
Master of Civil Engineering defended by SONNA DONKO Maël
NASPW Yaoundé 2019/2020

8

1.1.6.3.   Fatigue and fracture

Large variations in tensile stresses cause fatigue in steel which reduces the overall strength of the steel element making it liable to buckling. Also, due to high deformations and loss of ductility, fracture might occur in steel after the brittle strength is reached.

In order to prevent these defects, steel must be used under reasonable and designed conditions.

1.2. Plate girders

In most design cases, standard rolled shapes are large enough and able to satisfy design requirements, but if the requirements are severe and none of the standard rolled shapes satisfy the design (not high enough cross-sectional area or moment of inertia), then a built-up section may be needed. In such cases, plate girders can therefore be used. These can be I-shaped sections, with two flanges and a web, or box sections, with two flanges and two webs. The components can be welded together and be designed to have exactly the properties needed (T. Segui, 2013). As such, this part focuses on the structure of plate girders followed by its erection method, the cross-section classification, the description of the plate girder's behaviour during pre-critical, critical and post-critical states and ends with an overview of the analytical approaches to the stability design of plate girders.

1.2.1. Structure of plate girders

A plate girder is a beam that is made up of plate elements to achieve a more efficient arrangement of material than that possible with rolled beams. They are economical where spans are long enough to permit savings in cost by proportioning for the particular requirement (Salman & Johnson, 1996).

Plate girders are usually classified depending on the technique used to assemble their parts. The main ones, as shown in Figure 1.3, being:

- welding
- bolting
- riveting

Imperfection tolerances during the erection of steel plate girders and geometrical nonlinearities
Master of Civil Engineering defended by SONNA DONKO Maël
NASPW Yaoundé 2019/2020

9
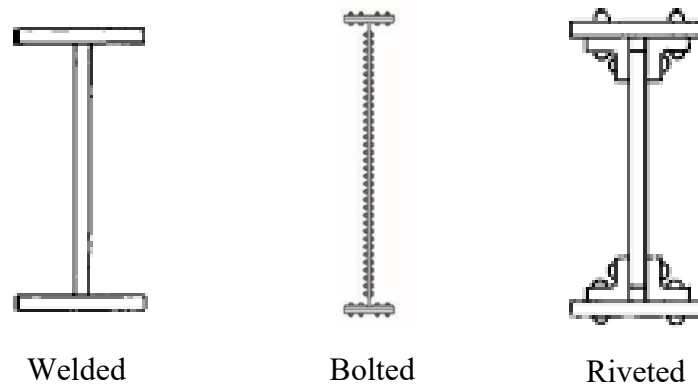
Figure 1.3. Welded, Riveted and Bolted Plate Girders (T. Segui, 2013)

Early railroad bridges constructed during the period 1870-1900 were mainly made up of riveted plate girders composed of angles connected to a web plate, with or without cover plates. In the 1950s, welding became more widely used due to the improved quality of welding and shop-fabricated economies. As such, shop welded steel plate girders composed of three plates gradually replaced riveted girders. During this period, high tensile strength bolts were gradually displacing rivets in construction fields. Since the 1960s, almost all plate girders are shop welded using two flange plates and one web plate to make a cross-section, the weld usually used is an Execution Class 3 weld as proposed by the European EN 1090 code.

I-shaped plate girders can be bisymmetric or monosymmetric, with bisymmetric plate girders (as seen in Figure 1.4) generating pure bending solicitations (neutral axis at the mid-depth of the web) while monosymmetric plate girders yield eccentric compression (pure bending plus pure compression).

In steel-concrete composite girders, monosymmetric steel plate girders are usually preferred to bisymmetric due to the fact that they possess a smaller upper flange (allowing most of the compression to the concrete that will be cast on it) thus reducing the cost of production. On the other hand, monosymmetric plate girders are very susceptible to web bend buckling during the erection phase as concrete is absent and the upper part of the web has to help the small upper flange to carry the heavy compressive solicitations.

Imperfection tolerances during the erection of steel plate girders and geometrical nonlinearities
Master of Civil Engineering defended by SONNA DONKO Maël
NASPW Yaoundé 2019/2020

10

Figure 1.4. Welded I-shaped bisymmetric plate girders (Structures, 2021)

1.2.2. Erection of plate girders

The balanced cantilever method, balanced lift method, movable scaffolding systems, climbing formworks and incremental launching methods are all different methods used for the erection of plate girders. In most cases where the bridge is too heavy, long, high over the ground or water, the most common method used is the incremental launching method. Here, the plate girder is launched from one end of the abutment to the other. This suggests that each part of the cross-section is manufactured and welded to the others in a workshop by fabricators, transported to the construction site and pushed out to the final position as seen in Figure 1.5.

A launching nose, usually a low weight steel truss, is usually placed in the front of the bridge girder to get it up on the next support and to decrease the bending moment and support reaction at the level of the launching shoe. However, large bending moments are present in plate girders during erection when the launching nose reaches a support. These large bending moments may cause local web bend-buckling that if not protected against, will cause the failure of the girder during its launching phase. As such, its behaviour during the launching phase needs to be studied for proper consideration during the design phase.

Imperfection tolerances during the erection of steel plate girders and geometrical nonlinearities
Master of Civil Engineering defended by SONNA DONKO Maël
NASPW Yaoundé 2019/2020

11

Figure 1.5. Incremental launching of a plate girder

(Techniques of Superstructure Construction, 2014)

1.2.3. Cross-section classification

It is of utmost importance to classify cross-sections based on their tendency to buckle locally before the overall failure of the member is envisaged. Special precautions need then to be taken in design for those cross-sections liable to buckle locally. However, local buckling involves distortion of the cross-section and does not always imply disaster. In the context of plate bucking, substantial reserve strength exists in plates beyond the point of elastic buckling, thus utilization of this reserve capacity may be the objective of the design. Therefore, in some cases, allowance of local buckling is made, provided care is taken to estimate the reduction in the capacity of the section due to its effect and the consequences clearly understood (Jayanta, 2016).

Cross-sections can be classified into four main groups, depending on their moment-rotation characteristics (Figure 1.6):

- Plastic (Class 1) cross-sections are those which can form a plastic hinge with a rotation capacity for plastic analysis.
- Compact (Class 2) cross-sections are those which can develop their plastic moment resistance but have limited rotation capacity.
- Semi-compact (Class 3) cross-sections are those in which the calculated stress in the extreme compression fibre of the steel member can reach its yield strength, but local buckling is liable to prevent the development of the plastic moment resistance.

Imperfection tolerances during the erection of steel plate girders and geometrical nonlinearities
Master of Civil Engineering defended by SONNA DONKO Maël
NASPW Yaoundé 2019/2020

12

- Slender (Class 4) cross-sections are those in which it is necessary to make explicit allowances for the effects of local buckling when determining their moment resistance or compression resistance (Loorits & Mekaniikka, 1995).

For each of the stated classes, codes specify limiting width to thickness ratios for component plates used to design.
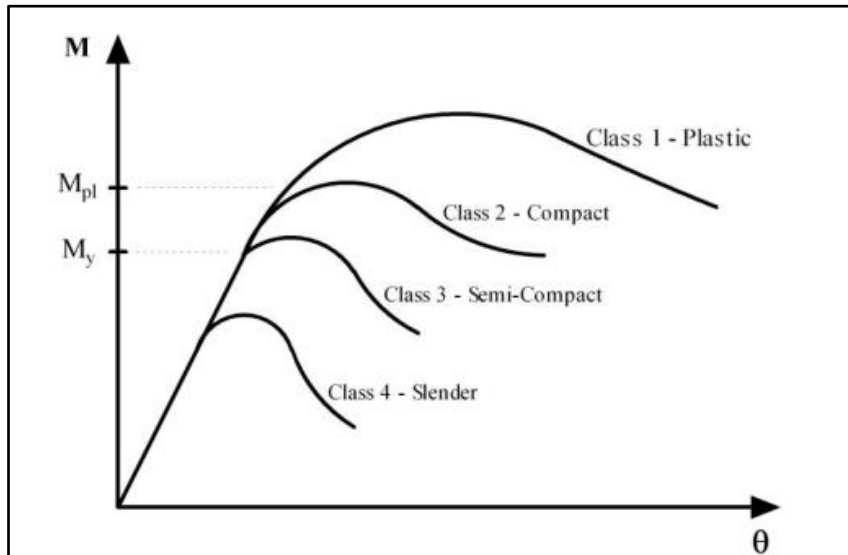
Figure 1.6. Cross-section classification (Jayanta, 2016)

1.2.4. Behaviour of plate girders

Even though the term plate girder is used for sections made up of plates, the correct use of the term applies to members with slender webs. As such, these members might be exposed to 3 behaviours: pre-critical, critical and post-critical behaviours.

1.2.4.1. Pre-critical behaviour of plate girders

During the erection of plate girders, a concrete slab is yet to be present and the steel plate girders are subjected to various actions due to bearing's reaction raised near the bridge piers, the effect of self-weight of the launching nose equipment as well as the distance between two consecutive bridge supports. These actions are exerted on the plate as concentrated loads, bending and shear forces or as the combined effect of loadings, thus, in this phase, the deep web of plate girders becomes very unstable (lateral-torsional instability, local instability of the flange and instability of the web).

As the aforementioned loads increase, the girder parts first resist elastically until the slender plate suddenly deflects from its original shape. At this point, the plate has buckled and the deformations might be so excessive that the girder will be discarded.

Imperfection tolerances during the erection of steel plate girders and geometrical nonlinearities
Master of Civil Engineering defended by SONNA DONKO Maël
NASPW Yaoundé 2019/2020

13

To increase the web's resistance to buckling, it is a common practice to provide girders, transversal and/or longitudinal stiffeners to limit the risk of local or global buckling of the structural element. Thus, to avoid unacceptable damage whether during the erection process or in the bridge's service, it becomes important, for the engineer, not to study only the failure of the structural element by reaching the admissible yield stress but also to focus on the elastic buckling and nonlinear post-buckling of the slender plate, get the ultimate load and design at lesser loads (Tetougueni et al., 2019).

1.2.4.2. Critical state

The critical state or buckling point is defined as the point where a perfect structure, or member, loses its stability. Buckling instability is a phenomenon in structural engineering, where a light increase in the load can lead to a sudden catastrophic failure. Bifurcation or critical stress can be calculated analytically based on the classical theory of elasticity by solving the differential equation of a plate or by using the energy method.

a) The direct approach to the differential equation

In 1870, Saint-Venant established the differential equation in (1.2) that describes the equilibrium of a loaded plate under small deformations in its mid-plane based on Kirchhoff-Love's plate theory.

$$\frac{\partial^4 w}{\partial x^4} + 2 \cdot \frac{\partial^4 w}{\partial x^2 \, \partial y^2} + \frac{\partial^4 w}{\partial y^4} = \frac{1}{D}\left[N_x \cdot \frac{\partial^2 w}{\partial x^2} + N_y \cdot \frac{\partial^2 w}{\partial y^2} + 2 \cdot N_{xy} \cdot \frac{\partial^2 w}{\partial x \, \partial y} \right] \quad (1.2)$$

$$D = \frac{E \cdot t^3}{12 \cdot (1 - v^2)} \quad (1.3)$$

where:

w: lateral displacement

D: flexural rigidity of the plate is given by equation (1.3)

E: Young's modulus

t: plate's thickness

v: Poisson's ratio

Imperfection tolerances during the erection of steel plate girders and geometrical nonlinearities
Master of Civil Engineering defended by SONNA DONKO Maël
NASPW Yaoundé 2019/2020

14

This was derived assuming that:

- the material is behaving in an ideally elastic way
- the plate is without initial imperfections such as initial curvature or residual stresses
- the plate deformations are small

Under the stated assumptions, the plate shows no lateral deformations until the critical state is reached. At this point, the deflection can either be negative or positive with respect to the coordinate system of the plate as seen in Figure 1.7
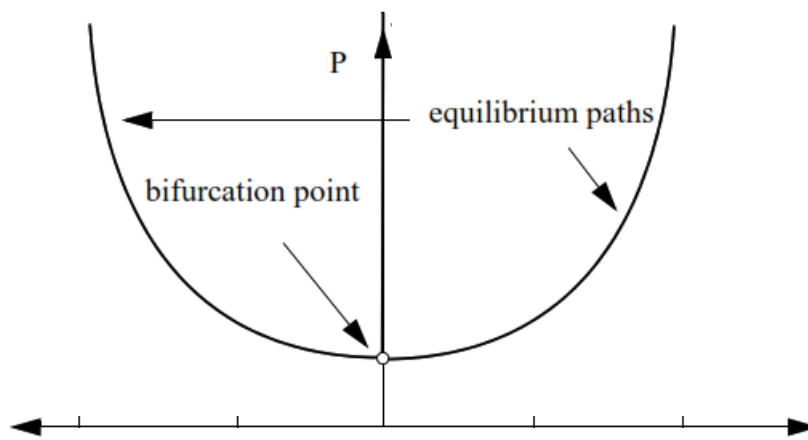
Figure 1.7. System bifurcation (Ritter, 2000)

b) Strain energy-based approach

In 1891, Bryan developed a strain energy-based approach, built on the classical correlation between the internal energy of bending, equation (1.4), and the external work done by the forces acting in the middle plane of the plate, equation (1.5). It consists of studying the plate's energy in the bifurcation point, where the plate ceases to be in its assumed perfectly flat state and instead follows its secondary equilibrium path in a laterally deformed state, as expressed in equation (1.6) (Clarin, 2007).

$$U = \frac{1}{2} \cdot D \iint \left[\left(\frac{\partial^2 w}{\partial x^2} + \frac{\partial^2 w}{\partial y^2} \right)^2 - 2 \cdot (1 - v) \cdot \left(\frac{\partial^2 w}{\partial x^2} \cdot \frac{\partial^2 w}{\partial y^2} - \left(\frac{\partial^2 w}{\partial x \, \partial y} \right)^2 \right) \right] dxdy \quad (1.4)$$

$$T = -\frac{1}{2} \cdot D \iint \left[N_x \cdot \frac{\partial^2 w}{\partial x^2} + N_y \cdot \frac{\partial^2 w}{\partial y^2} + 2 \cdot N_{xy} \cdot \frac{\partial^2 w}{\partial x \, \partial y} \right] dxdy \quad (1.5)$$

Imperfection tolerances during the erection of steel plate girders and geometrical nonlinearities
Master of Civil Engineering defended by SONNA DONKO Maël
NASPW Yaoundé 2019/2020

15

$$U = T \tag{1.6}$$

c) The solution to the buckling problem

Buckling stress solution to these differential equations depend on the boundary condition and load pattern applied to the plate under consideration.

In the case of a simply supported plate under uniform compression applied only along the edges $x = \frac{a}{2}$ and $x = -\frac{a}{2}$ as seen in Figure 1.8, this yields equation (1.7).
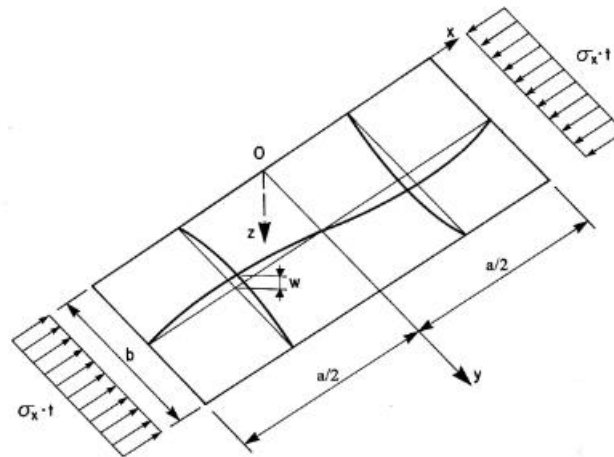
Figure 1.8. Simply supported plate under uniform compression (Clarin, 2007)

$$N_y = N_{xy} = 0 \tag{1.7}$$

Also, the assumed edge constraints of the plate lead to the boundary conditions in equation (1.8).

$$\begin{cases} w = \dfrac{\partial^2 w}{\partial x^2} = 0, & x = \dfrac{a}{2} \text{ and } x = -\dfrac{a}{2} \\ w = \dfrac{\partial^2 w}{\partial y^2} = 0, & y = 0 \text{ and } y = b \end{cases} \tag{1.8}$$

The specified boundary conditions imply that the deformed shape of the simply supported plate may be described, as in equation (1.9), by a double trigonometric Fourier series of the form:

$$w = \sum_{m=1}^{\infty} \sum_{n=1}^{\infty} a_{mn} \sin \frac{m\pi x}{a} \sin \frac{n\pi y}{b} \qquad m, n = 1,2,3 \dots \tag{1.9}$$

Imperfection tolerances during the erection of steel plate girders and geometrical nonlinearities
Master of Civil Engineering defended by SONNA DONKO Maël
NASPW Yaoundé 2019/2020

16

Thus, solving the differential equation of simply supported plates under uniform compression yields equation (1.10).

$$\sigma_{cr} = \frac{N_{cr}}{t} = k_{cr} \cdot \frac{\pi^2 E}{12(1-v^2)} \cdot \left(\frac{t}{b}\right)^2 \qquad (1.11)$$

$$k_{cr} = \left(\frac{m \cdot b}{a} + \frac{a}{m \cdot b}\right)^2 \qquad m = 1,2,3 \dots \qquad (1.10)$$

The buckling load coefficient, k_{cr}, as seen in equation (1.11) is a function of the plate width b, the length a and the number of sinus half waves over the length, m. For different values of aspect ratio $\frac{a}{b}$, the lowest critical stress level will be found for different numbers of half-waves as seen in Figure 1.9.
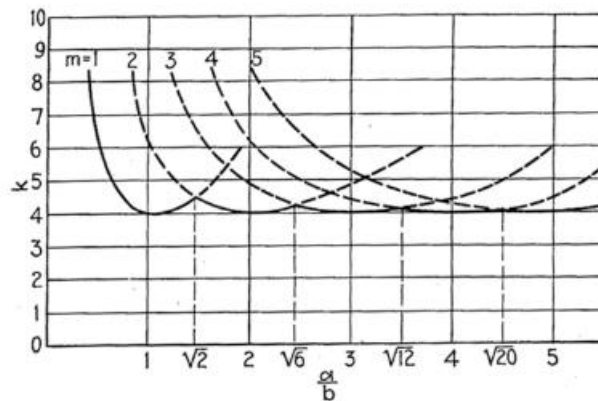
Figure 1.9. Buckling coefficient of a simply supported plate under uniform compression (Timoshenko et al., 1962)

For other common support conditions and loading cases, Timoshenko and Gere (1962) proposed different values of k for which equation (1.10) remains valid.

1.2.4.3. Post-critical behaviour of plate girders

In contrast to columns and beams which fail after buckling due to excessive deformations and do not exhibit any post-critical response, plates can often support stresses much higher than the buckling stress. When the plate starts to buckle, stresses are re-distributed in it. The plate behaviour under the excessive large deflections, or post-critical behaviour, is a quite complicated phenomenon to describe.

Mathematically, the large deflection (non-linear) phenomenon was described by the Föppl–von Kármán differential equations originally presented by von Kármán in 1910,

Imperfection tolerances during the erection of steel plate girders and geometrical nonlinearities
Master of Civil Engineering defended by SONNA DONKO Maël
NASPW Yaoundé 2019/2020

17

following Kirchhoff's work on small deflections in plates in 1876. The differential equation was later modified by Marguerre in 1938 to take into consideration initial geometric imperfections. The equilibrium equation is shown in equation (1.12) and the compatibility in equation (1.13).

$$\frac{\partial^4 w}{\partial x^4} + 2 \cdot \frac{\partial^4 w}{\partial x^2\,\partial y^2} + \frac{\partial^4 w}{\partial y^4} = \frac{t}{D}\left[\frac{\partial^2 F}{\partial y^2} \cdot \frac{\partial^2 (w+w_0)}{\partial x^2} - 2 \cdot \frac{\partial^2 F}{\partial x\,\partial y} \cdot \frac{\partial^2 (w+w_0)}{\partial x\,\partial y} + \frac{\partial^2 F}{\partial x^2} \cdot \frac{\partial^2 (w+w_0)}{\partial y^2}\right] \quad (1.12)$$

$$\frac{\partial^4 F}{\partial x^4} + 2 \cdot \frac{\partial^4 F}{\partial x^2\,\partial y^2} + \frac{\partial^4 F}{\partial y^4} = E \cdot \left[\left(\frac{\partial^2 w}{\partial x\,\partial y}\right)^2 - \frac{\partial^2 w}{\partial x^2} \cdot \frac{\partial^2 w}{\partial y^2} - \left(\frac{\partial^2 w_0}{\partial x\,\partial y}\right)^2 + \frac{\partial^2 w_0}{\partial x^2} \cdot \frac{\partial^2 w_0}{\partial y^2}\right] \quad (1.13)$$

where:

F: stress variation in the plate

w: out-of-plane deflection at any point on the plate

w_0: initial deflection (or imperfection) system in the plate

D: plate flexural rigidity

Despite the differential equations of this phenomenon formulated, methods for solving these are too complex. The finite difference method, Fourier series or different perturbation methods are possible tools that can be used to tackle this problem. Also, numerical methods can be used to solve these complex equations. An example is the finite element method (FEM), which probably is the most powerful tool available today. However, other methods have been used during the years of research. Analytical methods such as the Ritz energy method or a method based on a theory by Skaloud and Kristek called the "Folded plate theory method" are both excellent examples (Clarin, 2007).

From a more practical point of view, Wilson explained, in 1886, the source of the post-buckling (post-critical) strength of stiffened plate girder webs in shear. He discovered that: "By means of a paper model with a very thin flexible web, that when stiffeners were properly introduced, the web no longer resisted by compression, but by tension, the stiffeners taking up the duty of compressive resistance, like the posts of a Pratt truss, and dividing the girder into panels equivalent to those of an open truss, the web in each panel acting as an inclined tie."

Imperfection tolerances during the erection of steel plate girders and geometrical nonlinearities
Master of Civil Engineering defended by SONNA DONKO Maël
NASPW Yaoundé 2019/2020
18

Wilson stated that using this theory he obtained "results that quite agreed with practical examples".

Wagner (1931) developed a diagonal-tension theory of web shear. His work was extended by Kuhn (1956) for applications in aircraft design. Extensive studies, both analytical and experimental, were made in the late 1950s by Basler and Thürlimann on the post-buckling behaviour of web panels in bending as well as in shear (Basler and Thürlimann, 1960; Basler et al., 1960; Yen and Basler, 1962; Basler, 1963). Practical procedures were then developed and have been adopted in many specifications. Widespread interest in the subject resulted in several modifications to the Basler-Thürlimann approach to achieve a better correlation between theory and tests.

Many researchers showed that the ultimate load of a plate under compression may significantly surpass the critical load level. But since formulas for predicting buckling are relatively simple and have been known for many years, buckling was used for the design of plate girder webs almost exclusively until the early 1960s, while suitable analyses of post-buckling strength were not available. However, in most code specifications, smaller factors of safety for web buckling than for yielding or failure of other elements were used to acknowledge the presence of a post-buckling strength (Ziemian & Wiley, 2010).

Thus, slender plates in compression possess significant post-critical resistance that can be utilized in design procedures for plated structural elements. A typical response of slender plates in compression is shown in Figure 1.10.
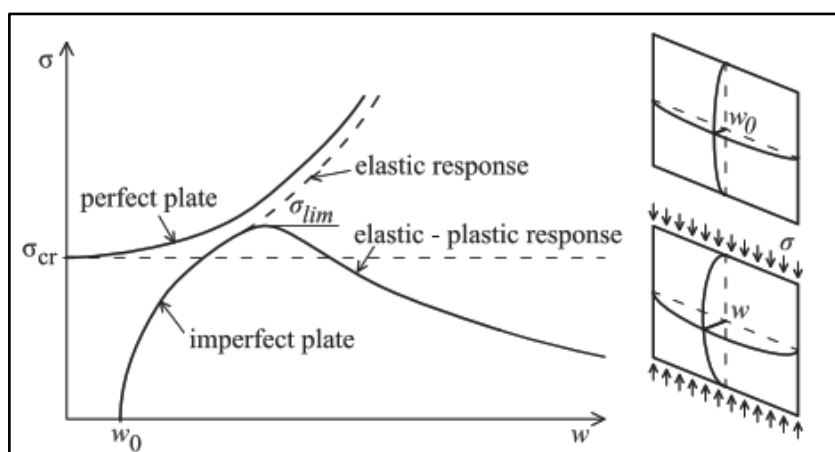
Figure 1.10. Post-critical response of slender plates in compression (Beg et al., 2011)

Imperfection tolerances during the erection of steel plate girders and geometrical nonlinearities
Master of Civil Engineering defended by SONNA DONKO Maël
NASPW Yaoundé 2019/2020

19

For geometrically perfect plates pre- and post-critical behaviour are very evident, while for imperfect plates the transition between pre- and post-critical behaviour is gradual and for larger imperfections, nearly imperceptible. It is important that after reaching the elastic critical stress, the resistance is not exhausted, but it increases further until plastic collapse occurs. In the post-critical state, the redistribution of compressive stresses takes place with the reduction of stresses in the middle-buckled part, where axial stiffness is decreased, and with the increase of stresses near straight plate edges. The ultimate resistance is reached soon after the maximum edge stress has reached the plate yield strength as, in general, slender plates do not have any ductility to redistribute stresses by developing zones of plastic strains (Beg et al., 2011).

1.2.5. Stability design approach

Structural steel design is often performed to provide stability, either locally or globally. Many, if not all, standard hot-rolled structural shapes are proportioned in such a way that local stability problems have been eliminated or brought to their minimum. However, when a plate girder is used, the designer will have to take into consideration factors that in many cases would not have been problematic with a hot-rolled shape. Deep and thin webs account for many of the special problems associated with plate girders, including local instability (T. Segui, 2013). Instability, which should be designed against, can be caused either by direct stresses or shear stresses acting in the plated structural member.

1.2.5.1. Direct stresses

As slender plates do not possess any ductility to redistribute stresses by developing zones of plastic strains, the ultimate resistance of the plate girder cross-section is reached soon after the maximum edge stress has reached the plate yield strength. The use of the non-linear distribution of actual stresses at this stage is not very practical for the design, as such two simplified methods appropriate in practical design procedures were developed.

The first method focuses on an appropriate reduction of the cross-section in the central buckled part of the plate, assuming effective widths adjacent to the edges as fully effective with stresses that have reached the plate yield strength all over the effective width. This method is called the effective width method or reduced cross-section method.

The second method, called the reduced stress method, deals with the average stress of the actual stress distribution at the ultimate limit state. The main idea behind these methods is shown in Figure 1.11.

Imperfection tolerances during the erection of steel plate girders and geometrical nonlinearities
Master of Civil Engineering defended by SONNA DONKO Maël
NASPW Yaoundé 2019/2020

20

Theodore von Kármán's work on effective width was a milestone concerning plates' simplified design methods. His hypothesis, to find the ultimate strength of a perfect plate, was that the fictitious plate of width b_{eff} would have the critical stress equal to the yield stress as given by equation (1.14).
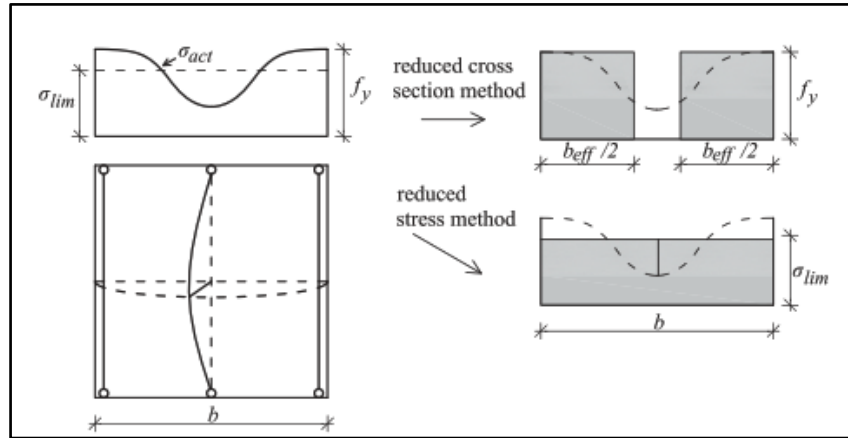
Figure 1.11. Basic ideas of reduced cross-section method and reduced stress method
(Beg et al., 2011)

$$\sigma_{cr} = f_y \qquad (1.14)$$

This was such that the effective width, b_{eff}, and width reduction factor, ρ, could be written as in equations (1.15) and (1.16) respectively. Where, $\bar{\lambda}_p$ is the von Kármán's slenderness ratio.

$$b_{eff} = b\sqrt{\frac{f_y}{\sigma_{cr}}} \qquad (1.15)$$

$$\rho = \frac{b_{eff}}{b} = \frac{1}{\bar{\lambda}_p} \qquad (1.16)$$

Many researchers followed his work, aiming to derive an expression describing a real plate with inherent initial imperfections. One of the most known and widely spread in design codes is the one proposed by Winter in 1947. Winter conducted numerous experimental tests on cold-formed specimens and proposed a refined expression for the effective width given by equation (1.17) (Clarin, 2007).

Imperfection tolerances during the erection of steel plate girders and geometrical nonlinearities
Master of Civil Engineering defended by SONNA DONKO Maël
NASPW Yaoundé 2019/2020

21

$$\rho = \begin{cases} 1, & \bar{\lambda}_p \leq 0.673 \\ \dfrac{1}{\bar{\lambda}_p}\left(1 - \dfrac{0.22}{\bar{\lambda}_p}\right), & \bar{\lambda}_p > 0.673 \end{cases} \qquad (1.17)$$

Although huge efforts have been put into this research field, the Winter function, based on cold-formed members is used in the present design rules of EN 1993-1-5 but it is highly contested. Also, modified width ratios were proposed to take into account loading conditions different from uniformly compressive loads.

1.2.5.2. Shear stresses

Under shear loading, plates undergo a behaviour that can be divided into 2 states prior to the plastic hinge mechanism: the state of pure shear stress and the tension field (Beg et al., 2011).

a) Pure shear stress

Before buckling, pure shear stresses occur in the plate. Transformed into principal stresses, these shear stresses, correspond to principal tensile stresses and principal compressive stresses with equal magnitude and inclined at an angle of 45° with respect to the longitudinal axis of the girder. Only constant shear stresses occur at the edges.

b) Tension field action

Slender plates under shear have a post-critical reserve as is the case for plates subjected to direct compressive stresses. After buckling, a shear buckle forms in the direction of the principal tensile stresses when the plate reaches the post-critical stress state. Due to buckling, there is no more possible increase of the stresses in the direction of the principal compressive stresses, whereas the principal tensile stresses can still increase. As a result, stress values of different magnitude occur such that tensile stresses become greater than compressive stresses. This then leads to a rotation of the stress field to attain equilibrium. This is termed tension field action. The development of such a tensile force is only possible if the boundary elements provide sufficient anchorage. When reaching ultimate load, a plastic hinge mechanism forms in the flange as seen in Figure 1.12.

Imperfection tolerances during the erection of steel plate girders and geometrical nonlinearities
Master of Civil Engineering defended by SONNA DONKO Maël
NASPW Yaoundé 2019/2020

22
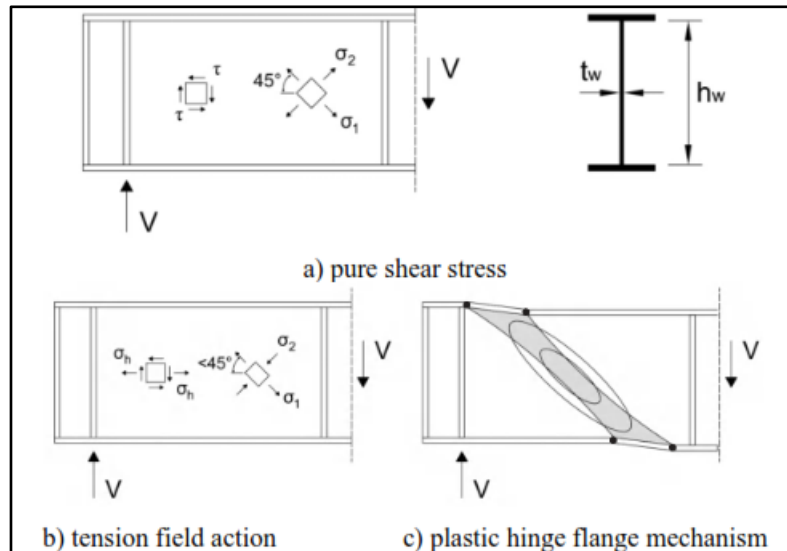
Figure 1.12. Stress states and collapse behaviour of a plate subjected to shear

(Beg et al., 2011)

1.3. Imperfections

The dimensions of any artefact usually vary from those initially defined by the designer, such variations exist from the nature and behaviour of the material as much as from the process of making it. In modern steel fabrication, dimensional variation from the design is inherent and unavoidable, as it involves the manufacture of large and often complex welded assemblies of components from rolled steel products, with high-temperature processes being used to produce the steel components and join them together. This behaviour has implications for the designer, for the steelwork contractor, for the bridge builder, and each has to anticipate the variations in carrying out their role (Hayward et al., 2002). As such, an in-depth understanding of the inevitable imperfections is important for a consistent and complete study of real-life pate girders. Thus, generalities on imperfections, followed by the types and modelling techniques of imperfections are studied. Then, guidance is given on how to reduce imperfections and a summary of the possible imperfection tolerance limits are presented.

1.3.1. Generalities

Imperfections are deviations and inconsistencies from the theoretically assumed perfect state in structural members which can affect the behaviour of the structure. Imperfections in structures are usually taken into consideration when their effects could be critical (Obinna, 2020).

Imperfection tolerances during the erection of steel plate girders and geometrical nonlinearities
Master of Civil Engineering defended by SONNA DONKO Maël
NASPW Yaoundé 2019/2020

23

The important questions dealing with imperfections are:

- which dimensional variations are critical?
- what limits should be defined on the critical ones?
- how can imperfections be managed to ensure that the implemented design meets its performance requirements?

In steel bridge engineering, imperfections are quite important as they involve mechanical components, structural steelwork manufactured remote from the site, and civil engineering works. The following are imperfections usually found in bridge engineering:

- Mechanical fit, for example for the function between nut and bolt, between bearing and girder, between machined faces of compression members.
- Fit up of fabricated members, essential for efficient assembly for example of a bolted site splice, yet the dimensional accuracy of the bolt group is immaterial to the strength.
- Deviation from flatness or straightness affects the strength or function of components for example in reduced buckling capacity.
- Accuracy of assembly at the site where steel spans must match the substructure positions and girder profiles must correspond to maintain deck slab thicknesses.
- Interface with substructures where the designer has to provide adjustment in construction, say by variable grout layers to accommodate relatively inaccurate concrete to precise steel components.
- Distortion in steel used to describe shrinkages that take place when heat is applied in cutting or welding processes. Welding causes shrinkage which will lead to deformation from the original shape (Hayward et al., 2002).

1.3.2. Types of imperfections

The type of imperfections depends on their origin, as such, there are 2 types of imperfections: geometric and material imperfections.

1.3.2.1. Geometric imperfections

a) Generalities

Geometric imperfections are deviations of an actual member from the perfect geometry. Most structural steel members have initial geometric imperfections as a result of manufacturing, transporting, and handling processes.

Imperfection tolerances during the erection of steel plate girders and geometrical nonlinearities
Master of Civil Engineering defended by SONNA DONKO Maël
NASPW Yaoundé 2019/2020

24

Geometric imperfections can be classified into two main categories, which are local (cross-sectional) and global (overall) imperfections (Ellobody, 2014).

- Local geometric imperfections represent the change of the cross-section from its ideal shape and can be found in any region of the outer or inner surfaces of structural members like dents and plate waviness as in Figure 1.13 (a).

- Overall geometric imperfections are global profiles for the whole structural member which represents the deviation of the member centreline from its straightness along the member length in any direction. These imperfections include bowing, warping, or twisting of a member as in Figure 1.13 (b).
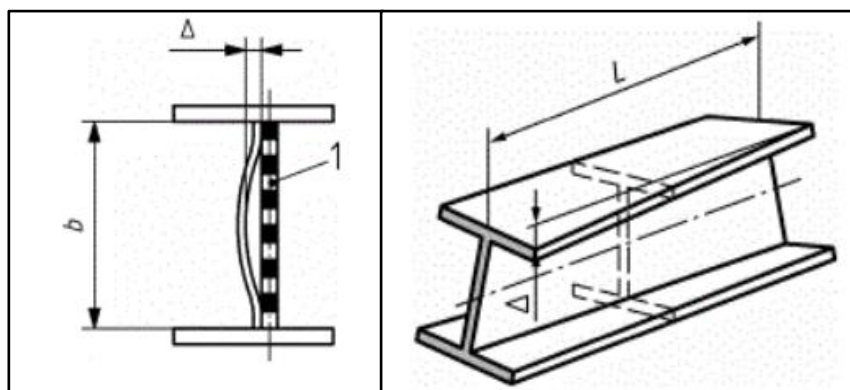
(a) Local imperfection   (b) Global imperfection

Figure 1.13. Geometrical imperfections (EN 1090-2:2018 (E), 2018)

b) **Measuring methods**

Geometric imperfection measurement methods and procedures usually employed are:

- photogrammetry
- laser scanning
- the manual method (dial gauges mounted on a precision rail) (McAnallen et al., 2014)

Figure 1.14 shows a widely used on-site manual method.

Imperfection tolerances during the erection of steel plate girders and geometrical nonlinearities
Master of Civil Engineering defended by SONNA DONKO Maël
NASPW Yaoundé 2019/2020

25

Figure 1.14. Measurements of web imperfections with dial gauges

(Helwig et al., 2015)

It is important to note that, practically, a detailed understanding of the complete imperfection pattern existing in a member is not generally required. The strength of a given member is particularly sensitive to imperfections in the shape of its eigenmodes. Thus, the most structurally influential geometric imperfection can be adequately characterized if the amplitude of imperfections in the lowest eigenmode is known. To this end, existing experimental data is gathered, and new experiments are conducted to make conclusions about what magnitude of imperfection analysts should use (Schafer, 1996).

c) Effects

Due to imperfections, instead of an abrupt change from pre-buckling, buckling to post-buckling as is the case in perfect members, buckling processes rather occur gradually. This situation leads to an unclear buckling point seen in Figure 1.15 (Pham et al., 2018).

Geometric imperfections lead to out-of-plane deflections which vary as a function of the applied loads. Tensile-type stresses tend to reduce the imperfections while compressive stresses cause the imperfections to grow. Due to this behaviour, compressive regions of the girders are much more sensitive to plate imperfections. Figure 1.15 shows the typical effect of imperfections on the load-displacement relationship of the part of a plate subjected to compression. The first curve shows the post-buckling strength developed due to stiffening that occurs as displacements increase. Also, it is noticed that plates with larger imperfections experience larger deformations than plates with smaller imperfections. Hence, geometric

Imperfection tolerances during the erection of steel plate girders and geometrical nonlinearities
Master of Civil Engineering defended by SONNA DONKO Maël
NASPW Yaoundé 2019/2020

26

imperfections tend to reduce the initial stiffness of the plate. Therefore, larger initial imperfections lead to larger plate displacements at low loads. However, as shown in Figure 1.15, with any level of imperfection, the plate still approaches the path of the ideal plate at higher levels of strain, but a plate with high imperfections will undergo large displacements to approach the path of the ideal plate (Helwig et al., 2015).
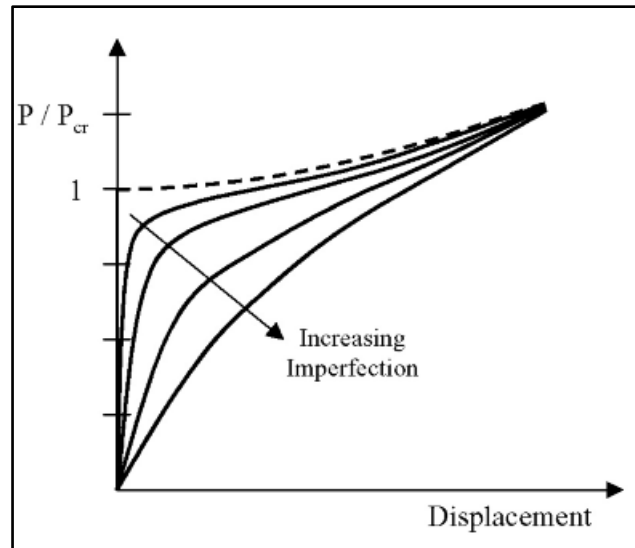
Figure 1.15. Effects of geometrical imperfections on plates
(Helwig et al., 2015)

1.3.2.2.   Material imperfections

a) Generalities

Material imperfections are those which arise from deviations in the assumed material properties. They are residual stresses, concrete grade deviation, modulus of elasticity deviation from the ideal properties etc. The main material imperfection in steel plate girders is residual stress. These are stresses that remain within a material or body after manufacture and material processing occur in the absence of external forces or thermal gradients. They are generated during most manufacturing processes involving material deformation, heat treatment, machining or processing operations that transform the shape or change the properties of a material. Thus, they cannot be avoided and in most cases are not desirable (Rossini et al., 2012).

Residual stresses produce internal membrane forces and bending moments, which are in equilibrium inside the cross-sections. Residual stresses in structural cross-sections are usually attributed to the uneven cooling of parts of cross-sections after hot rolling. The parts

Imperfection tolerances during the erection of steel plate girders and geometrical nonlinearities
Master of Civil Engineering defended by SONNA DONKO Maël
NASPW Yaoundé 2019/2020

27

that cool quicker have residual compressive stresses, while parts that cool lower have residual tensile stresses as seen in Figure 1.16 (Ellobody, 2014).
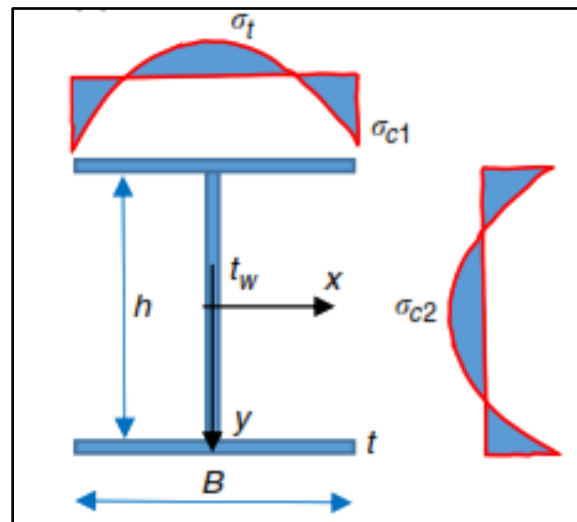
Figure 1.16. Stress distribution due to residual stresses (Di Pietro et al., 2012)

b) Measuring methods

The measurement of residual stresses is important for an accurate understanding of the performance of appropriate structural members. Extensive experimental investigations have been conducted to determine the distribution and magnitude of residual stresses inside cross-sections. These experimental investigations can be classified into two main categories, which are:

- Non-destructive methods, suitable for measuring stresses close to the outside surface of cross-sections. Examples of these methods are X-ray diffraction and Neutron diffraction.
- Destructive methods, involving machining/cutting of the cross-section to release internal stresses and measure the resulting change of strains. These methods are based on the destruction of the state of equilibrium of the residual stresses in the cross-section. In this way, the residual stresses can be measured by relaxing these stresses.

One of the main destructive methods is to cut the cross-section into slices and measure the change in strains before and after cutting. After measuring the strains, some simple analytical approaches can be used to evaluate resultant membrane forces and bending moments in the cross-sections (Ellobody, 2014).

Imperfection tolerances during the erection of steel plate girders and geometrical nonlinearities
Master of Civil Engineering defended by SONNA DONKO Maël
NASPW Yaoundé 2019/2020
28

c) Effects

Like geometric imperfections, residual stresses (material imperfections) also have compromising effects on the behaviour of plate girders. Residual stresses and their distribution are of particular importance for slender structural steel members as they affect their strength.

As loads acting on girders increase, some parts of the structural member will quickly reach the yield stress and become plastic due to the presence of initial residual compressive stresses. The stiffness will then tend to reduce and become a function of the inelastic part of the cross-section. A member with residual stresses can be seen to behave like one that has a reduced cross-section, the reduced cross-section or elastic portion of the member will change as the applied load changes. Nonetheless, residual stresses reduce the flexural capacity of plate girders by less than 3% (Shin et al., 2013).

Buckling and post-buckling analysis can be carried out by using an effective second moment of area of the elastic portion of the cross-section or by using the tangent modulus.

1.3.3. Modelling imperfections

In frames, all types of imperfections are usually merged and considered as equivalent geometric imperfections with a higher value of amplitude. On the other hand, in cold-formed plated structures, geometric imperfections and residual stresses are both introduced separately to derive buckling factors (Obinna, 2020).

Initial local and overall geometric imperfections can be modelled using finite element programs by first conducting eigenvalue buckling analysis to obtain the worst cases of local and overall buckling modes. The obtained deflections from the local and overall buckling modes are then multiplied by measured magnitudes from tests. Superpositions are used to obtain models for final combined local and overall buckling modes. The resulting combined buckling modes are added to the initial coordinates of the perfect structural member, the final coordinates obtained (imperfect model) can be used in any subsequent nonlinear analysis. The results obtained will be accurate enough if finite element models incorporate both initial local and overall geometric imperfections in the analysis. Therefore, efficient test programs must include the measurement of initial local and overall geometric imperfections.

Experimental investigations used to measure residual stresses are costly and time-consuming. As such, previous works have been done to simulate some typical and simple procedures to introduce residual stresses through numerical methods. Dixit and Dixit modelled

Imperfection tolerances during the erection of steel plate girders and geometrical nonlinearities
Master of Civil Engineering defended by SONNA DONKO Maël
NASPW Yaoundé 2019/2020

29

cold rolling and found a simplified procedure to determine the longitudinal residual stresses in steel. Also, Kamamato et al. have analysed residual stresses and distortion of large steel shafts due to quenching. The results showed that residual stresses are strongly related to transformational behaviour. Also, numerical simulations have provided a means to investigate the effects of different parameters on the magnitude and distribution of residual stresses such as material characteristics and boundary conditions (Ellobody, 2014). Though complex, these procedures have provided a way to model residual stresses.

When refined analysis on geometric and material imperfections are not carried out, codes provide equivalent geometric imperfections, as in the case of frames, that can be used to model all imperfection types at once.

1.3.4. Guides to reduce imperfections

It has been shown that imperfections are caused as a result of manufacturing, transporting, and handling processes. As such, imperfections are inherent and unavoidable. Therefore, it is understandable that various standards require that these imperfections should be kept under control via prescribed tolerances and that in the case of need the magnitude of the initial imperfections can be reduced using the following techniques:

- Use of more accurate machines and increased levels of inspections during each process
- Each member should either be fabricated overlength then cut to length after welding, or an estimate of shrinkage should be added to anticipate its effect during the fabrication of the member.
- Sections can be straightened with the aid of special bar bending or straightening machines.
- Heat can be applied to the side opposite to that carrying the welds which caused the distortion. (Hayward et al., 2002).

These techniques are usually not desirable due to 2 main reasons:

- They are rather costly, both directly (as the process is expensive) and indirectly (as they block some space in the steel fabricator that can be used for other operations).
- It cannot be ascertained that the new stability behaviour is better than that of the original member. As, straightening a member-only means that one initial imperfection (initial web curvature) is replaced by another initial imperfection (additional induced residual stresses) (Kala et al., 2010).

Imperfection tolerances during the erection of steel plate girders and geometrical nonlinearities
Master of Civil Engineering defended by SONNA DONKO Maël
NASPW Yaoundé 2019/2020

30

If the aim is to go as far as entirely to disregard the effect of unavoidable initial imperfections, it must be certain that the influence of larger than usually adopted imperfection tolerances will not imperil the safety of the member. For this reason, authors have recently started extensive investigations on the impact of various (but practically important) configurations and magnitudes of imperfections on limit states.

1.3.5. Tolerances

Tolerances are defined as limits above which no guarantee can be given on the structural strength of a member.

Given that manufacturing and erection processes will always result in imperfections in a structure, there is a need to define tolerances that will help to guide whether a process can be seen as successful or not, depending on the influence of the imperfections on the structural strength of a member.

Thus, it can be understood that the strength of a member is independent of imperfections when imperfection amplitudes are below the code's maximum tolerance. When its amplitude exceeds the limit tolerance, a significant reduction in strength occurs which may render the structural part vulnerable to early collapse. Thus, tolerances are provided to engineers for adequate designs.

Tolerances are divided into three distinct categories (EN 1090-2:2018 (E), 2018):

- Essential tolerances represent the limits of permissible deviation for the mechanical resistance and stability of the structure. They are used to support conformity assessment to BS EN 1090-1.
- Functional tolerances provide limits of permissible deviation for fit-up and appearance. Two classes of deviation exist, class 1 being the cheaper and default class for routine fabrication and class 2 which requires more expensive and special measures during fabrication and erection.
- Special tolerances usually specified in individual projects either as a modification of the essential or functional tolerances or for aspects not already covered.

For plated structural members, simple criteria based on maximum eccentricity with respect to the undeformed vertical plane are usually given in codes. Some imperfection limits are shown in Table 1.1 for several different codes (Maiorana et al., 2009).

Imperfection tolerances during the erection of steel plate girders and geometrical nonlinearities
Master of Civil Engineering defended by SONNA DONKO Maël
NASPW Yaoundé 2019/2020

31

Table 1.1. Allowable out-of-plane deviations for steel plates (Maiorana et al., 2009)

Code/Recommendation	Nation	f_{adm}	Note
ÖNORM B 4600	Austria	$a/250$ or $b/250$	a = length of stiffener or length of the half wave of stiffener buckling mode
NBN B51-001	Belgium	$a/250$ or $b/250$ max: 4 mm	
DASt 012	Germany	$a/250$ or $b/250$	
CNR	Italy	$a/400$ or $b/400$	Stated for web panels
SIA-161 (1979)	Switzerland	$a/250$ or $b/250$	For unstiffened webs of plate girders, the maximum out-of-plane deflections f are prescribed with reference to a gauge length of 2 m
St.BK-N1	Sweden	$b/150$	Valid for the web of a beam subjected to a bending moment
ECCS	Europe	$a/500$ or $b/500$	
NS 3472	Norway	$b/133$	Valid for the web plate
AASHTO	USA	$\frac{0.159a}{144/\sqrt{t}}$ (m) or 4.8 mm	These tolerances are valid for orthotropic deck bridges only
SETRA	France	$\pm\frac{1}{3}(t+40 \text{ mm})\pm\frac{6}{3000}\pm\frac{1.5t}{10\,000}$	For orthotropic bridge deck
BS5400	UK	$\frac{2b}{165}\sqrt{\frac{\sigma_r}{355}}(a > 2b)\ \frac{2a}{165}\sqrt{\frac{\sigma_r}{355}}(a < 2b)$ but not less 3 mm	Applicable when $\frac{b}{t} > 25\sqrt{\frac{355}{\sigma_r}}$

Tolerances have been provided, to guide both manufacturers and designers in their jobs, through current international codes/recommendations based on experiences and traditions of the countries but not on the load configuration. Therefore, there is a need to redefine the codes' tolerances by studying the structural element's behaviour under varying load configurations and support conditions.

1.4. Nonlinearities

Most structures in civil engineering exhibit a linear elastic behaviour under service loads. Exceptions are slender structures such as steel plate girders, arches, tall buildings, and structures subjected to early localized yielding or cracking. Almost all structures, prior to reaching their limit of resistance, would exhibit significant nonlinear behaviours (McGuire et al., 1999). As such, there is a need to study the different types of nonlinear behaviours, their methods of analysis and the techniques used to solve these problems. Thus, leading to proper consideration during subsequent studies.

1.4.1. Nonlinear behaviour

Many sources of nonlinearity in the behaviour of structures were discovered recently. The main nonlinear effects that are considered in the analysis of civil engineering structures today can be grouped into geometric and material nonlinearities.

Imperfection tolerances during the erection of steel plate girders and geometrical nonlinearities
Master of Civil Engineering defended by SONNA DONKO Maël
NASPW Yaoundé 2019/2020

32

1.4.1.1. Geometric nonlinearity

Geometric nonlinearity represents an inherent realistic nonlinear relationship between the strain and the displacement of a structure. They are taken into consideration when the deflections are large enough to cause significant changes in the geometry of the structure so that the equations of equilibrium must be formulated for the deformed configuration (Przemieniecki, 1968).

In the following cases, it is important to consider a geometric nonlinear model:

- Significant initial imperfections such as member camber and out-of-plumb erection of a frame.
- Influence of axial force on the flexural stiffness of an individual member ($P - \delta$ effect)
- Significant lateral displacement of the supporting structure causing a destabilizing moment equal to a gravity load times the horizontal displacement ($P - \Delta$ effect) (McGuire et al., 1999).

1.4.1.2. Material nonlinearity

Material nonlinearities are due to the real-life nonlinear behaviour of structural materials. The usually used linear elastic constitutive laws of elementary structural analysis are rough approximations of the real material behaviour. They are used when approximate behaviour results in a response similar to the real-life response of the structure. More precise approximations are specific nonlinear constitutive models such as nonlinearly elastic, nonlinearly plastic, elasto-plastic, visco-elastic and visco-plastic behaviour of different types of materials (Galishnikova et al., 2009).

The following are a few cases where material nonlinearity should be considered:

- plastic deformation of steel structures
- cracking or creep of reinforced concrete structures
- inelastic interaction of axial force, bending, shear, and torsion

1.4.2. Nonlinear analysis

In structures, many practical phenomena simply cannot be considered using a linear formulation. Examples are buckling, post-buckling, formation of plastic hinges, nonlinear material behaviour of concrete, structural collapse. The elementary theory of structures does not work in these cases and needs to be completed (Wood, 1997). The fundamental aim of all

Imperfection tolerances during the erection of steel plate girders and geometrical nonlinearities
Master of Civil Engineering defended by SONNA DONKO Maël
NASPW Yaoundé 2019/2020
33

nonlinear analyses is to improve the quality of design by providing the engineer with a more reliable prediction of the performance of a system that is under design or investigation. In the following lines, the matrix approach is used to represent equilibrium equations of the most common nonlinear analyses used to define structures that experience high degrees of nonlinearities.

1.4.2.1.   Geometrically nonlinear elastic analysis (GNA)

A geometrically nonlinear (second-order) elastic analysis is an analysis that takes into account nonlinear large deflection theory for the displacements during the formulation of equations of equilibrium of the system. It includes any change in geometry due to the actions on the structure. This analysis yields an excellent representation of destabilizing influences but is unable to detect material nonlinearity as it uses a linear elastic material behaviour.

The following are possible modes of nonlinear elastic behaviours as shown in Figure 1.17:

- Bifurcation of the loading path with the system following an alternative path in the post-critical state
- Gradually increasing nonlinearity culminating in elastic instability at a limit point
- Increasing stiffness either from the onset of loading or, as shown, following a period of gradual softening

Equation (1.18) shows the matrix notation of the equations of equilibrium used for second-order elastic analysis.

$$[K_e + K_g]\{d\Delta\} = \{dP\} \tag{1.18}$$

Where $[K_e]$ is the linear elastic stiffness matrix and $[K_g]$ is the geometric stiffness matrix, which represents the change in stiffness resulting from these effects.

GNA analyses that adopt a model for the geometry of the structure including the imperfect shape (i.e. the geometry of the middle surface includes unintended deviations from the ideal shape) is termed a geometrically nonlinear elastic analysis with imperfections included (GNIA). The explicitly included imperfection may also cover the effects of deviations in boundary conditions and/or the effects of residual stresses.

Imperfection tolerances during the erection of steel plate girders and geometrical nonlinearities
Master of Civil Engineering defended by SONNA DONKO Maël
NASPW Yaoundé 2019/2020
34

1.4.2.2. Materially nonlinear analysis (MNA)

In first-order inelastic analysis (or MNA), inelastic behaviour is considered in the formulation of the equations of equilibrium. Also, the equations are written in terms of the geometry of the perfect structure and are therefore not able to detect geometric nonlinear effects. When the destabilizing effects of finite displacements are relatively insignificant, first-order inelastic analysis can produce an excellent representation of simple elastic-plastic behaviour and failure through mechanism formation, that is, the simple plastic limit load of Figure 1.17.

Thus,

$$[K_e + K_m]\{d\Delta\} = \{dP\} \qquad (1.19)$$

where $[K_m]$ which shall be called the plastic reduction matrix, represents the change in stiffness that results from the inelastic behaviour of the system.

1.4.2.3. Geometrically and materially nonlinear analysis (GMNA)

This is an analysis based on the perfect structure, using the assumptions of nonlinear large deflection theory and nonlinear elasto-plastic material property. This type of analysis has the potential for accommodating all of the geometric, elastic, and material factors that influence the response of a structure. Thus, it enables the preparation of analytical models that can precisely simulate the actual behaviour of structures and calculating the inelastic stability limit, that is, the point at which a system's capacity is exhausted and an increase in deformation results in a decrease in load resisting capacity. It is usually referred to as a second-order inelastic analysis.

The path of increasingly nonlinear response (elastic or inelastic) leading to instability is probably the most common mode of failure in real civil engineering structures.

In second-order inelastic analysis, both geometric and material nonlinearities are considered in the equations of equilibrium which takes the form of equation (1.20)

$$[K_e + K_g + K_m]\{d\Delta\} = \{dP\} \qquad (1.20)$$

If the GMNA analysis also includes the intrinsic imperfect shape of the structure, then the analysis is called a geometrically and materially nonlinear analysis with imperfections included (GMNIA).

Imperfection tolerances during the erection of steel plate girders and geometrical nonlinearities
Master of Civil Engineering defended by SONNA DONKO Maël
NASPW Yaoundé 2019/2020
35

It is not possible to model all sources of nonlinearity of a practical structure with complete details and represent its exact behaviour. Therefore, the problem of finding solutions to nonlinear problems is one of selecting a method that is sufficiently close to the real one and which provides adequate analytical simulation of the case at hand. The most common levels of analysis are shown in Figure 1.17 of the response curve of a statically loaded structure (McGuire et al., 1999). The precision with which each level can model the actual behaviour varies, but each gives important information to the engineer.
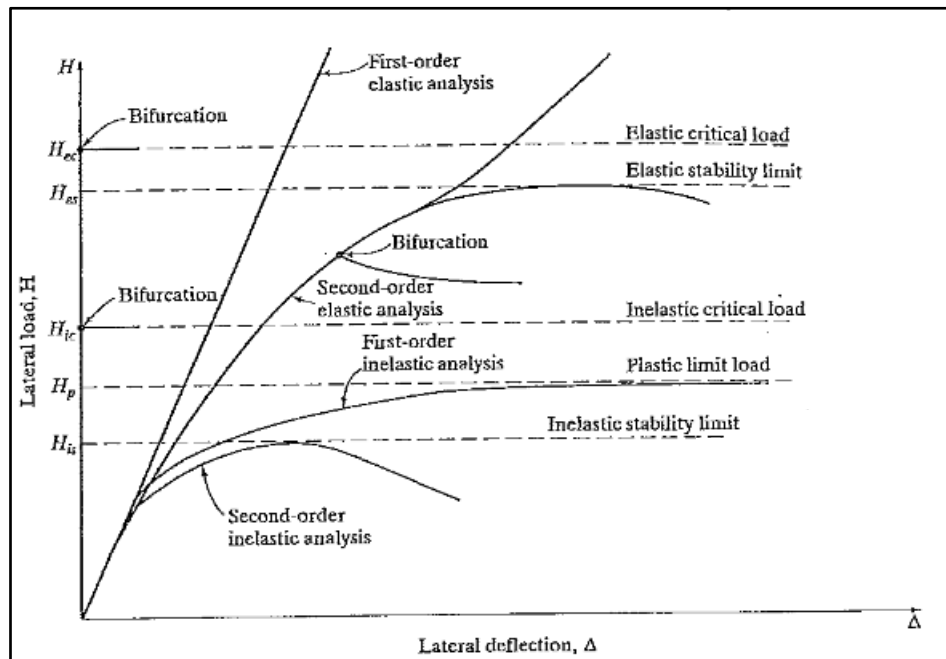
Figure 1.17. Levels of analysis (McGuire et al., 1999)

1.4.3. Numerical solution techniques

Various techniques can be used to solve the nonlinear problems discussed above. As analytical techniques have already been treated, this section will be used to discuss the possible numerical solution techniques. Numerical techniques solve problems by dividing the interval between the undeformed shape of the structure and the applied load step into various increments. The basic objective of all of these techniques is the establishment of equilibrium at the end of the load increment (McGuire et al., 1999). The incremental single-step methods, iterative methods and automatic load incrementation methods will be presented in this part.

Imperfection tolerances during the erection of steel plate girders and geometrical nonlinearities
Master of Civil Engineering defended by SONNA DONKO Maël
NASPW Yaoundé 2019/2020
36

1.4.3.1. Incremental single-step methods

The incremental single-step methods employ a strategy that is similar to solving systems of linear or nonlinear differential equations by the Runge-Kutta methods.

Here, the analyst prescribes the size of the load ratio for the first increment, usually about 10%-20% of the anticipated maximum applied load, then increment of unknown displacements is found in a single step by solving the linear system of equations.

The two most popular methods are the Euler and midpoint Runge-Kutta methods. The Euler method is schematised in Figure 1.18.
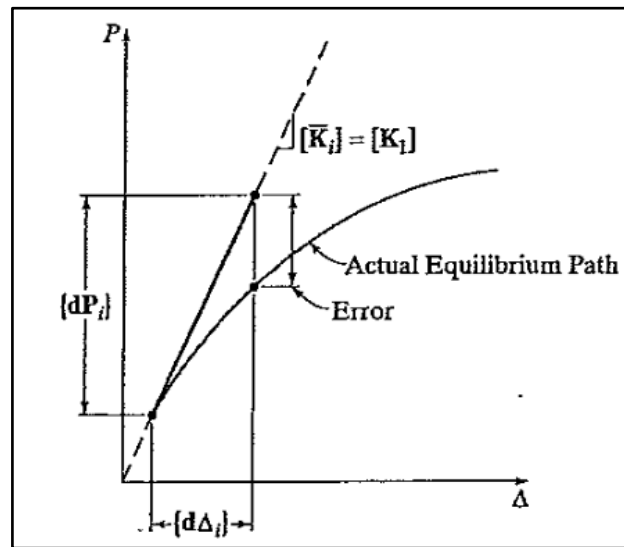
Figure 1.18. Euler method (McGuire et al., 1999)

The main advantages of the single-step methods are their simplicity and efficiency. One or two analyses are performed in each increment for almost all cases. In this regard, for the analysis of structures exhibiting little to moderate nonlinearities, these methods are particularly attractive.

The disadvantage of these techniques resides in the fact that the error resulting from the use of a single representative stiffness in every load increment can accumulate. Hence, displacements become inaccurate and total internal element forces are not necessarily in equilibrium with the externally applied forces. This discrepancy is termed the drift-off error. This error can be reduced by using a smaller load ratio, rendering the additional number of increments required for analysing highly nonlinear systems unreasonable. In these cases, the use of an iterative scheme becomes more appropriate.

Imperfection tolerances during the erection of steel plate girders and geometrical nonlinearities
Master of Civil Engineering defended by SONNA DONKO Maël
NASPW Yaoundé 2019/2020

37

1.4.3.2. Incremental iterative methods

Iterative methods do not need to use a single representative stiffness in each load increment as is the case of single-step schemes. On the contrary, increments are subdivided into several steps, each step is then used as a cycle in an iterative process which terminates when the requirements of equilibrium are satisfied within the specified tolerance. Some of the methods available to perform these multistep or iterative tasks are presented in the following paragraphs.

a) Load control method

Also called the Newton-Raphson method, here (Figure 1.19) a fixed amount of load is employed in each increment. All of this fixed amount of load is applied in the first step and additional iterations are performed to help satisfy equilibrium requirements.
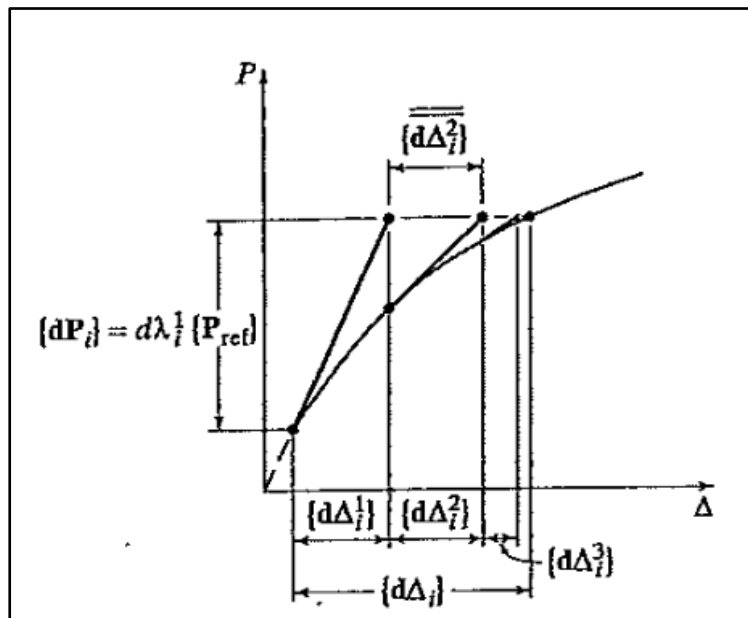
Figure 1.19. Load control method (McGuire et al., 1999)

Newton's method is not the best choice in cases where the stiffness matrix of the structure is not purely positive definite like structures that exhibit instabilities in the form of buckling. As seen in Figure 1.20, Newton's method fails in load control as it snaps through.

To solve such problems, the displacement control method which can continuously increase displacements and remain on the equilibrium (actual behaviour) curve is used (Vasios, 2015).

Imperfection tolerances during the erection of steel plate girders and geometrical nonlinearities
Master of Civil Engineering defended by SONNA DONKO Maël
NASPW Yaoundé 2019/2020
38
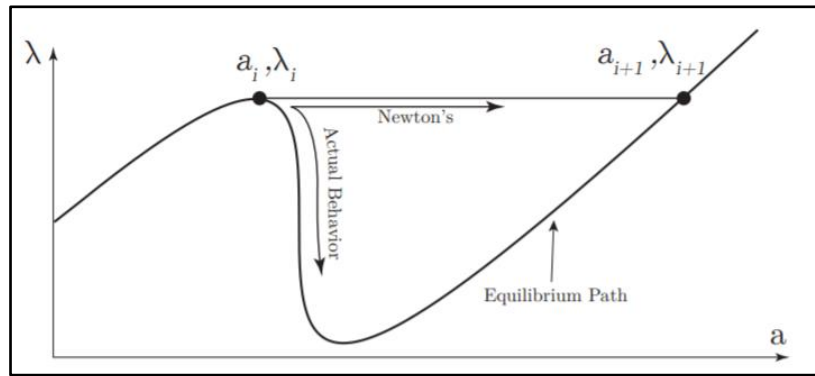
Figure 1.20. Snap-through behaviour (Vasios, 2015)

b) Displacement control method

In a traditional displacement control method, the load ratio used in the first step of an increment is chosen to induce a prescribed displacement amount following a "key" displacement component.

The load ratios for the remaining iterations are then fixed in such a way that this key displacement component will not change. Such a method tends to experience snap-back behaviours as shown in Figure 1.21.
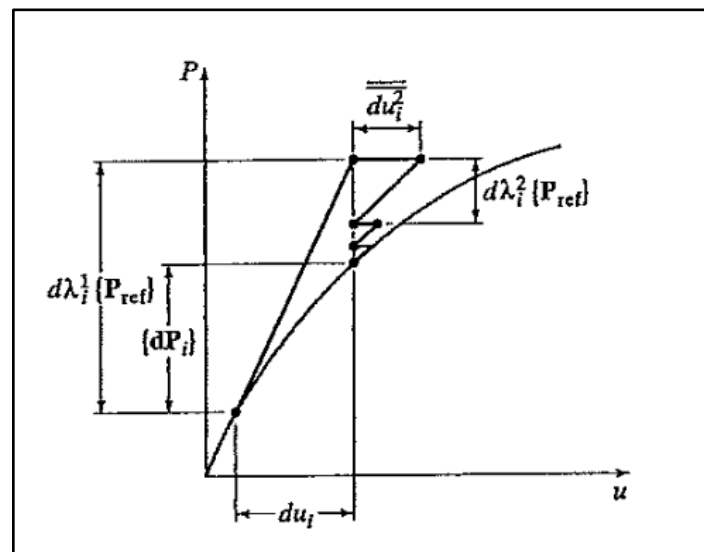
Figure 1.21. Displacement control method (McGuire et al., 1999)

c) Arc-length method

The Arc Length Method, commonly called "The modified Riks method" is a powerful numerical technique for solving systems of nonlinear equations. This method iterates neither at fixed load nor at fixed displacement, instead, it is based on defining and further constraining an arbitrary arc length in each equilibrium iteration. The method (Figure 1.22) postulates a

Imperfection tolerances during the erection of steel plate girders and geometrical nonlinearities
Master of Civil Engineering defended by SONNA DONKO Maël
NASPW Yaoundé 2019/2020
39

simultaneous variation in both the displacements and the load vector coefficient which enables to solve highly nonlinear systems of equations efficiently and accurately even when the former methods fail (Vasios, 2015).
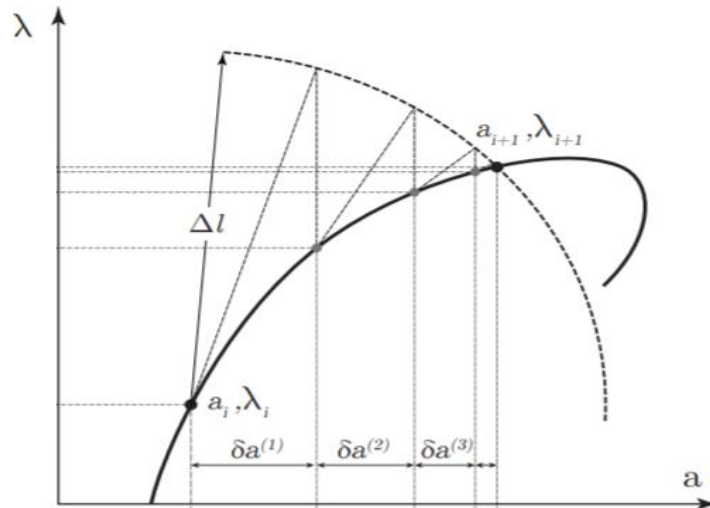
Figure 1.22. Arc-length method (McGuire et al., 1999)

In most situations, the arc length methods can solve problems that exhibit limit point behaviour, but also snap-through and snapback response as shown in Figure 1.23.

Usually, the structural response of a structure under consideration is unknown, and therefore one does not know what type of behaviour to expect. If strong nonlinearities may arise in finite deformation problems this numerical technique should be used.
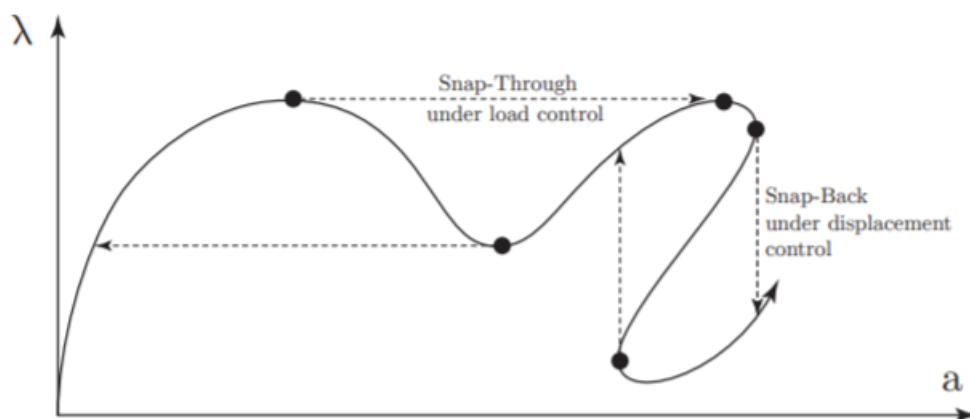
Figure 1.23. Snap-through and snap-back behaviours (Vasios, 2015)

Also, Crisfield (1981), Ramm (1981), and Powell and Simons (1981) presented other formulations of the arc-length method which could be readily implemented in any commercial finite element software. The fact that all of these other formulations are based on the basic Riks method makes the arc-length methods to be commonly known as the modified Riks method.

Imperfection tolerances during the erection of steel plate girders and geometrical nonlinearities
Master of Civil Engineering defended by SONNA DONKO Maël
NASPW Yaoundé 2019/2020
40

1.4.3.3. Automatic incrementation methods

The load, displacement or arc-length ratio chosen in each increment of the analysis can have a drastic effect on the solution. In the single-step methods, a correct selection of the ratio is the only means to control drift-off errors. In the iterative methods, a poor definition of the initial ratio could result in the solution not converging within a practical number of iterations. In both methods, an exceedingly small ratio may lead to a significant computational effort with a negligible increase in accuracy.

To assist in determining the ratio, several types of automated procedures are employed by software. In most cases, the automated procedure provides a higher ratio when it forecasts a linear behaviour of the structure and a lower otherwise.

Computer-aided engineering (CAE) and finite element (FE) software such as Abaqus, Ansys, Strand 7 and others have incorporated solvers which use these numerical solution techniques to solve the easiest to the most complex nonlinear problems. The choice of the appropriate software, solver and solution technique depends on the nonlinear problem at hand.

Conclusion

Throughout this chapter, understanding the theories and concepts that surround imperfections and tolerances in steel plate girders from a pre-critical to a nonlinear post-critical behaviour during its erection was the aim. Thus, steel, as the main component of most plate girders was discussed by giving a brief history of its evolution, its manufacturing techniques, then, explaining how important its properties, especially the mechanical ones, are for different applications and how to deal with possible defects. The structure of plate girders, their erection, the cross-section classification and its behaviour and design against stability were discussed. Also, imperfections, their tolerances and nonlinear behaviours were explained and it was seen that web-bend stability of imperfect plate girders could be analysed through analytical code provisions, GNIA or GMNIA analyses performed by adequate numerical techniques such as the automatic incrementation methods used in most FE software packages based on the Föppl-von Kármán-Marguerre differential equations.

Imperfection tolerances during the erection of steel plate girders and geometrical nonlinearities
Master of Civil Engineering defended by SONNA DONKO Maël
NASPW Yaoundé 2019/2020

41

CHAPTER 2. METHODOLOGY

Introduction

As opposed to codes' analytical formulations on linear buckling and geometrically and materially nonlinear analyses with imperfections included (GMNIA) analyses, finite element (FE) formulations after thorough verifications can accurately be used to study the effects of various influential parameters on the ultimate strength of imperfect webs of plate girders and thus study their effects on tolerances during the erection phase. This chapter aims at giving the methods used for a concise study of the most influential parameters affecting the web's imperfection tolerance limit. As such, the chapter starts by specifying the methods used in preliminary studies of the FE modelling procedures, then, provides the method used for the selection of the range of values of the influential parameters under study and the strategy adopted for the parametric study procedures are given. The chapter provides the European code formulation of critical buckling stress and ultimate strength based on the classical theory of elasticity solved by Timoshenko and Winter's effective width method respectively. Also, it gives the tolerance limits stated in the American and European codes, gives the FE modelling methodology used for both linear buckling and GMNIA analyses, provides criteria for the comparison of the analytical and FE results and then ends with the methodology used to derive an ultimate strength and a tolerance limit equation.

2.1. Preliminary studies

Preliminary studies are done to provide scientific evidence that specific methods are reliable and consistent before they can be used in routine analysis. In the course of this study, analytical and experimental comparisons were performed to assure that FE modelling procedures and their results are well-grounded before their extensive use in the parametric study. Accurate FE results were assured by first getting accurate boundary conditions and meshing for appropriate convergence of the results, then analytical and experimental comparisons were made with the FE model.

Imperfection tolerances during the erection of steel plate girders and geometrical nonlinearities
Master of Civil Engineering defended by SONNA DONKO Maël
NASPW Yaoundé 2019/2020

42

2.1.1. Method for boundary condition (BC) selection

2.1.1.1. Objective

This section aimed to determine the most suitable boundary condition to be used for further linear buckling and nonlinear post-buckling analyses.

2.1.1.2. Approach

3 different sets of boundary conditions (BCs) were chosen for this study. These BCs were chosen in such a way that they reflect the effect of the adjacent flanges and stiffeners. The plate chosen was modelled with both buckling and post-buckling analyses.

For each set of boundary conditions, 4 stress ratios were used; $\psi = -1, \frac{1}{3}, \frac{1}{2}$ and 1. A plate with geometrical properties of $a = b = 1000$ mm and $t = 4$ mm was used as depicted in Figure 2.1.
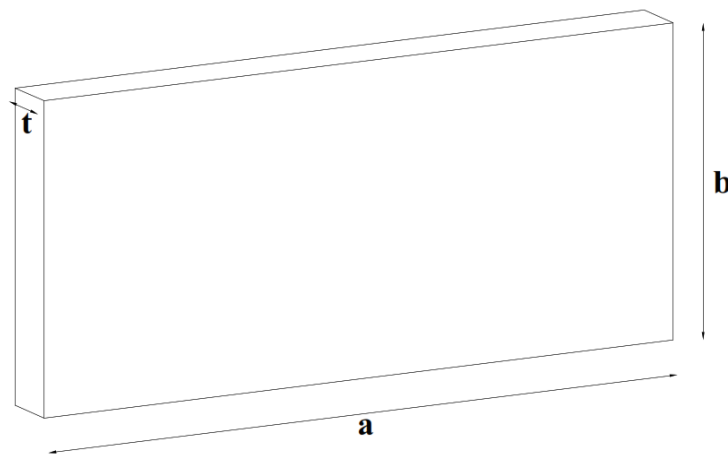
Figure 2.1. Geometry of the web of a plate girder

An elastic perfectly plastic steel behaviour was used with $E = 206\,000$ MPa, $\nu = 0.3$ and $f_y = 355$ MPa. The chosen geometry and material was taken from the domain of the upcoming parametric study.

2.1.1.3. Selection criteria

The selection of a BC depends on the coherence of the:

- FE critical stress with respect to the analytical results derived theoretically by Timoshenko and used analytically in EC3-1-5
- FE ultimate strength with respect to the analytical results derived theoretically by von Kármán and Winter then used analytically in EC3-1-5.

Imperfection tolerances during the erection of steel plate girders and geometrical nonlinearities
Master of Civil Engineering defended by SONNA DONKO Maël
NASPW Yaoundé 2019/2020

43

The analytical formulations of EC3-1-5 are given in part 2.2.2.

The BC taken as the most suitable was that whose FE results had a maximum deviation of 10% from the analytical results.

2.1.2. Mesh convergence study

2.1.2.1. Objective

A mesh convergence study is a study that is aimed at finding an optimum mesh size enabling to obtain solutions closer to a real and/or ideal model's solution. In finite element analyses, modelling with finer mesh results leads to a more accurate solution, but as the mesh is made finer, the computation time increases. As such, this section was aimed at determining the mesh density and size that will be used for subsequent analyses.

2.1.2.2. Approach

In the context of this study, buckling analyses were used to verify the mesh convergence and post-buckling analyses were used further to confirm this convergence during experimental verification studies.

For a concise mesh convergence study, buckling analyses, aimed at finding the critical stress under 3 different loading conditions ($\psi = 1, -0.5$ and 1) were done on a commercial square web of side, $a = b = 1500$mm and thickness, $t = 12$mm.

The following steps were used in the course of this mesh convergence study:

- use of the already selected boundary condition for the modelling process
- creation of a mesh using a reasonable mesh density and running of the buckling analyses to obtain the critical stress (trial T_i)
- recreation of the mesh with a denser element distribution, re-analyses, and comparison of the results to those of the previous mesh (trial T_{i+1})
- further increase in the mesh density and re-analyses of the model until the results converge satisfactorily
- graph plot of mesh density against FE critical stress obtained
- deduction from the graph of the mesh density against result convergence (AutoDesk Inc, 2017).

These stated steps were done for the 3 loading conditions characterising the domain of the upcoming parametric study.

Imperfection tolerances during the erection of steel plate girders and geometrical nonlinearities
Master of Civil Engineering defended by SONNA DONKO Maël
NASPW Yaoundé 2019/2020

44

2.1.2.3. Selection criteria

To identify the most suitable mesh density, one had to compare the graph of mesh density against results convergence for each loading condition. The mesh density at which every curve tends was set to be the most appropriate mesh density.

2.1.3. FE modelling method for comparison with analytical expression

2.1.3.1. Objective

Also termed analytical verification, this verification is used to confirm that the finite element modelling method employed is suitable to represent analytical methods with a strong theoretical basis. In the case of the present study, the critical stress result obtained from the plates FE modelling for buckling, described in part 2.2.3.2, was assessed and compared to EC3-1-5 analytical results to judge the FE model quality, reliability and consistency.

2.1.3.2. Approach

In the course of this work, the analytical verification study was approached as follows:

- choice of a suitable plate to reflect the range of values of parameters under study
- use of the already selected appropriate boundary condition and mesh density for modelling
- FE modelling of the chosen plate
- computation of buckling stress value from the eigenvalue result obtained at the end of the FE process
- comparison with the analytical result

2.1.3.3. Verification criteria

The FE modelling process for buckling in plates was considered valid when the deviation of the obtained FE critical stress from the analytically computed critical stress was less than 10%.

2.1.4. FE modelling method for comparison with experiment

2.1.4.1. Objective

Also termed experimental verification, this is aimed at confirming finite element (FE) procedures that were used in subsequent FE analyses. This was done by comparing the FE results of an FE modelled experiment with the results obtained directly from the experiment to verify the FE modelling method and result. Thus, the aim here was to model a renowned experiment using the post-buckling analysis procedures described in part 2.2.3.2. This

Imperfection tolerances during the erection of steel plate girders and geometrical nonlinearities
Master of Civil Engineering defended by SONNA DONKO Maël
NASPW Yaoundé 2019/2020
45

verification passed; the quality of the results obtained in subsequent FE analyses was guaranteed.

2.1.4.2. Approach

Here, this experimental verification was approached as follows:

- choice of a suitable experiment that reflects the range of values of parameters and also pre- and post-buckling behaviours under study
- use of the already selected appropriate boundary condition and mesh density for modelling
- FE modelling of the experiment
- computation of buckling stress value from the eigenvalue result obtained at the end of the FE buckling process
- a plot of the lateral displacement vs applied stress to capture pre- and post-buckling behaviours
- computation of ultimate strength and maximum vertical deflection
- comparison with experimental results.

2.1.4.3. Criteria

The FE modelling process was considered valid when the deviation of the:

- FEA curve of vertical displacement vs applied stress from that of the experimentally obtained curve was found less than 10%
- FE maximum vertical displacement from the experimental maximum displacement was found less than 10%
- Obtained FE ultimate load and strength values from the experimental ultimate values was less than 10%.

2.2. Parametric study

A parametric study is a study that deals with the influence of parameters on the solution of a particular problem. Many different parameters may influence the ultimate strength of the web of steel plate girders. In the course of their study, researchers (Alinia et al., 2011; Ghadami & Broujerdian, 2019; Graciano et al., 2011; Maiorana et al., 2009; Sadovský & Baláž, 1996) have focused on aspect ratio, slenderness ratio, plate loading condition or initial imperfection amplitude as they are the most influential parameters. Thus, this section starts by providing the

Imperfection tolerances during the erection of steel plate girders and geometrical nonlinearities
Master of Civil Engineering defended by SONNA DONKO Maël
NASPW Yaoundé 2019/2020

46

selection methodology of the appropriate webs for the study then the analytical and FE methods are detailed explicitly. The section ends with the criteria for results comparison and the methodology used for equation derivation.

2.2.1. Web selection

In this study, each of the above-mentioned parameters is detailed in the first part, then the strategy used for the selection of the necessary webs for the parametric study is given.

2.2.1.1. Parameters under study

a) Geometrical properties

A plate's geometry, as seen in Figure 2.2, is one of the most crucial parameters to consider when doing a parametric study on the behaviour of the web of plate girders. The geometry used in the analyses was based on current real-life bridge engineering situations. An initial web of plate girder was chosen and then geometrical parameters (aspect ratio and web slenderness ratio) varied to take into account a maximum of the real-life geometry of webs.

i) Aspect ratio

The aspect ratio, α, of a plate panel is the ratio of its length to its depth given by equation (2.1).

$$\alpha = \frac{a}{b} \qquad (2.1)$$

Plates selected for this study were those whose aspect ratios are usually encountered in bridge engineering. Also, values less than 1 were not considered to avoid column type buckling
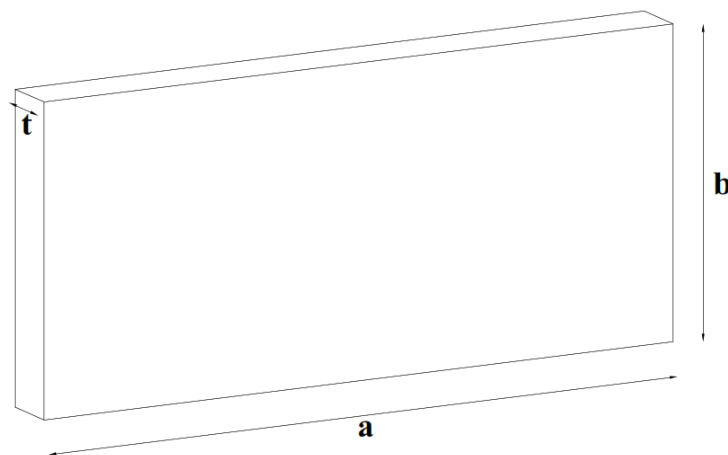
Figure 2.2. Geometry of the web of a plate girder

Imperfection tolerances during the erection of steel plate girders and geometrical nonlinearities
Master of Civil Engineering defended by SONNA DONKO Maël
NASPW Yaoundé 2019/2020
47

in the web. As such, the study focused on $\alpha \in [1,2]$. Analyses were done on a subset $\{1, 1.5, 2\}$ and the results were generalised to the initial interval.

ii) Slenderness ratio

Also, in the course of the parametric study, variation was done on the thickness of the plate by varying the slenderness ratio, where the slenderness ratio is the ratio of the plate's depth, b, to its thickness, t. It is given by $\beta = \dfrac{b}{t}$.

Here, the range of slenderness ratio values on which parametric analyses were studied is a range that considers that buckling occurs always before the most compressed part of the plate yields, $f_y \geq \sigma_{cr}$. This condition ensures that the studied plates are always prone to web buckling. A plate under this limit condition is said to be critically slender, $\beta = \beta_{cr}$. The situation is expressed using equation (2.2) as:

$$f_y \geq k_{cr} \cdot \frac{\pi^2 E}{12(1 - \nu^2)} \cdot \left(\frac{t}{b}\right)^2 \implies \beta = \frac{b}{t} \geq \sqrt{k_{cr} \cdot \frac{\pi^2}{12(1 - \nu^2)} \cdot \frac{E}{f_y}} = \beta_{cr} \quad (2.2)$$

Also, slenderness ratios considered were those bounded from above by a value that prevents flange-induced buckling, given as $\beta = 250$.

Therefore, the range of slenderness ratio values used here was $[\beta_{cr}, 250]$.

b) Loading conditions

The loading conditions selected for parametric analyses were those regularly encountered during the erection of a bridge's plate girder without forgetting the basic load condition of pure compression.

During a plate girder's erection, its loading conditions is influenced by the position of the neutral axis (N.A.) as seen in Figure 2.3. Loading conditions of pure bending are encountered by doubly symmetric plate girders as their global neutral axis coincides with the centroid of the web, thus, compressive and tensile solicitations are equally distributed along the web. In contrast, singly symmetric plate girders encounter eccentric compression (combination of pure bending and pure compression) due to the eccentricity between the neutral axis and the web's centroid, causing uneven compressive and tensile solicitations.

Imperfection tolerances during the erection of steel plate girders and geometrical nonlinearities
Master of Civil Engineering defended by SONNA DONKO Maël
NASPW Yaoundé 2019/2020
48

(a) Singly symmetric plate girder　　　　　(b) Singly symmetric plate girder
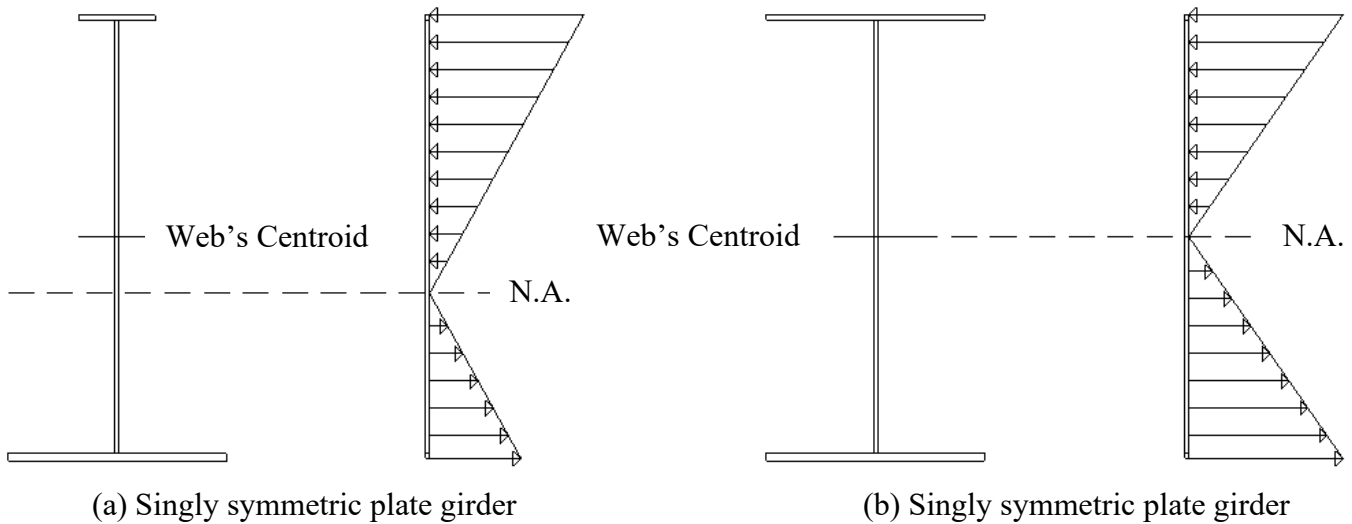
Figure 2.3. Position of the neutral axis during girder's erection

Loading conditions are easily expressed using the stress ratio factor given by equation (2.3) and schematised in Figure 2.4. Thus, real-life plate girders during erection experience stress ratio values in the range $[-1, 0[$. Also, the basic loading condition of pure compression is considered for completeness.

$$\psi = \frac{\sigma_t}{\sigma_c} \tag{2.3}$$
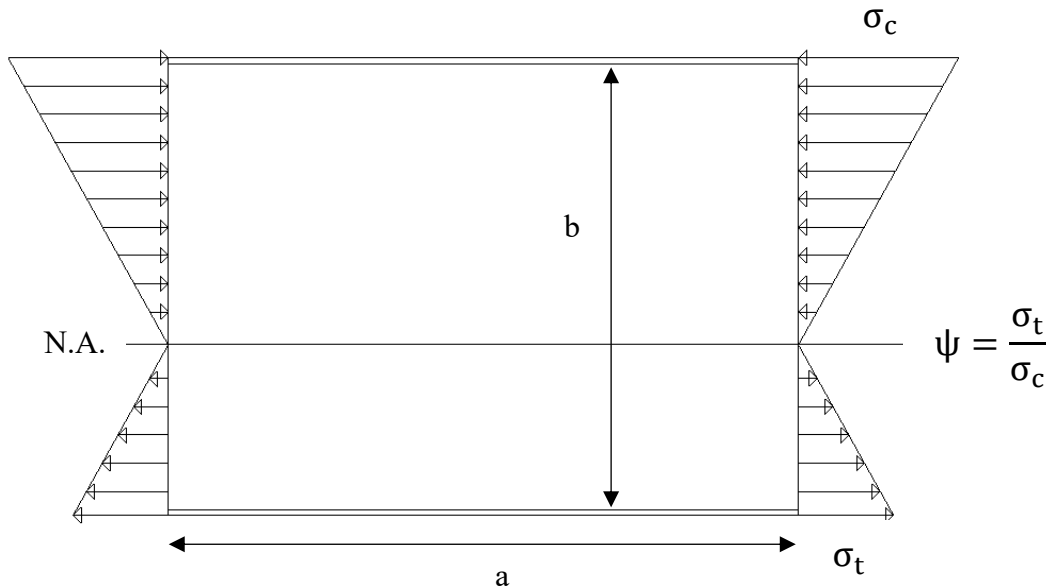
Figure 2.4. Generic loading of the web of a plate girder

Imperfection tolerances during the erection of steel plate girders and geometrical nonlinearities
Master of Civil Engineering defended by SONNA DONKO Maël
NASPW Yaoundé 2019/2020

49

Thus, 3 loading conditions were under study:

- pure compression, $\psi = 1$
- pure bending, $\psi = -1$
- a combination of pure compression and pure bending (eccentric), $\psi = -0.5$

c) Initial imperfection amplitudes

Initial imperfection amplitude is a function of the parameter called the imperfection parameter, k, implicitly defined by equation (2.4).

$$\text{Imp} = \frac{b}{k} \qquad (2.4)$$

where Imp: initial imperfection amplitude.

Thus, initial imperfection amplitude is inversely proportional to the imperfection parameter. Imperfection amplitudes are bounded from below by a small imperfection amplitude (high imperfection parameter) which cannot be captured by a measuring instrument thus simulating a perfect structure but is one that allows bifurcation type buckling. Also, the values are bounded from above by an acceptably high value (low imperfection parameter). In the course of this study, this range was taken to be $\left[\frac{b}{100\,000}, \frac{b}{10}\right]$ with $k \in [10, 100\,000]$.

2.2.1.2. Strategy adopted

To achieve an extensive parametric study on selected ranges, this study was done by first selecting the geometry of webs of plate girders to be used. This was done by:

- First choice of the web of a plate girder's geometry based on real-life encountered geometry
- Calculate its aspect ratio, then fix it
- For the fixed aspect ratio, vary the slenderness ratio within the given range to get the specific length, depth and thickness.
- Choose another aspect ratio within the range and vary the slenderness ratio as mentioned in the previous point
- Repeat the previous step for all the possible values of the aspect ratio.

After the web geometries have been varied and appropriate ones chosen, selected imperfection amplitudes were applied to simulate real-life webs. Then, the 3 loading conditions (stress ratios) under study were applied and the ultimate strength monitored.

Imperfection tolerances during the erection of steel plate girders and geometrical nonlinearities
Master of Civil Engineering defended by SONNA DONKO Maël
NASPW Yaoundé 2019/2020

50

2.2.2. Analytical methods

A structural element is built to provide minimum requirements of safety, serviceability and durability, as such analytical code provisions are used as practical guidance by those who design the structural elements to confirm that the minimum requirements are respected. Thus, plate girders and more specifically their webs are subjected to specific code requirements and therefore, any in-depth study must be compared to the well-established analytical code provisions. This section provides code provision requirements of a web plate during buckling and post-buckling, then specifies codes' tolerance limits on the web of plate girders.

2.2.2.1. Buckling stress

The nominal local buckling resistance of the web plate of Figure 2.5 was quantified by the classical elastic critical stress formula previously derived in part 1.2.3.3 and given in equation (2.5).

$$\sigma_{cr} = k_{cr} \cdot \frac{\pi^2 E}{12(1 - v^2)} \cdot \left(\frac{t}{b}\right)^2 \qquad (2.5)$$

where:

σ_{cr}: Critical (buckling) stress of a plate

E: Young's modulus of the plate's material

v: Poisson's ratio

t: Web plate's thickness

b: Web plate's depth

k_{cr}: Buckling factor or buckling coefficient

Imperfection tolerances during the erection of steel plate girders and geometrical nonlinearities
Master of Civil Engineering defended by SONNA DONKO Maël
NASPW Yaoundé 2019/2020

51
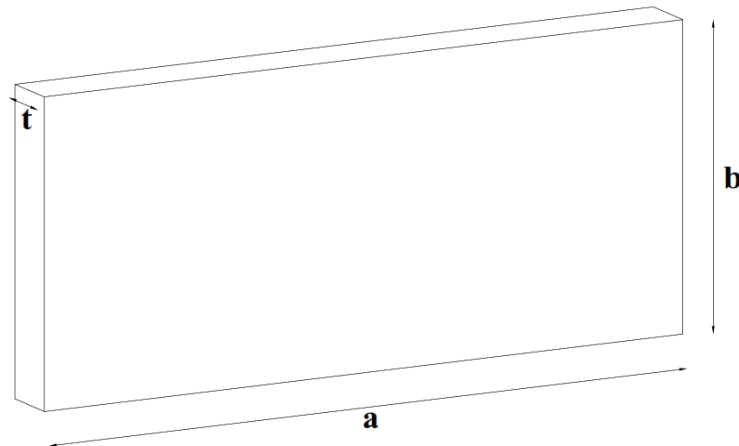
Figure 2.5. Geometry of the web of a plate girder

Tables 4.1 and 4.2 of Eurocode's EN 1993-1-5 gives various values of the buckling factor, k_σ, of a simply supported plate, depending on the stress distribution over the cross-section (EN 1993-1-5:2006 (E), 2011).

Equation (2.6) summarises Eurocode's provision for internal compression parts.

$$k_{cr} = \begin{cases} 4\,, & \psi = 1 \\ \dfrac{8.2}{1.05 + \psi}\,, & 0 < \psi < 1 \\ 7.81\,, & \psi = 0 \\ 7.81 - 6.29\psi + 9.78\psi^2\,, & -1 < \psi < 0 \\ 23.9, & \psi = -1 \\ 5.98(1 - \psi)^2\,, & -3 \le \psi < -1 \end{cases} \qquad (2.6)$$

$\psi = \dfrac{\sigma_2}{\sigma_1}$ is the stress ratio, in which:

σ_1: larger compressive stress

σ_2: smaller stress (compressive or tensile) as shown in Figure 2.6.

2.2.2.2.   Post-buckling (Ultimate) strength

As only direct stresses were dealt with in this study, Eurocode's effective width method was chosen for subsequent analyses. The ultimate strengths of plates subjected to direct stresses were calculated by: finding the plate buckling reduction factor, ρ; calculating the effective section characteristics $b_{eff}, y_{eff,sup}, A_{eff}$ and I_{eff}; determining its ultimate strength, f_u.

Imperfection tolerances during the erection of steel plate girders and geometrical nonlinearities
Master of Civil Engineering defended by SONNA DONKO Maël
NASPW Yaoundé 2019/2020

52

a) Plate buckling reduction factor

Eurocode adopted Winter's expression for the reduction factor of plate buckling as found in Section 4.4 (2) of EN 1993-1-5. The expression for internal compression elements is given by equation (2.7).

$$\rho = \begin{cases} 1, & \bar{\lambda}_p \leq 0.5 + \sqrt{0.085 - 0.055\psi} \\ \dfrac{\bar{\lambda}_p - 0.055(3 + \psi)}{\bar{\lambda}_p^{\,2}} \leq 1.0, & \bar{\lambda}_p > 0.5 + \sqrt{0.085 - 0.055\psi} \end{cases} \qquad (2.7)$$

$$\text{where } \bar{\lambda}_p = \sqrt{\frac{f_y}{\sigma_{cr}}}$$

b) Effective section characteristics

Tables 4.1 and 4.2 of EN 1993-1-5 provide effective width values (b_{eff}, b_{e1} and b_{e2}) of class 4 cross-sections, depending on the stress distribution over it.

Given that class 3 cross-sections can fully attain the yield stress, its effective width equals its normal width (no reduction in cross-section). Table 2.1 shows Eurocode's provision for internal compression elements ($\bar{b} = b$).

Table 2.1. Effective width provision for internal compression elements (EN 1993-1-5:2006 (E), 2011)

Stress distribution (compression positive)	Effective[p] width b_{eff}
	$\psi = 1$: $b_{eff} = \rho\,\bar{b}$ $b_{e1} = 0{,}5\,b_{eff}$ $b_{e2} = 0{,}5\,b_{eff}$
	$1 > \psi \geq 0$: $b_{eff} = \rho\,\bar{b}$ $b_{e1} = \dfrac{2}{5-\psi}\,b_{eff}$ $b_{e2} = b_{eff} - b_{e1}$
	$\psi < 0$: $b_{eff} = \rho\,b_c = \rho\,\bar{b}/(1-\psi)$ $b_{e1} = 0{,}4\,b_{eff}$ $b_{e2} = 0{,}6\,b_{eff}$

$\psi = \sigma_2/\sigma_1$	1	$1 > \psi > 0$	0	$0 > \psi > -1$	-1	[AC1]$-1 > \psi \geq -3$[AC1]
Buckling factor k_σ	4,0	$8{,}2/(1{,}05+\psi)$	7,81	$7{,}81 - 6{,}29\psi + 9{,}78\psi^2$	23,9	$5{,}98(1-\psi)^2$

Imperfection tolerances during the erection of steel plate girders and geometrical nonlinearities
Master of Civil Engineering defended by SONNA DONKO Maël
NASPW Yaoundé 2019/2020

53

Also, the other section characteristics are given by equations (2.8) to (2.12).

$$y_{eff,sup} = \begin{cases} \left(\dfrac{b}{b_{eff}} - 1\right) \cdot \left(\dfrac{b_{e2} - b_{e1}}{2}\right) + \dfrac{b}{2}, & \text{for} \quad 0 \leq \psi \leq 1 \\[3mm] \left(\dfrac{b}{1-\psi} - b_{eff}\right) \cdot \left(\dfrac{(b_{e2} - b_{e1})(1-\psi) - b\psi}{2(b_{eff}(1-\psi) - b\psi)}\right) + \dfrac{b}{2}, & \text{for} \quad -1 \leq \psi \leq 0 \end{cases} \qquad (2.8)$$

$$A_{eff} = \begin{cases} b_{eff} \cdot t, & \text{for} \quad 0 \leq \psi \leq 1 \\[3mm] \dfrac{b_{eff}(1-\psi) - b\psi}{1-\psi} \cdot t, & \text{for} \quad -1 \leq \psi \leq 0 \end{cases} \qquad (2.9)$$

$$I_{eff} = \begin{cases} I + A y_{eff,G}{}^2 - \left[t(b - b_{eff})(y_{eff,G} + y_{\Delta A})^2 + \dfrac{t(b - b_{eff})^3}{12} \right] & \text{for} \quad 0 \leq \psi \leq 1 \\[3mm] I + A y_{eff,G}{}^2 - \left[t\left(\dfrac{b}{1-\psi} - b_{eff}\right)(y_{eff,G} + y_{\Delta A})^2 + \dfrac{t\left(\dfrac{b}{1-\psi} - b_{eff}\right)^3}{12} \right] & \text{for} -1 \leq \psi \leq 0 \end{cases} \qquad (2.10)$$

where:

$$y_{eff,G} = \begin{cases} \left(\dfrac{b}{b_{eff}} - 1\right) \cdot \left(\dfrac{b_{e2} - b_{e1}}{2}\right), & \text{for} \quad 0 \leq \psi \leq 1 \\[3mm] \left(\dfrac{b}{1-\psi} - b_{eff}\right) \cdot \left(\dfrac{(b_{e2} - b_{e1})(1-\psi) - b\psi}{2(b_{eff}(1-\psi) - b\psi)}\right), & \text{for} \quad -1 \leq \psi \leq 0 \end{cases} \qquad (2.11)$$

and

$$y_{\Delta A} = \begin{cases} \dfrac{b_{e2} - b_{e1}}{2}, & \text{for} \quad 0 \leq \psi \leq 1 \\[3mm] \dfrac{(b_{e2} - b_{e1})(1-\psi) - b\psi}{2(1-\psi)}, & \text{for} \quad -1 \leq \psi \leq 0 \end{cases} \qquad (2.12)$$

c) Ultimate strength

The ultimate strength of plates was gotten by calculating the stress (maximum compressive) in the normal (real) cross-section for which the reduced cross-section is at the onset of yielding in the most compressed fibre. Thus, this yields:

$$\begin{cases} f_u = \dfrac{N}{A} + \dfrac{N \cdot e}{I} y_{sup} \\[3mm] f_y = \dfrac{N}{A_{eff}} + \dfrac{N \cdot e}{I_{eff}} y_{eff,sup} \end{cases} \implies \dfrac{f_u}{f_y} = \dfrac{A_{eff}}{A} \cdot \dfrac{I_{eff}}{I} \cdot \dfrac{I + A \cdot e \cdot y_{sup}}{I_{eff} + A_{eff} \cdot e \cdot y_{eff,sup}} \qquad (2.13)$$

Imperfection tolerances during the erection of steel plate girders and geometrical nonlinearities
Master of Civil Engineering defended by SONNA DONKO Maël
NASPW Yaoundé 2019/2020

54

where y_{sup}, A, I are the properties of the real section and $e = \frac{1-\psi}{1+\psi} \cdot \frac{b}{6}$
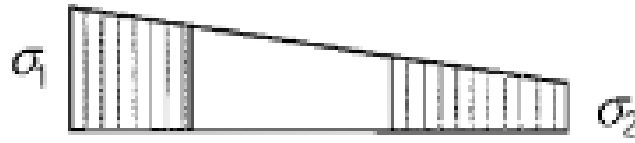
Figure 2.6. Generic stress distribution across the depth of the web
(EN 1993-1-5:2006 (E), 2011)

2.2.2.3.   Imperfection tolerance limits

In the course of this study, only out-of-plane imperfections encountered during the fabrication of welded plate girders were dealt with. Only these imperfections were used because researchers have found that the most susceptible buckling modes of plate girders are associated with out-of-plane manufacturing imperfections. As stated in part 1.3.5 of this thesis, three types of out-of-plane imperfection tolerances exist: essential, functional and special tolerances. In the course of this study, only the essential tolerances will be dealt with, as they are responsible for the mechanical resistance and stability of the structure.

a) American specification (AWS D1.1/D1.1M)

The American specification guiding the fabrication of steel welded structures in Table D.2 of AWS D1.1/D1.1M:2010 provides that steel girders with no intermediate stiffeners and depth of web, D, have a maximum allowable variation from the flatness of webs given by $D/150$.

Variation from the flatness of webs (out-of-plane imperfections) is determined by measuring the offset from the actual web centreline to a straight edge whose length is greater than the least panel dimension and placed on a plane parallel to the nominal web plane. Measurements are taken prior to erection (AWS D1.1/D1.1M:2010, 2010).

b) Eurocode specification (EN 1090-2)

Eurocode provides manufacturing tolerance limits for webs of welded plated structural elements, like the one under study, in Table B.1 of EN 1090-2. The specific essential tolerance considered in this study is expressed as shown in equation (2.14).

Imperfection tolerances during the erection of steel plate girders and geometrical nonlinearities
Master of Civil Engineering defended by SONNA DONKO Maël
NASPW Yaoundé 2019/2020

55

$$\text{Imp}_{\text{EN }1090-2} = \begin{cases} \dfrac{b}{200}, & \text{when } \beta \leq 80 \\ \dfrac{b^2}{16000t}, & \text{when } 80 \leq \beta \leq 200 \quad \text{but } \geq t \\ \dfrac{b}{80}, & \text{when } \beta \geq 200 \end{cases} \qquad (2.14)$$

where Imp stands for imperfection and β is the slenderness ratio.

2.2.3. FE methods (FEM)

The Finite Element (FE) software, Abaqus/CAE, was chosen to solve both linear and nonlinear problems that govern buckling and post-buckling in the web of plate girders subjected to various in-plane loading conditions. Also, the effects of local geometrical imperfections and material nonlinearity were included in this study. The following sections describe the FE software, Abaqus/CAE, used to conduct parametric studies then presents the modelling procedures and analyses performed.

2.2.3.1. FE software package

Abaqus/CAE used in the course of this study is a finite element analysis software developed by Abaqus Inc. and owned by Dassault Systèmes Simulia Corp., a subsidiary of Dassault Systèmes. Abaqus/CAE is a Complete Abaqus Environment that provides a simple, consistent interface for FE modelling, monitoring, and evaluation of results from Abaqus/Standard and Abaqus/Explicit simulations (ABAQUS, 2014). It is divided into modules, where each module defines a logical aspect of the modelling process. Movement from one module to another module is used to build the model from which Abaqus/CAE generates an input file is submitted to the Abaqus/Standard or Abaqus/Explicit analysis product depending on the type of analysis to be done. The analysis product performs the analysis, sends information to Abaqus/CAE to allow monitoring the progress of the job, and generates an output database. Finally, Abaqus/Viewer, incorporated as the Visualization module of Abaqus/CAE is used to read the output database and view the results of your analysis.

2.2.3.2. FE modelling methodology and analyses

a) FE modelling methodology

For the study on the web of plate girders, the web was modelled as a deformable shell-type part with elastic perfectly plastic steel properties. These properties are considered

Imperfection tolerances during the erection of steel plate girders and geometrical nonlinearities
Master of Civil Engineering defended by SONNA DONKO Maël
NASPW Yaoundé 2019/2020

56

necessary and sufficient for subsequent analyses, so no additional property modelling was required.

The appropriate geometric characteristics are given after the selection of the webs. The loads were applied at the vertical edges as normal traction-type. The boundary conditions used at the shell's edges were those chosen after the preliminary studies. An S4R FE was used, this is a three-dimensional, doubly-curved, four-node shell element with six degrees of freedom per node that uses bilinear interpolation with reduced integration. The S4R FE was used to mesh the web to the mesh density and size found after the preliminary studies. The FE model well prepared, the type of analysis to be performed was selected and the whole model sent to Abaqus/Standard for analysis. Specifications like the scratch directory, sub-routine file and parallelisation were configured to speed up the analysis procedure. Abaqus/CAE gives the possibility to monitor the analysis and hence, be aware of potential warnings and errors that might be present.

b) Analyses performed

i) Buckling analyses

The aim of buckling analyses in this study was to obtain the eigenvalues and eigenmodes, of a perfectly flat web, that will further be used to model an inherent imperfect web for post-buckling analyses. Also, the buckling (critical) stress was computed from the eigenvalues.

To perform buckling analysis in Abaqus/CAE, a step that permits Abaqus/Standard to solve the system of equations given in part 1.2.4.2 was added to the modelling methodology given in a) and thus eigenvalues and eigenmodes were obtained.

The step to be added is given in Abaqus/Standard as a buckle, linear perturbation type. Geometrical nonlinearity is not considered as the aim was to obtain the results of a perfect web. Input parameters to this step are the number of eigenvalues required and the number of iterations to be performed by the solver as shown in Figure 2.7.

Imperfection tolerances during the erection of steel plate girders and geometrical nonlinearities
Master of Civil Engineering defended by SONNA DONKO Maël
NASPW Yaoundé 2019/2020

57
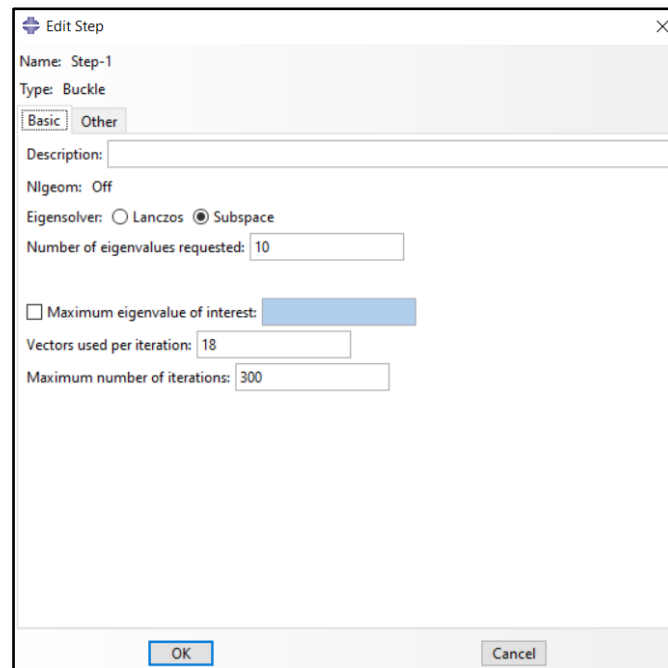
Figure 2.7. Step editing dialogue box

At the end of this analysis, the eigenvalues and eigenmodes obtained were stored to be used in the subsequent analysis. Also, the buckling (critical) stress was calculated by dividing the fundamental eigenvalue, λ_1, obtained by the web's thickness as given in equation (2.15). This was done through a Microsoft Excel spreadsheet.

$$\sigma_{cr,FE} = \frac{\lambda_1}{t} \tag{2.15}$$

ii) GMNIA analyses

In the course of this study, GMNIA analyses were used to capture both the pre- and post-buckling responses of an imperfect web under a given loading condition and most importantly, to get the ultimate strength of the web.

As imperfections were included in this analysis, the perfect web drawn in the model was modified to include imperfections by calling the eigenmode obtained in the previous buckling analysis and setting an imperfection amplitude. This was done by:

- Saving the deformed shape (eigenmode) obtained at the end of the buckling analysis in an output file. This was done by adding the keywords highlighted in Figure 2.8 (a), to the model used for buckling analysis

Imperfection tolerances during the erection of steel plate girders and geometrical nonlinearities
Master of Civil Engineering defended by SONNA DONKO Maël
NASPW Yaoundé 2019/2020

58

- Calling the saved deformed shape from buckling to the new model created for post-buckling purposes, then defining the amplitude which models best the imperfect web. This was done by adding keywords to the new model used for post-buckling as shown in Figure 2.8 (b)
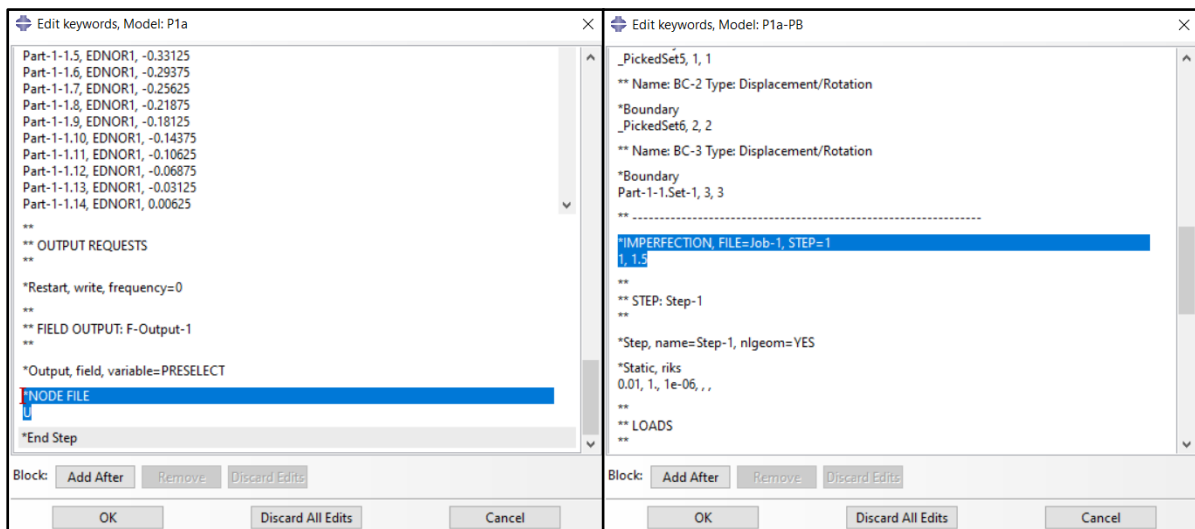
(a) Keyword for saving a deformed shape

(b) Keyword for inputting an amplitude to a deformed shape

Figure 2.8. Keyword definition dialogue boxes

At this stage, an imperfect web was ready for analysis. Abaqus/Standard dealt with this by finding, through a Static Riks step, the static equilibrium solutions of the system of nonlinear equations given part 1.2.4.3 which includes both geometric and material nonlinearities.

The Static Riks step was added by proceeding as follows:

- Create a Static Riks step in the step module
- Activate geometrical nonlinearity and define the analysis stopping criteria
- Set automatic incrementation, a numerical technique explained in part 1.4.3.3
- Define the initial, minimum and maximum arclength increments as well as the estimated total arc-length. This will be used by the solver to compute the initial Load Proportionality Factor (LPF) to be used in the analysis. Figure 2.9 shows an example of how the parameters can be defined.

Imperfection tolerances during the erection of steel plate girders and geometrical nonlinearities
Master of Civil Engineering defended by SONNA DONKO Maël
NASPW Yaoundé 2019/2020

59
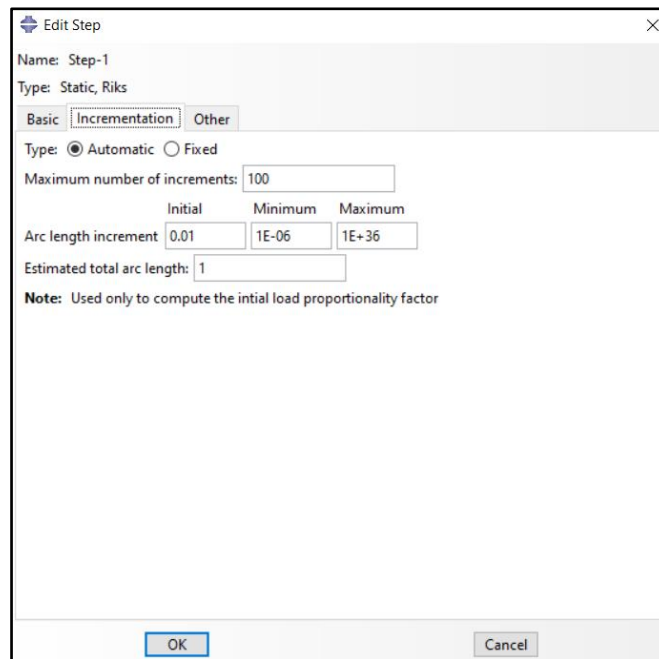
Figure 2.9. Step editing dialogue box

At the end of the analysis, the pre- and post-buckling 3D behaviours can be visualised through Abaqus/Viewer incorporated module.

Also, the ultimate strength was gotten by multiplying the obtained buckling stress by the maximum LPF captured before a possible softening behaviour. This was done through a Microsoft Excel spreadsheet.

2.2.4. Criteria for analytical and FE methods comparison

The FE and analytical methods were compared based on the criteria of the critical stress results for linear buckling analyses and that of ultimate strength results for nonlinear GMNIA analyses. This was done by computing the deviation, Δ, of the analytical method from the FE method (a method that simulates the actual behaviour) using equation (2.16).

$$\Delta = \frac{|\text{Analytical} - \text{Finite Element}|}{\text{Finite Element}} * 100 \qquad (2.16)$$

The deviation obtained helped to conclude whether both methods could be considered equivalent ($\Delta \leq 10\%$) or different ($\Delta > 10\%$).

Also, for a clearer comparison, the graphs of slenderness ratio against the ratio of analytical to FE results are plotted. A horizontal line at unity was drawn to separate the cases for which the analytical results are greater and that where the FE results dominated.

Imperfection tolerances during the erection of steel plate girders and geometrical nonlinearities
Master of Civil Engineering defended by SONNA DONKO Maël
NASPW Yaoundé 2019/2020

60

2.2.5. Regression analysis

Regression analysis is a set of statistical processes used to estimate the relationships that exist between a dependent variable and one or more independent variables.

In the course of this work, the effects of each parameter under study were first investigated by plotting graphs of the FE ultimate strength and FE tolerance limits against the necessary parameters. After obtaining the trends from the graphs, regression hypotheses were stated by formulating the relationship that existed between the dependent and independent variables. The independent variables that did not affect the dependent variable were considered as constants, then the rest of the independent variables were analysed through a multiple nonlinear regression technique provided by software Curve Expert Professional (Hyams, 2018).

The analysis done provided a wide number of nonlinear equations. The equation selected was that whose graph visually provided a consistent relationship between the independent and dependent variables. The constant terms in the selected equation were chosen such that the corresponding correlation coefficients of determination (R^2 and R) had values greater than 90%. After obtaining the constant terms, a manual refinement of these constants was done to reduce the errors between the FE results and the results obtained from the equation. This, keeping in mind the 95% confidence interval obtained. For the refined equation obtained, a verification test was done within the range of values of the specified independent variables to check whether the derived equation was valid. The equation was confirmed as valid only when the obtained results had a maximum deviation of 10% from the FE results.

Conclusion

A successful parametric study passes through the correct implementation of the necessary verification procedures described in the chapter. This chapter aimed at given detailed step by step procedures used throughout the thesis work. As such, it started with the aim, the steps used in the approach of each preliminary study and the criteria for verification. Then followed an elaborate procedure for the choice of a range of values of influential parameters and the strategy adopted. A good description of codes' analytical provisions on buckling stress, ultimate strength and imperfection tolerance limits was also given. The presentation of the FE software package Abaqus/CAE used throughout this work followed by a detailed procedure of the use of Abaqus/CAE in FE modelling was presented. This chapter ended with the criteria for analytical and FE methods comparison and a detailed procedure used for regression analysis.

Imperfection tolerances during the erection of steel plate girders and geometrical nonlinearities
Master of Civil Engineering defended by SONNA DONKO Maël
NASPW Yaoundé 2019/2020

61

CHAPTER 3. PRELIMINARY RESULTS AND INTERPRETATION

Introduction

Appropriate FE parametric results are strongly dependent on verified FE procedures. An analogy can be done with laboratory tests where before any experiment is done, the laboratory equipment must be well-calibrated and certified. Similarly, before any FE parametric analysis is performed using the Abaqus/CAE "laboratory", boundary conditions (BCs) and mesh density must be well-calibrated, then linear buckling and GMNIA modelling procedures must be certified through analytical and experimental basis. Thus, this chapter is aimed at verifying the necessary and crucial tools used for further parametric study. It begins with analyses performed to calibrate and present the BCs and mesh density used for modelling webs of plate girders. Then comes an analytical process to confirm the FE linear buckling modelling procedure used for critical stress determination. The last part of this chapter is dedicated to a whole experimental process aimed at confirming GMNIA modelling procedures through the FE modelling of a renowned experiment.

3.1. Presentation of boundary conditions (BC)

The main study consists of a local analysis of the behaviour of the web of a plate girder. As such, part of the web was extracted from the plate girder. Thus, for the analysis to be consistent with the web's behaviour under a global analysis of the whole plate, appropriate boundary conditions were chosen to model the behaviour of the adjacent flanges and stiffeners in the local model. To do so, a study of different BCs was done to determine the most appropriate one. This was done through a presentation of sets of BCs under study, presentation of analytical and FE results and then a result comparison for decision making.

3.1.1. Sets of BC

The sets of BCs chosen for the study were such that they simulate the real behaviour of the global plate. Therefore, the effect of the flanges was simulated by using horizontal and out-of-plane restraints, the effects of both stiffeners and adjacent webs were simulated using vertical and out-of-plane restraints. Also, having in mind that the rotational stiffness provided by the webs and stiffeners are negligible, no restraint was used to simulate it. In addition to the common set of restraints, each set had its particularity as seen in Table 3.1.

Imperfection tolerances during the erection of steel plate girders and geometrical nonlinearities
Master of Civil Engineering defended by SONNA DONKO Maël
NASPW Yaoundé 2019/2020
62

Table 3.1. Presentation of sets of BC

Set	Static Scheme	Description of the set
Common to all sets		Out-of-plane restraints in all the nodes of the 4 sides
Set 1		Restraints on both horizontal and vertical displacements in the 4 middle nodes of the plate's sides
Set 2		Horizontal restraints in the 2 middle nodes of the horizontal sides and vertical restraints on all the nodes of the vertical sides
Set 3		Horizontal restraints in the 2 middle nodes of the horizontal sides and vertical restraints in the 2 middle nodes of the vertical sides
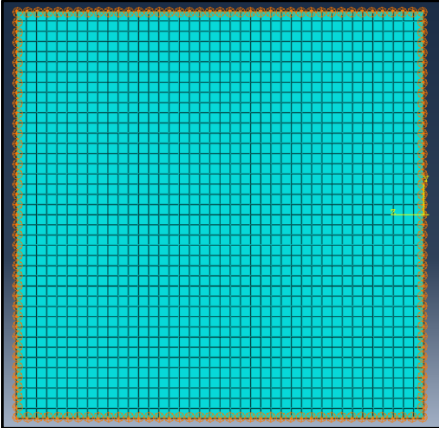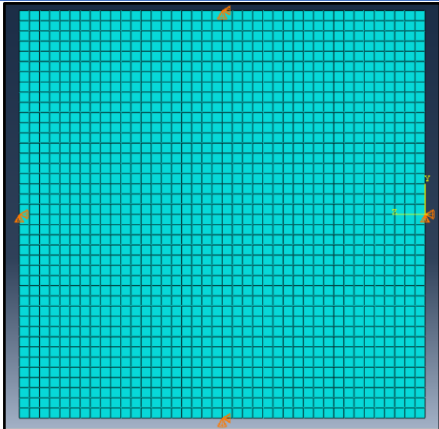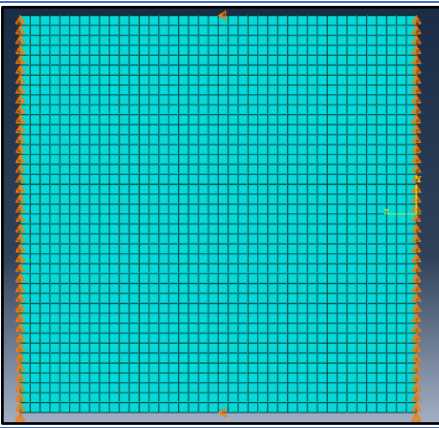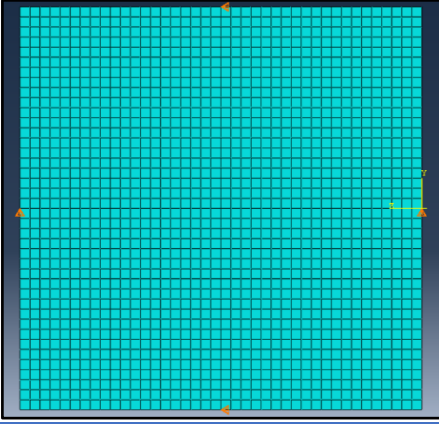
Imperfection tolerances during the erection of steel plate girders and geometrical nonlinearities
Master of Civil Engineering defended by SONNA DONKO Maël
NASPW Yaoundé 2019/2020

63

3.1.2. Analytical results

3.1.2.1. Critical stress

The analytical critical stress formula is given by equation (3.2) and results by equations (3.1) and (3.3).

$$\sigma_{cr,Ana} = k \cdot \frac{\pi^2 E}{12(1 - v^2)} \cdot \left(\frac{t}{b}\right)^2 \tag{3.3}$$

k: buckling factor which depends on the aspect ratio, stress ratio and boundary condition

$$k = \begin{cases} 4.00\,, & \psi = 1 \\ 5.29\,, & \psi = \frac{1}{2} \\ 5.80\,, & \psi = \frac{1}{3} \\ 25.60\,, & \psi = -1 \end{cases} \text{ from EC3-1-5} \tag{3.2}$$

$$\Rightarrow \sigma_{cr,Ana} = \begin{cases} 11.92\,, & \psi = 1 \\ 15.76\,, & \psi = \frac{1}{2} \\ 17.67\,, & \psi = \frac{1}{3} \\ 71.20\,, & \psi = -1 \end{cases} \tag{3.1}$$

3.1.2.2. Ultimate strength

The ultimate strength formulation provided by Winter, used in EC3-1-5 and detailed in part 2.2.2.2 gives $\sigma_{ult} = 62.40$ MPa.

3.1.3. FE results

3.1.3.1. Critical stress

a) Set 1

Table 3.2 summarises the FE and analytical critical stress results obtained. Its deviation was also calculated to determine its suitability.

The results obtained show that the deviations of the FE results are always greater than 10% that of the analytical formulation, with a minimum deviation of 12.23%. As such, BC set 1 will not suitably comply with the analytical formulation of critical stress. Thus, it is not a good model for the web under study.

Imperfection tolerances during the erection of steel plate girders and geometrical nonlinearities
Master of Civil Engineering defended by SONNA DONKO Maël
NASPW Yaoundé 2019/2020
64

Table 3.2. FE and analytical critical stress results for Set 1
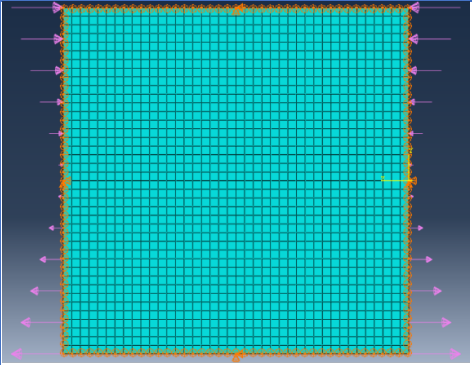
Stress Ratio	Static Scheme and Loads	λ_1 (N/mm)	$\sigma_{cr.\ FE}$ (MPa)	$\sigma_{cr.\ Ana}$ (MPa)	$\Delta\sigma_{cr}\%$
$\psi = -1$		319.62	79.91	71.20	12.23
$\psi = 1/3$		81.22	20.30	17.67	14.91
$\psi = 1/2$		72.44	18.11	15.76	14.91
$\psi = 1$		54.48	13.62	11.92	14.26
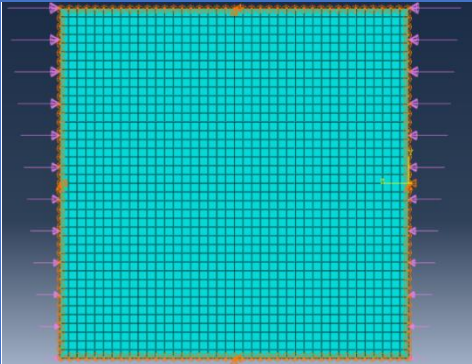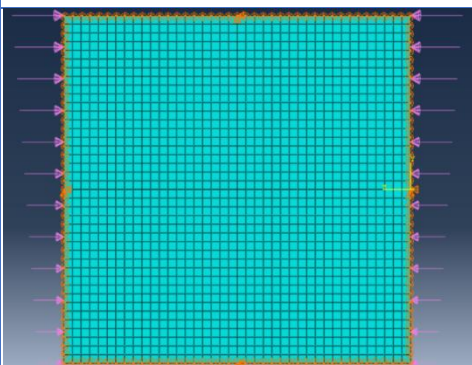
Imperfection tolerances during the erection of steel plate girders and geometrical nonlinearities
Master of Civil Engineering defended by SONNA DONKO Maël
NASPW Yaoundé 2019/2020

65
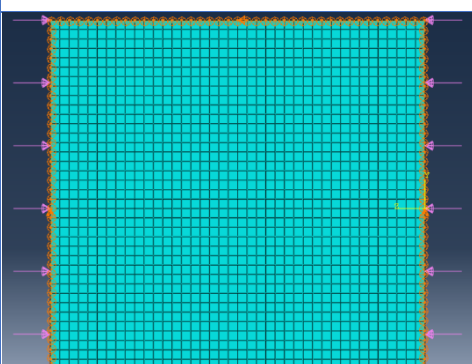
b) Set 2

Table 3.3 summarises the FE and analytical critical stress results obtained. Deviations are also calculated to determine their suitability.

The results obtained show that the deviations of the FE results are always less than 5% that of the analytical formulation, with a maximum deviation of 4.88%. As such, BC set 2 complies well with the analytical formulation of critical stress. Thus, it is a good model to study the web up to its critical state.

Imperfection tolerances during the erection of steel plate girders and geometrical nonlinearities
Master of Civil Engineering defended by SONNA DONKO Maël
NASPW Yaoundé 2019/2020

66

Table 3.3. FE and analytical critical stress results for Set 2
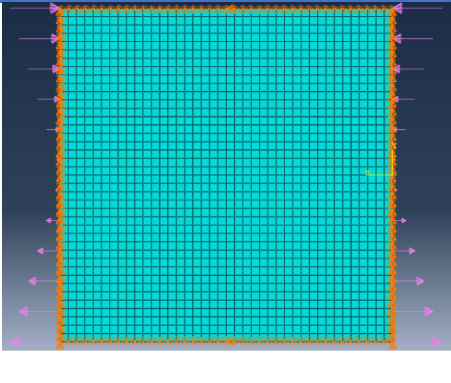
Stress Ratio	Static Scheme and Loads	λ_1 (N/mm)	$\sigma_{cr.\ FE}$ (MPa)	$\sigma_{cr.\ Ana}$ (MPa)	$\Delta\sigma_{cr}\%$
$\psi = -1$		295.13	73.78	71.20	3.63
$\psi = 1/3$		67.64	16.91	17.67	4.31
$\psi = 1/2$		60.31	15.08	15.76	4.33
$\psi = 1$		45.35	11.34	11.92	4.88
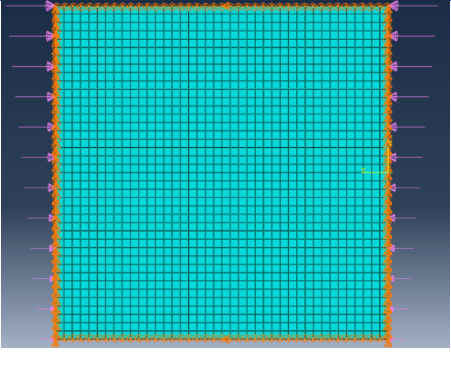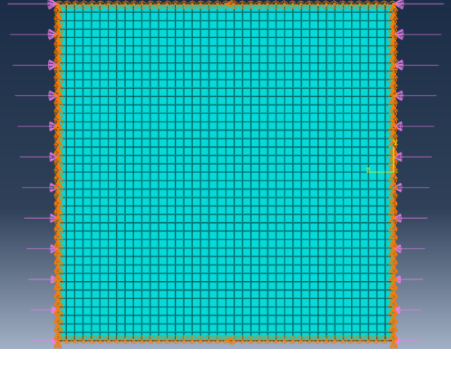
Imperfection tolerances during the erection of steel plate girders and geometrical nonlinearities
Master of Civil Engineering defended by SONNA DONKO Maël
NASPW Yaoundé 2019/2020

67
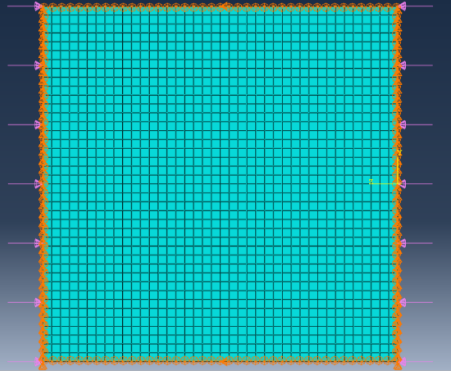
c) Set 3

Table 3.4 summarises the FE and analytical critical stress results obtained. Deviations are also calculated to determine their suitability.

The results obtained show that the deviations of the FE results are always less than 10% that of the analytical formulation, with a maximum deviation of 7.11%. As such, BC set 3 suitably complies with the analytical formulation of critical stress. Thus, it is a good model to study the web up to its critical state.

Imperfection tolerances during the erection of steel plate girders and geometrical nonlinearities
Master of Civil Engineering defended by SONNA DONKO Maël
NASPW Yaoundé 2019/2020

68

Table 3.4. FE and analytical critical stress results for Set 3
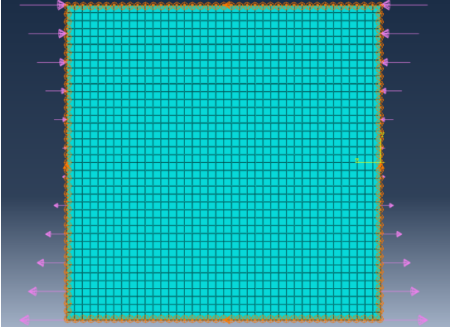
Stress Ratio	Static Scheme and Loads	λ_1 (N/mm)	$\sigma_{cr.\ FE}$ (MPa)	$\sigma_{cr.\ Ana}$ (MPa)	$\Delta\sigma_{cr}\%$
$\psi = -1$		305.05	76.26	71.20	7.11
$\psi = 1/3$		71.05	17.76	17.67	0.52
$\psi = 1/2$		63.37	15.84	15.76	0.52
$\psi = 1$		47.65	11.91	11.92	0.05
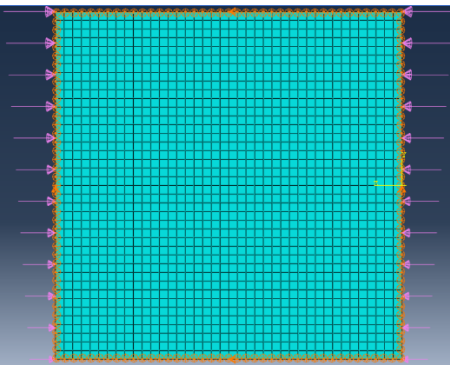
Imperfection tolerances during the erection of steel plate girders and geometrical nonlinearities
Master of Civil Engineering defended by SONNA DONKO Maël
NASPW Yaoundé 2019/2020

69
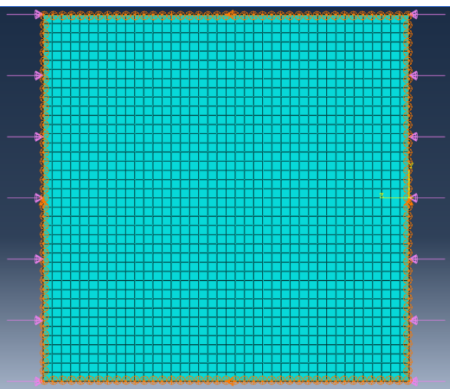
3.1.3.2. Ultimate strength

After determining the suitability of every set of BC at the critical state, it was also necessary to find its suitability at post-buckling, and necessarily at its ultimate state. Here, after a GMNIA analysis on the selected modelled web, through Abaqus/CAE Static Riks step, the ultimate strength of the web was calculated by multiplying the maximum load proportionality factor (LPF) by the appropriate critical stress. This was done for each set and the results presented in Table 3.5. Also, the stress distribution at the ultimate state, the analytical results and the deviations are presented.

Table 3.5. FE and analytical ultimate strength results for all the Sets

Set	Stress Distribution at Ultimate state	$f_{u.FE}$ (MPa)	$f_{u.\,Ana}$ (MPa)	$\Delta f_u \%$
Set 1		70.82	62.4	13.49
Set 2		57.26	62.4	8.24
Set 3		46.46	62.4	25.54
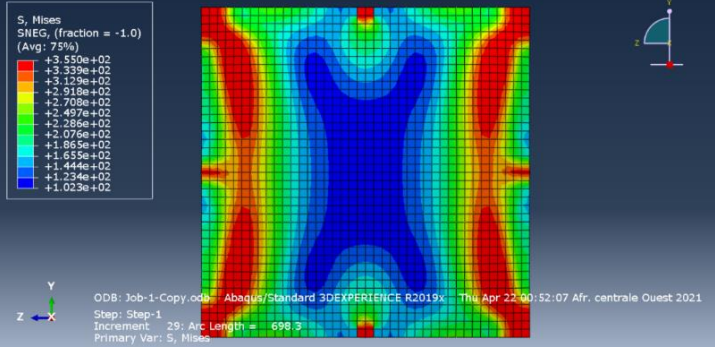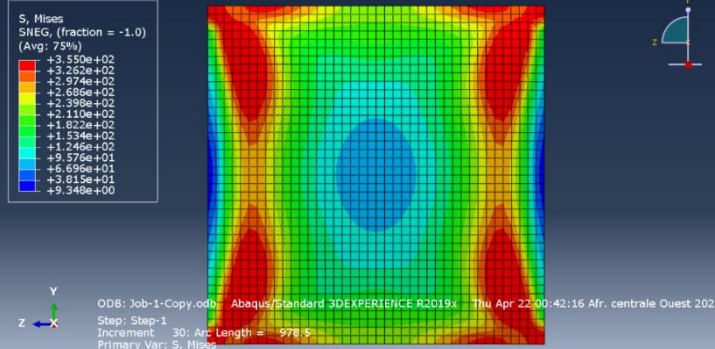
Imperfection tolerances during the erection of steel plate girders and geometrical nonlinearities
Master of Civil Engineering defended by SONNA DONKO Maël
NASPW Yaoundé 2019/2020
70
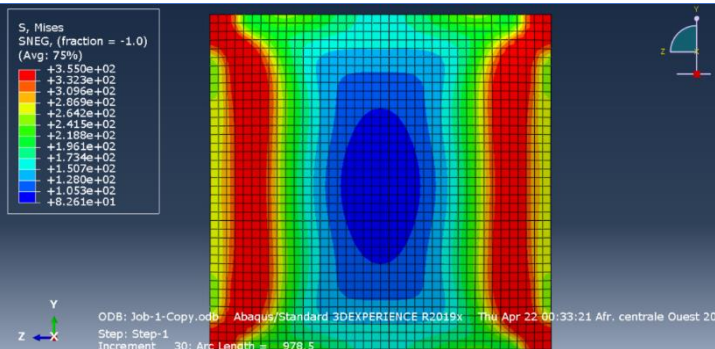
The results obtained show that set 1 cannot be used to model the web at the post-critical state as there are stress accumulations at the edges which are not seen in the behaviour of the web under real global plate girder analysis. Set 2 and 3 seem to give realistic stress distributions, with set 2 chosen as the best as it gives FE ultimate strength result with the lowest deviation of 10%.

3.1.4. Results comparison and interpretation

The critical stress and ultimate strength deviations are summarised in Table 3.6. It is observed that:

- Set 1 always has a deviation of more than 10% with a maximum deviation of up to 14.91%
- Set 2 always has a deviation of less than 10%
- Set 3 has less than 10% deviations at pre-critical states but a deviation of up to 25.54% at its ultimate state.

Table 3.6. Summary of critical stress and ultimate strength results deviations

Deviation of Set (%)			
Case	Set 1	Set 2	Set 3
$\psi = -1$	12.23	3.63	7.11
$\psi = \dfrac{1}{3}$	14.91	4.31	0.52
$\psi = \dfrac{1}{2}$	14.91	4.33	0.52
$\psi = 1$	14.26	4.88	0.05
Ultimate Strength $(\psi = 1)$	13.49	8.24	25.54

These results can also be presented in an "accuracy" form (Table 3.7) instead of a "deviation" form (Table 3.6). In this form, the graph (Figure 3.1) is plotted for better visualisation and ease in the choice of the appropriate set.

Imperfection tolerances during the erection of steel plate girders and geometrical nonlinearities
Master of Civil Engineering defended by SONNA DONKO Maël
NASPW Yaoundé 2019/2020

71

Table 3.7. Summary of critical stress and ultimate strength results accuracy

Accuracy of Set (%)			
Case	**Set 1**	**Set 2**	**Set 3**
$\psi = -1$	87.77	96.37	92.89
$\psi = \dfrac{1}{3}$	85.09	95.69	99.48
$\psi = \dfrac{1}{2}$	85.09	95.67	99.48
$\psi = 1$	85.74	95.12	99.95
Ultimate Strength ($\psi = 1$)	86.51	91.76	74.46

Graph of Figure 3.1 shows that Set 3 looks to be very accurate in 4 cases, but not at the ultimate state where the FE ultimate strength obtained is far less than the analytical result (74.46% accuracy). From all the 5 cases studied, Set 2 always has an accuracy of at least 90% (error less than 10%), thus Set 2 will be used for further buckling and post-buckling studies.
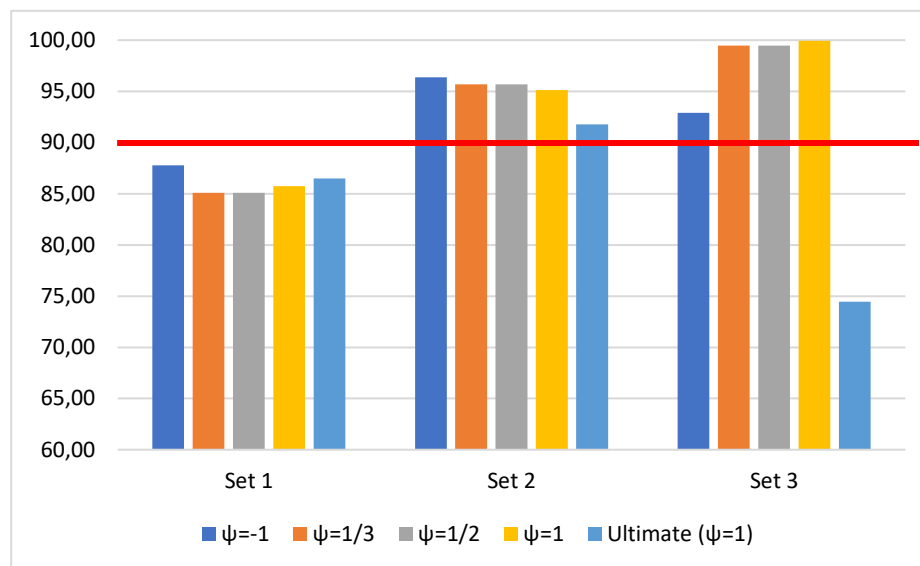
Figure 3.1. Graphical representation of critical stress and ultimate strength results accuracy

Imperfection tolerances during the erection of steel plate girders and geometrical nonlinearities
Master of Civil Engineering defended by SONNA DONKO Maël
NASPW Yaoundé 2019/2020

72

3.2. Mesh density and size

3.2.1. FE results

3.2.1.1. Pure compression ($\psi = 1$)

The results obtained under pure compression are presented in Table 3.8.

Table 3.8. FE results under pure compression

Trial	Mesh density b/S	Mesh size S (mm)	λ_1 (N/mm)	Critical stress $\sigma_{cr,FE}$ (N/mm^2)	Change (%)
T_1	5	300	582.66	48.56	-
T_2	10	150	552.73	46.06	5.14
T_3	20	75	545.16	45.43	1.37
T_4	30	50	543.38	45.28	0.33
T_5	40	37.5	542.52	45.21	0.16

The results obtained here show that if both mesh densities 30 and 40 (< 1%) are used, the results obtained will be convenient enough. The graph shown in Figure 3.2 appropriately describes the effect of mesh density on the obtained FE result.
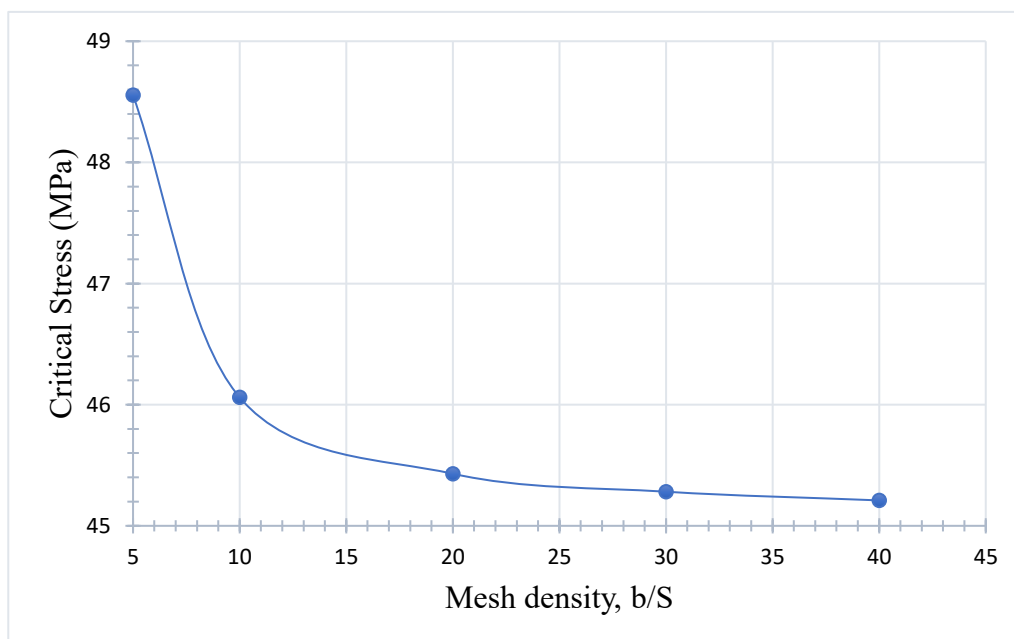
Figure 3.2. Graphical representation of FE results under pure compression

Imperfection tolerances during the erection of steel plate girders and geometrical nonlinearities
Master of Civil Engineering defended by SONNA DONKO Maël
NASPW Yaoundé 2019/2020

73

3.2.1.2. Eccentric compression ($\psi = -0.5$)

The results obtained under eccentric compression are presented in Table 3.9.

Table 3.9. FE results under eccentric compression

Trial	Mesh density b/S	Mesh size S (mm)	λ_1 (N/mm)	Critical stress $\sigma_{cr,FEM}$ (N/mm^2)	Change (%)
T_1	5	300	2080.5	173.38	-
T_2	10	150	1904.3	158.69	8.47
T_3	20	75	1861	155.08	2.27
T_4	30	50	1851.7	154.31	0.50
T_5	40	37.5	1847.7	153.98	0.22

Again, the results obtained here show that if both mesh densities 30 and 40 ($< 1\%$) are used, the results obtained will be convenient enough. The graph of Figure 3.3 describes well the effect of mesh density on the obtained FE result.
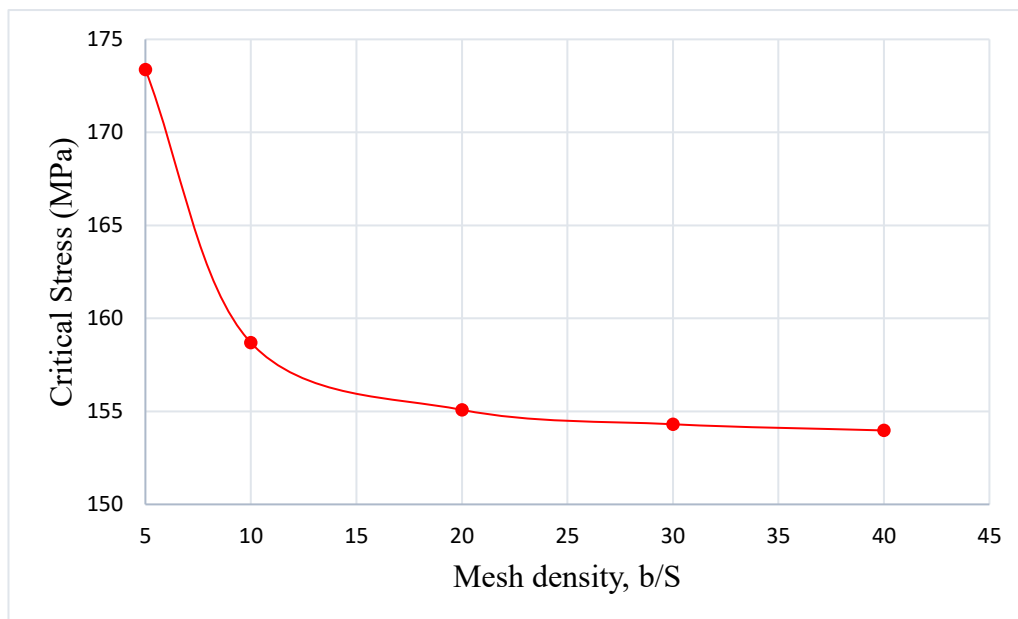
Figure 3.3. Graphical representation of FE results under eccentric compression

Imperfection tolerances during the erection of steel plate girders and geometrical nonlinearities
Master of Civil Engineering defended by SONNA DONKO Maël
NASPW Yaoundé 2019/2020

74

3.2.1.3. Pure bending ($\psi = -1$)

The results obtained under pure bending are presented in Table 3.10.

Table 3.10. FE results under pure bending

Trial	Mesh density b/S	Mesh size S (mm)	λ_1 (N/mm)	Critical stress $\sigma_{cr,FEM}$ (N/mm^2)	Change (%)
T_1	5	300	4562.6	380.22	-
T_2	10	150	3774.6	314.55	17.27
T_3	20	75	3579.8	298.32	5.16
T_4	30	50	3542.4	295.20	1.04
T_5	40	37.5	3527.9	293.99	0.41

Conversely to that obtained for pure compression and eccentric compression, the results obtained here show that only mesh density 40 ($< 1\%$) will conveniently yield the appropriate result. The graph of Figure 3.4 describes well the effect of mesh density on the obtained FE result.
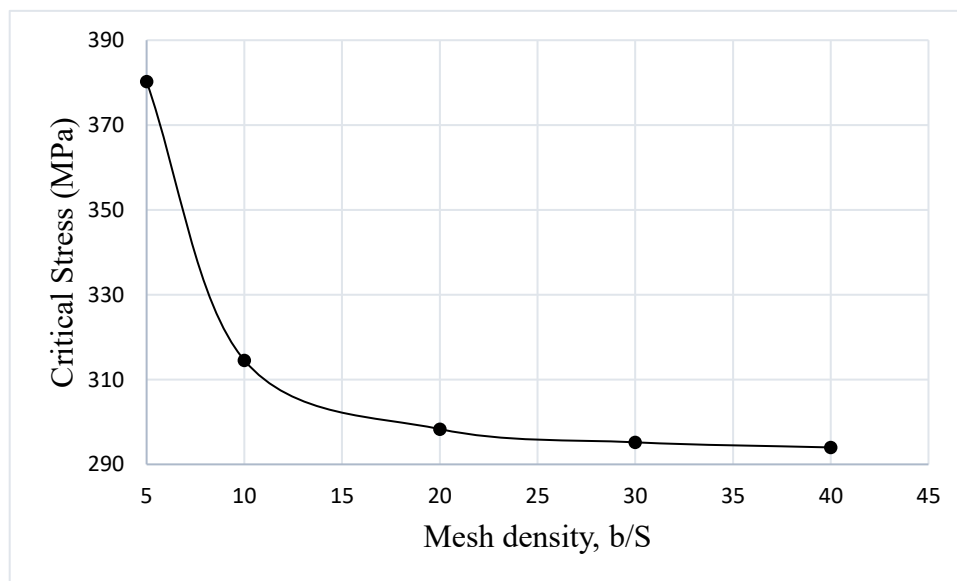
Figure 3.4. Graphical representation of FE results under pure bending

Imperfection tolerances during the erection of steel plate girders and geometrical nonlinearities
Master of Civil Engineering defended by SONNA DONKO Maël
NASPW Yaoundé 2019/2020

75

3.2.2. Results comparison and interpretation

Change in FE critical stress results is summarised in Table 3.11. It is observed that:

- Mesh density 30 is enough for subsequent analyses under pure compression and eccentric compression conditions

- A finer mesh density of 40 is needed for good analyses of webs under pure bending.

Table 3.11. Change in FE critical stress results

Trial	Mesh density, b/S	Change (%)		
		$\psi = 1$	$\psi = -0.5$	$\psi = -1$
T2	10	5.14	8.47	17.27
T3	20	1.37	2.27	5.16
T4	30	0.33	0.50	1.04
T5	40	0.16	0.22	0.41

These results can also be presented with a "convergence" format (Table 3.12) instead of a "change" format (Table 3.11). In this format, the graph (Figure 3.5) is plotted for better visualisation and ease in the choice of the appropriate mesh density.

Table 3.12. Convergence in FE critical stress results

Trial	Mesh density, b/S	Convergence (%)		
		$\psi = 1$	$\psi = -0.5$	$\psi = -1$
T2	10	94.86	91.53	82.73
T3	20	98.63	97.73	94.84
T4	30	99.67	99.50	98.96
T5	40	99.84	99.78	99.59

As seen on the graph, as the mesh density increases, convergence increases for each stress ratio. Also, the 2 extreme loading conditions (pure bending and pure compression) curves tend towards a fixed value of 99.74% convergence. Thus, this shows that any intermediate loading condition between these 2, will have a curve found between the stated 2 curves and will definitely tend to a 99.74% convergence value that corresponds to a mesh density of 40. This situation is experienced by the 3rd middle curve of Figure 3.5 which tends to 99.74%.

Imperfection tolerances during the erection of steel plate girders and geometrical nonlinearities
Master of Civil Engineering defended by SONNA DONKO Maël
NASPW Yaoundé 2019/2020
76
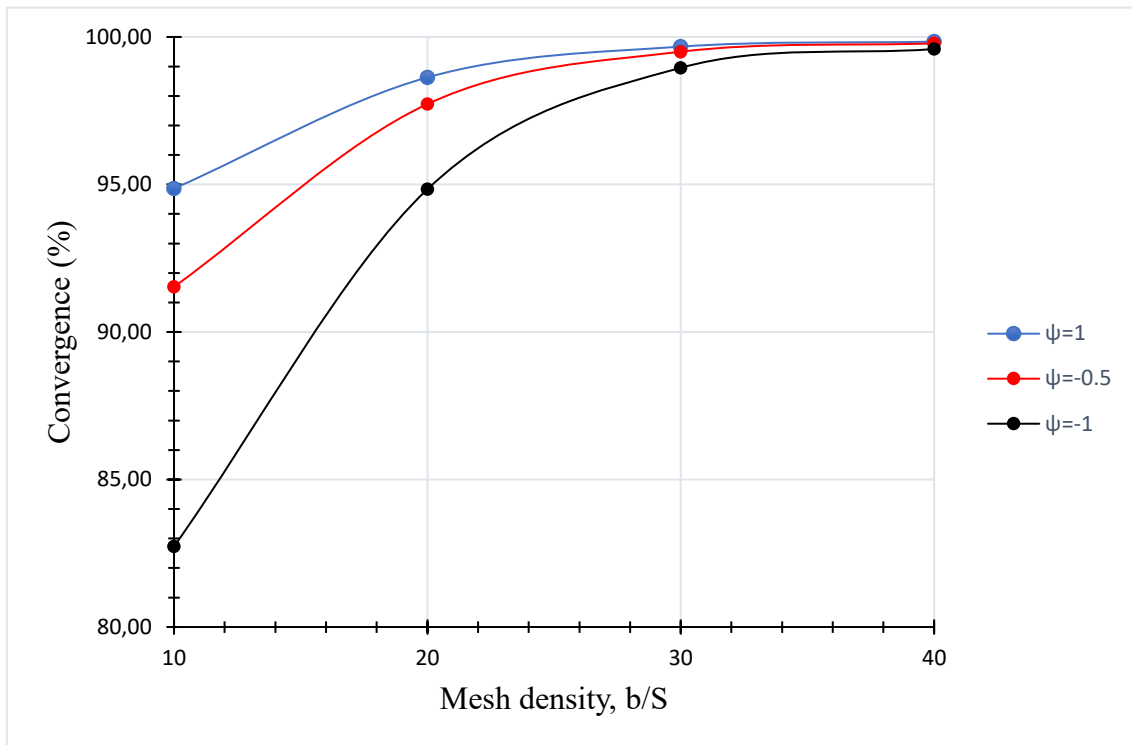
Figure 3.5. Graphical representation of convergence in FE critical stress results

The results obtained show that, using a mesh density of $\frac{b}{S} = 40$ in subsequent analyses will yield very accurate results. It is also noticed that the increase in computation time due to an increase in mesh density is very negligible.

3.3. FE and analytical results comparison

In the case of the present study, the critical stress result obtained from the FE formulation of plates was assessed and compared to the analytical result in order to confirm the FE methodology used for buckling analyses. This was achieved by first setting up the approach, then analytical and FE results were presented then compared for final approval of FE formulation.

3.3.1. Set-up

The plate girder's panels used for this study are Basler's panels subjected to pure bending and used in the subsequent experimental verification. These panels, of aspect ratio 0.75 and 1.5, were chosen for completeness of the verification procedures on girder G4 of Basler's web buckling tests (K. Basler et al., 1960). The panels used in the experiment have geometrical properties, mechanical properties and boundary conditions given in the following paragraphs.

Imperfection tolerances during the erection of steel plate girders and geometrical nonlinearities
Master of Civil Engineering defended by SONNA DONKO Maël
NASPW Yaoundé 2019/2020
77

3.3.1.1.   Geometrical properties

Panels P1 and P2 of test T1 on girder G4 have the geometrical properties given by equations (3.4) and (3.5). Note that $1 \text{ in} = 2.54 \text{ cm}$.

$$\text{Panel 1: } \begin{cases} a = 75 \text{ in} \\ b = 50 \text{ in} \\ t = {}^{1}/_{8} \text{ in} \end{cases} \Rightarrow \text{aspect ratio } \alpha = 1.5 \qquad (3.4)$$

$$\text{Panel 2: } \begin{cases} a = 37.5 \text{ in} \\ b = 50 \text{ in} \\ t = {}^{1}/_{8} \text{ in} \end{cases} \Rightarrow \text{aspect ratio } \alpha = 0.75 \qquad (3.5)$$

3.3.1.2.   Mechanical properties of the material

In the course of Basler's experiment, the mechanical properties of the steel used were explicitly determined through tests. It was found that an elastic perfectly plastic behaviour can be used as a model for the steel used. Thus, girder G4 used in this study has the following mechanical properties: $E = 3 * 10^7$ psi, $\nu = 0.3$, $f_y = 43\,400$ psi. Note that $1 \text{ lbf} = 4.45 \text{ N}$ and $1 \text{ psi} = 6.89 \text{ kPa}$.

3.3.1.3.   Boundary condition (BC)

The BC chosen in the previous study (Set 2) is used for this analytical verification. Set 2 BC restrains out-of-plane displacements on all nodes in the four edges, provides horizontal restrains in the 2 middle nodes of the horizontal edges and vertical restraints on all vertical nodes.

3.3.2. Analytical result

The critical stress was calculated in Basler's report using the formula given in 2.2.2.1. The critical stress result both for $\alpha = 1.5$ and 0.75 was thus found to be $\sigma_{cr,Ana} = 4.05$ ksi. Note that $1 \text{ ksi} = 6.89 \text{ MPa}$.

3.3.3. FE result

For the finite element formulation, an S4R, Quad-shaped, mesh element is applied on the panel using Abaqus/CAE structured meshing technique with the verified mesh density of 40 (mesh size of $b/40$). Then, linear buckling perturbation analysis is run with a predefined unity shell edge load such that $\psi = -1$.

Imperfection tolerances during the erection of steel plate girders and geometrical nonlinearities
Master of Civil Engineering defended by SONNA DONKO Maël
NASPW Yaoundé 2019/2020

78

The buckling shell edge load (fundamental eigenvalue) is obtained and used to determine the buckling stress of the panel as given in Table 3.13.

Table 3.13. FE critical stress results

Aspect Ratio	First Eigenmode	λ_1 (lpf/in)	$\sigma_{cr,FEM}$ (ksi)
$\alpha = 1.5$		502.28	4.02
$\alpha = 0.75$		493.28	3.95
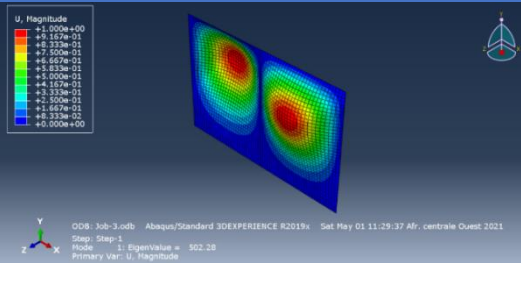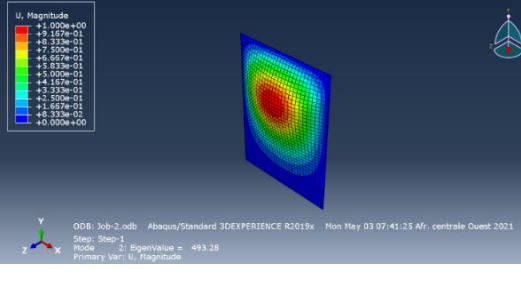
3.3.4. Comparison and interpretation

Table 3.14 summarises the FE and analytical critical stress results obtained for the 2 panels of girder G4.

Table 3.14. FE and analytical critical stress results comparison

Aspect Ratio	$\sigma_{cr,FE}$ (ksi)	$\sigma_{cr,Ana}$ (ksi)	$\Delta\sigma_{cr}\%$
$\alpha = 1.5$	4.02	4.05	0.75
$\alpha = 0.75$	3.95	4.05	2.56

The results obtained show that the FE deviation is so small (less than 2.56%) that the FE modelling process is considered valid for subsequent critical stress determination.

Imperfection tolerances during the erection of steel plate girders and geometrical nonlinearities
Master of Civil Engineering defended by SONNA DONKO Maël
NASPW Yaoundé 2019/2020
79

3.4. FE and experimental result comparison

Basler et al. (1960) experiment on welded plate girders was simulated numerically in view of obtaining results similar to the experimental ones and thus, confirm the finite element modelling procedures used to study the behaviour of the web through geometrically and materially nonlinear analysis with imperfections included (GMNIA). This was done by defining the test set-up, specifying the experimental data and experimental results, then presenting the FE results for comparison and interpretation.

3.4.1. Set-up

Basler's Test T1 on Girder G4 (Figure 3.6) is chosen as it experiences direct stresses which are the stresses considered in this study. The properties of the model used in the experiment are collected from the report, modelled in Abaqus/CAE and the results are compared with experimental results.
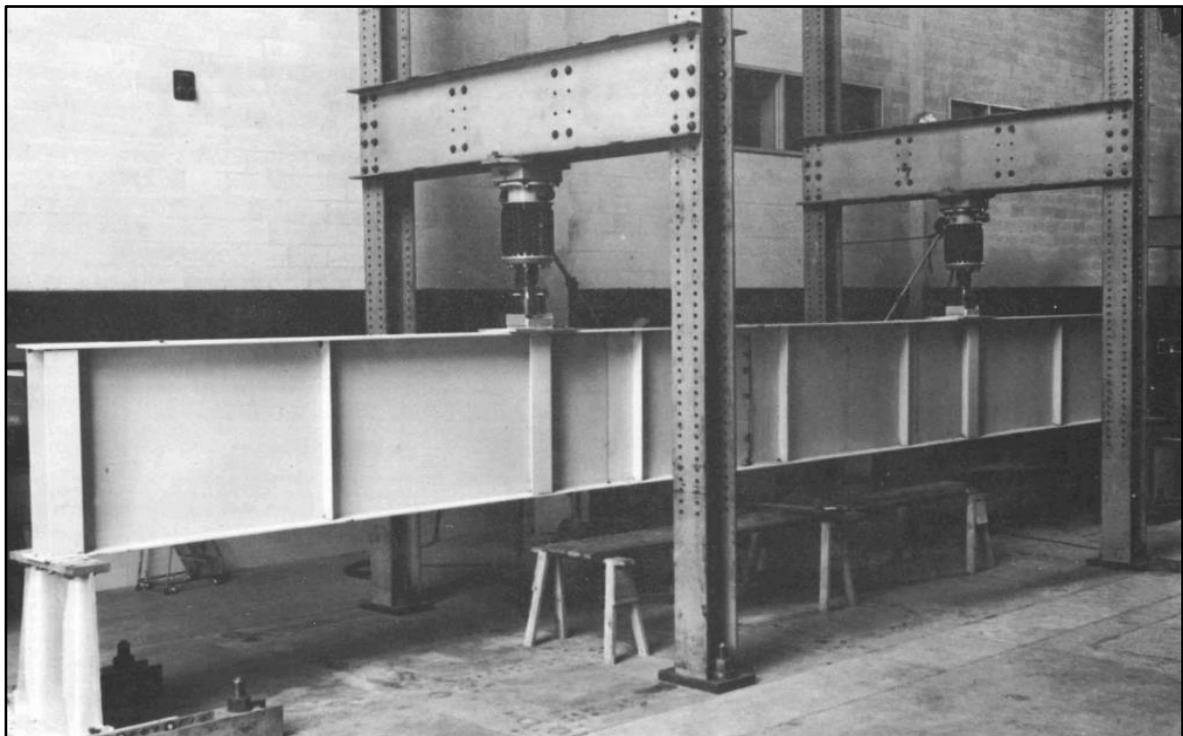
Figure 3.6. Experimental setup of girder G4 (Konrad Basler et al., 1960)

Imperfection tolerances during the erection of steel plate girders and geometrical nonlinearities
Master of Civil Engineering defended by SONNA DONKO Maël
NASPW Yaoundé 2019/2020

80

3.4.2. Experimental data

Basler's experimental data on geometrical properties, static scheme and material properties are collected from the experiment's report (K. Basler et al., 1960) and presented in the following parts.

3.4.2.1. Geometrical properties

The geometrical properties of girder G4 collected from the experiment's report are summarized in Table 3.15, Figure 3.7 and Figure 3.8.

Table 3.15. Geometrical properties of girder G4

Plate	Size (in)	Thickness (in)
Test web	50	$1/8$
Test flange	12	$3/4$
End web	50	$3/8$
End flange	12	$3/4$
Intermediate stiffener	4	$1/4$
Bearing stiffener web	4	$1/4$
Bearing stiffener flange	12	$3/8$
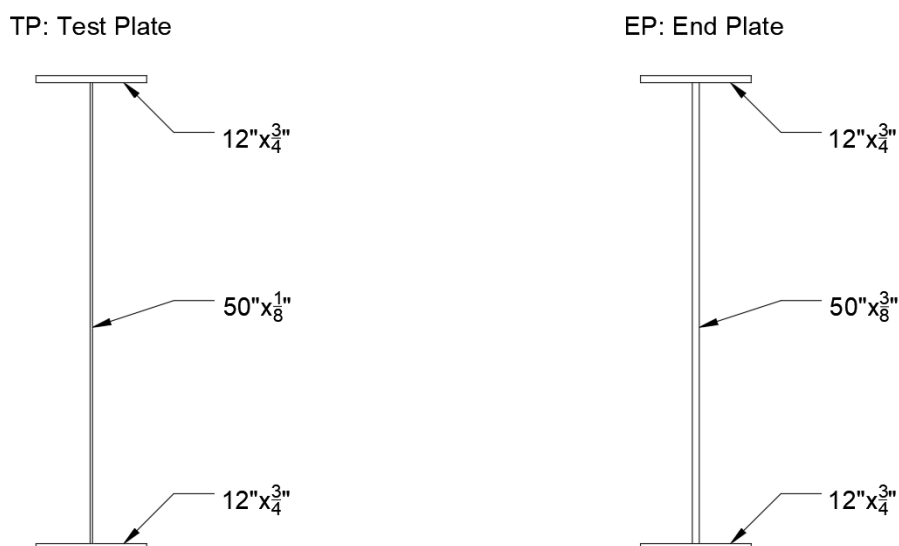
Figure 3.7. Cross-section of plates that form girder G4

Imperfection tolerances during the erection of steel plate girders and geometrical nonlinearities
Master of Civil Engineering defended by SONNA DONKO Maël
NASPW Yaoundé 2019/2020

81
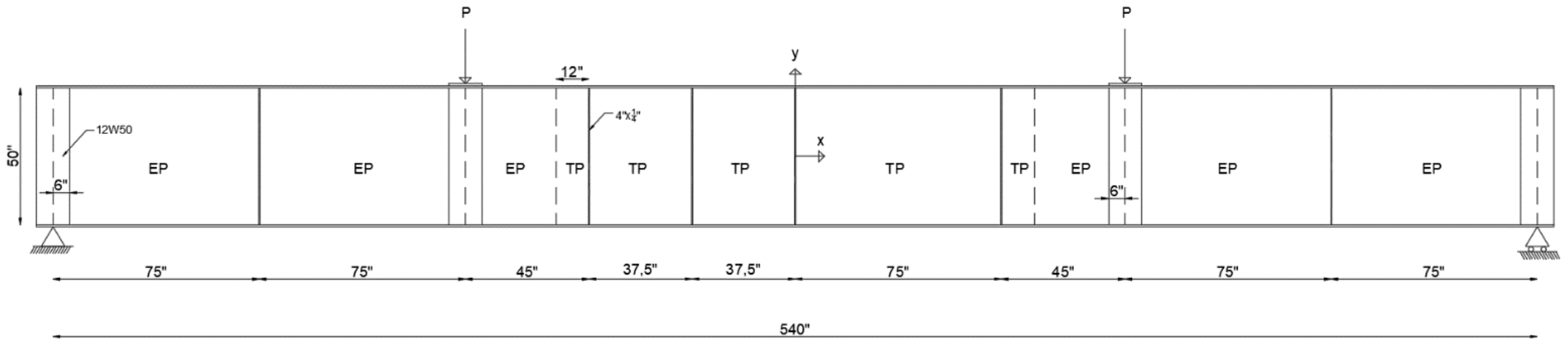
Figure 3.8. Longitudinal view of girder G4

3.4.2.2. Static scheme

Girder G4 is a, 540 inches, simply supported girder disposed in such a way that the system remains isostatic in the X-Y plane and is restrained from out-of-plane displacements. Also, girder G4 is loaded in such a way that it generates direct stresses from pure bending as displayed in Figure 3.9.
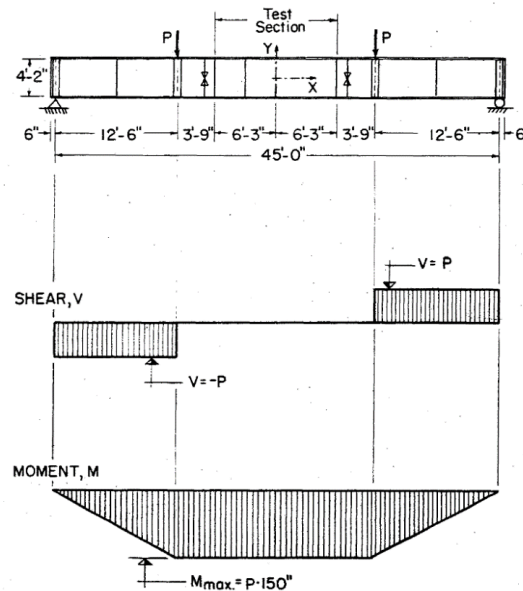
Figure 3.9. Test setup for bending girders (K. Basler et al., 1960)

3.4.2.3. Mechanical properties of the materials

The mechanical properties of the steel used for the experiment were determined through coupon tests in the laboratory, approximated as elastic perfectly plastic, documented in the report book and summarized here in Table 3.16 with $E = 3 * 10^7$ psi and $v = 0.3$.

Table 3.16. Mechanical properties of the steel of girder G4 (K. Basler et al., 1960)

Plate	Static yield stress (psi)
Test web	43 400
Test top flange	37 600
Test bottom flange	37 000
End web	40 000
End top flange	37 600
End bottom flange	37 000
Intermediate stiffener	43 400
Bearing stiffener web	40 000
Bearing stiffener flange	40 000

Imperfection tolerances during the erection of steel plate girders and geometrical nonlinearities
Master of Civil Engineering defended by SONNA DONKO Maël
NASPW Yaoundé 2019/2020

83

3.4.3. Experimental results

The ultimate load and lateral displacement results presented in Basler's report are given in Table 3.17.

Table 3.17. Experimental results (K. Basler et al., 1960)

Experimental Results			
Girder	**Test**	**P_u**	**v (P = 100 kips)**
G4	T1	118 kips	1.20 in

The load vs displacement graph obtained during the experiment (Figure 3.10) and drawn in the report are extracted using the graph digitizer tool of Graph Expert Professional (Hyams, 2014). The snap behaviour shown with the dashed curve from step 22 to 23 is not represented using the graph digitizer, as it indicates a dynamic response of the girder, which will not be captured with the static Riks step of the FE program used Abaqus/CAE. The graph obtained by the digitizer is given in Figure 3.11.
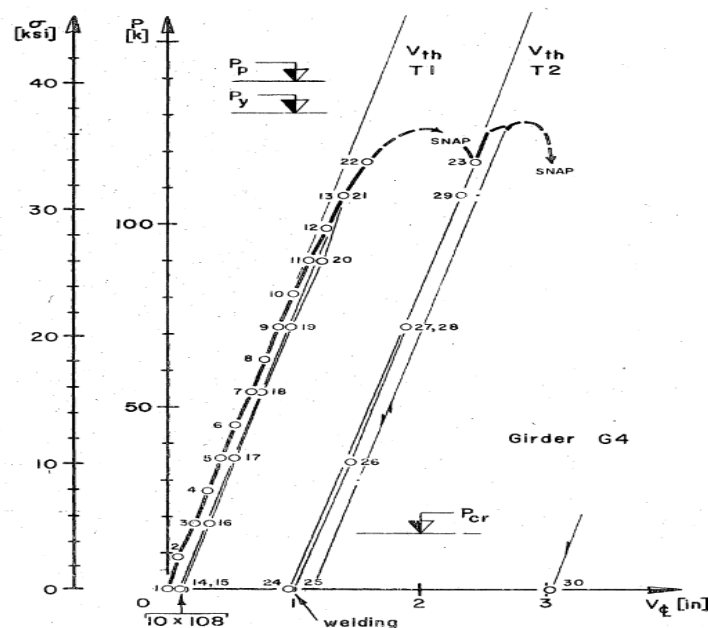
Figure 3.10. Experimental load vs displacement graph of girder G4 (Konrad Basler et al., 1960)

Imperfection tolerances during the erection of steel plate girders and geometrical nonlinearities
Master of Civil Engineering defended by SONNA DONKO Maël
NASPW Yaoundé 2019/2020
84
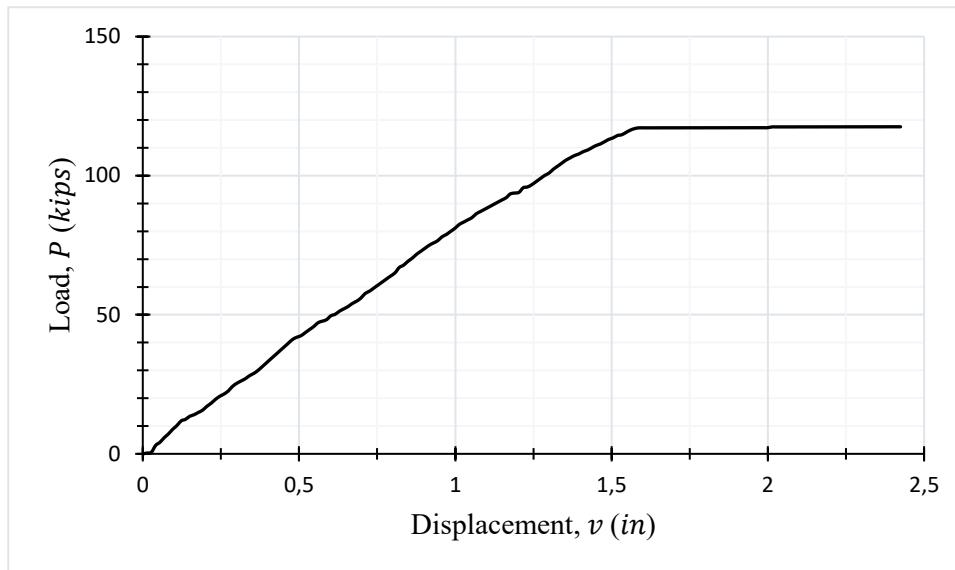
Figure 3.11. Extracted curve of the experimental load vs vertical displacement graph of girder G4

3.4.4. FE model

The experiment is modelled in Abaqus/CAE using the modelling techniques described in part 2.2.3.2. Geometrical, material, loading conditions and boundary conditions are modelled using the experimental data given above. An S4R, Quad-shaped, mesh element is applied on the whole girder model using the structured meshing technique with the calibrated mesh density of 40 (mesh size of $b/40$). Figure 3.12 and Figure 3.13 show the FE model obtained.
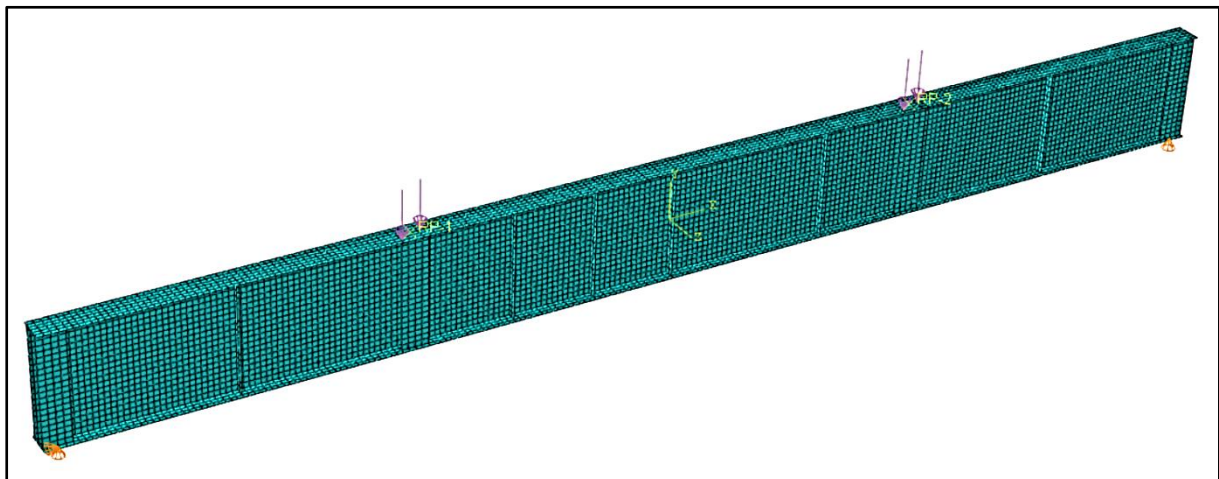
Figure 3.12. Front view of FE model of girder G4

Imperfection tolerances during the erection of steel plate girders and geometrical nonlinearities
Master of Civil Engineering defended by SONNA DONKO Maël
NASPW Yaoundé 2019/2020

85
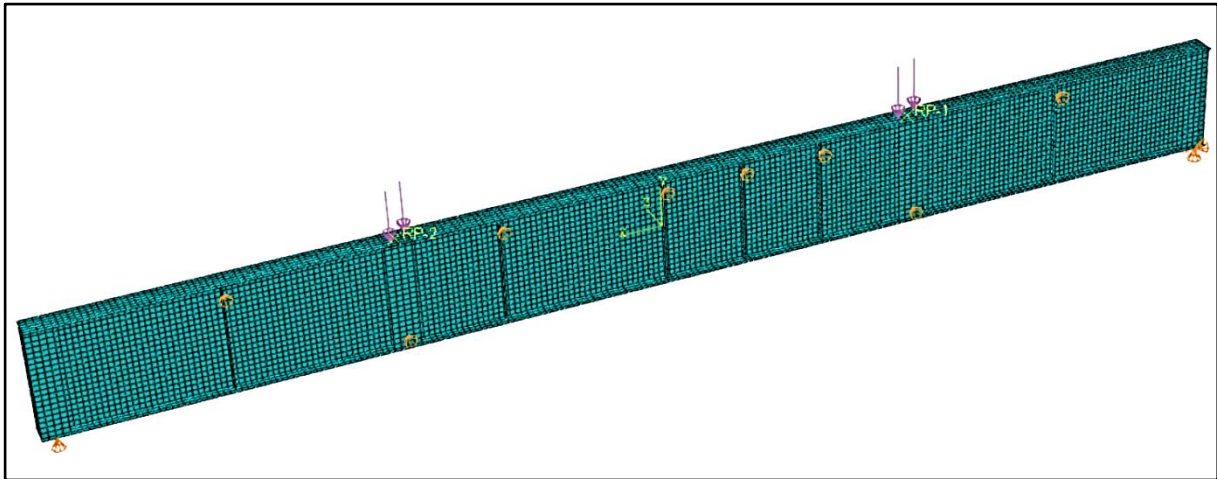
Figure 3.13. Backward view of FE model of girder G4

3.4.5. FE results

Abaqus/CAE linear buckling perturbation step is used for buckling analysis to obtain the fundamental buckling mode and load. This will help to model imperfections for the subsequent GMNIA analyses. The result obtained (Figure 3.14) is in perfect agreement with the setup put in place in the laboratory to create local bend buckling in the web.
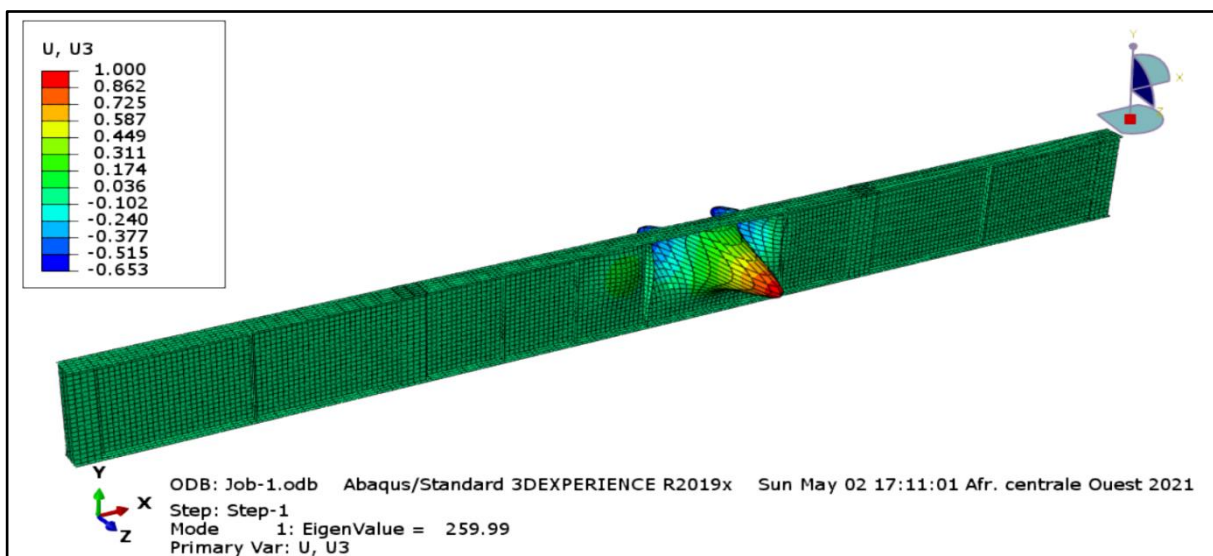
Figure 3.14. 1st eigenmode of girder G4

The GMNIA analysis is run through Abaqus/CAE static Riks step. The imperfect (real) girder inputted here has the shape obtained in the previous buckling analysis with a magnitude equal to that of the test web's initial imperfection amplitude given in the experiment's report (0.2 in). The deformed shape in Figure 3.15 is then obtained.

Imperfection tolerances during the erection of steel plate girders and geometrical nonlinearities
Master of Civil Engineering defended by SONNA DONKO Maël
NASPW Yaoundé 2019/2020

86
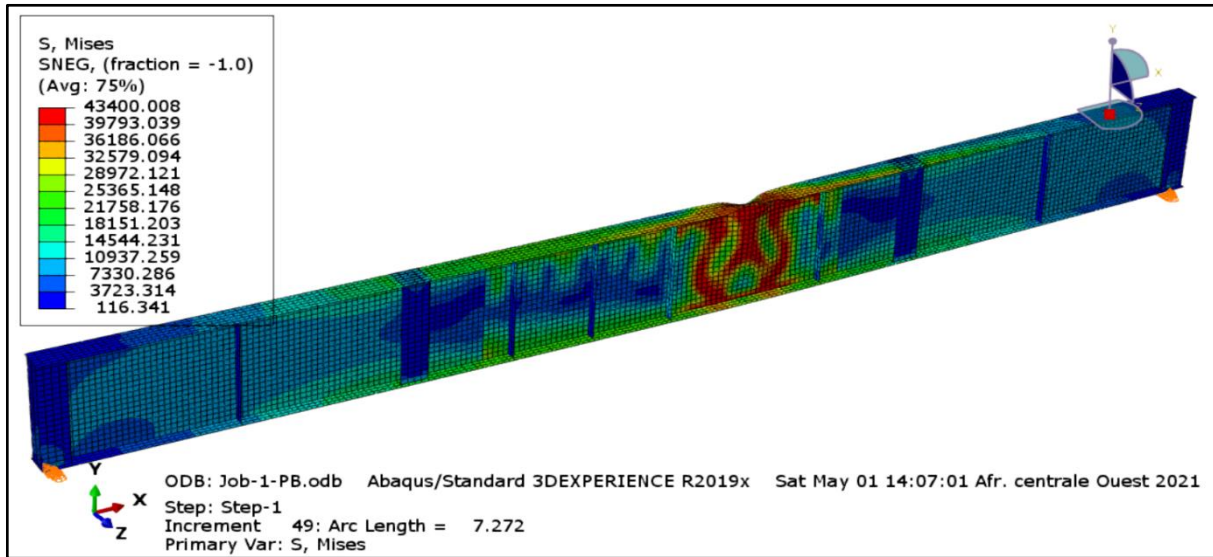
Figure 3.15. Shape of girder G4 at ultimate load

To view both pre- and post-buckling behaviour of girder G4, load values were calculated with equation (3.6) from load proportionality factor (LPF) extracted results from Abaqus/CAE and plotted against extracted vertical displacement values in the middle of the girder (Figure 3.16).
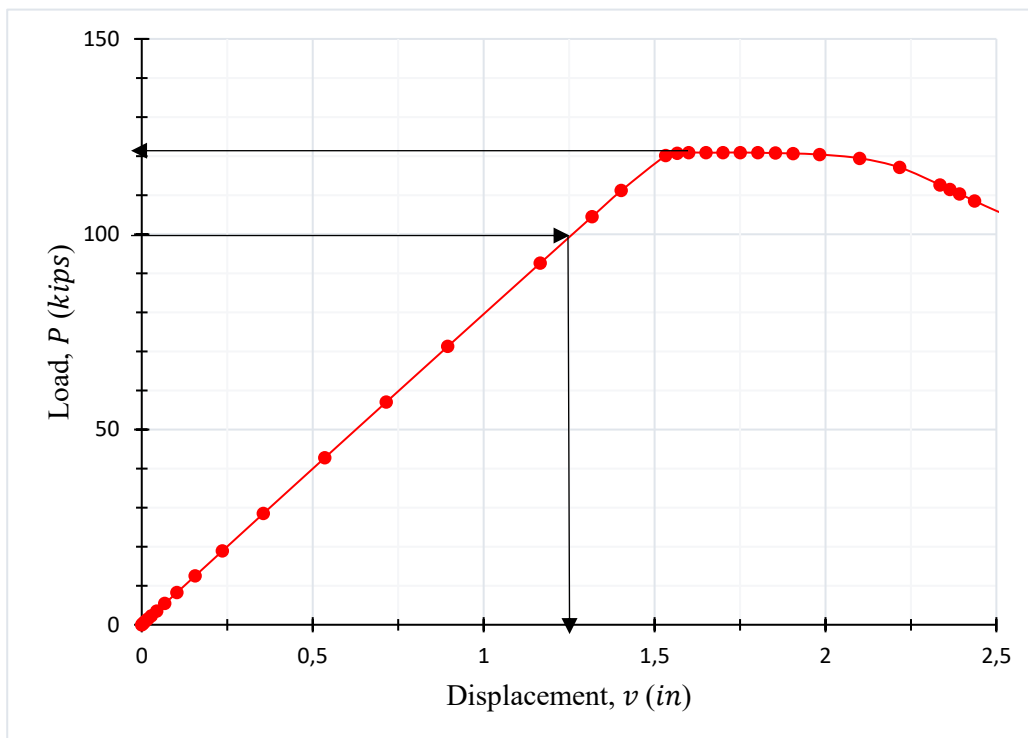
Figure 3.16. Applied load vs vertical displacement graph of FE model of girder G4

Imperfection tolerances during the erection of steel plate girders and geometrical nonlinearities
Master of Civil Engineering defended by SONNA DONKO Maël
NASPW Yaoundé 2019/2020

87

$$P = \frac{\lambda_1 * LPF * A}{1000} \qquad (3.6)$$

where:

$$\lambda_1 = 259.99 \text{ psi (from Abaqus/CAE FE results)}$$

$$\text{Loaded Area}, A = 12 \text{ in} * 8 \text{ in} = 96 \text{ in}^2$$

The FE ultimate load obtained is $P_u = 120.92$ kips and the FE vertical displacement at $P = 100$ kips is $v \, (P = 100 \text{ kips}) = 1.26$ in.

3.4.6. Comparison and interpretation

3.4.6.1. The behaviour of G4 under loading

Experimental and finite element load vs vertical displacement curves were plotted on the same graph of Figure 3.17 and compared.
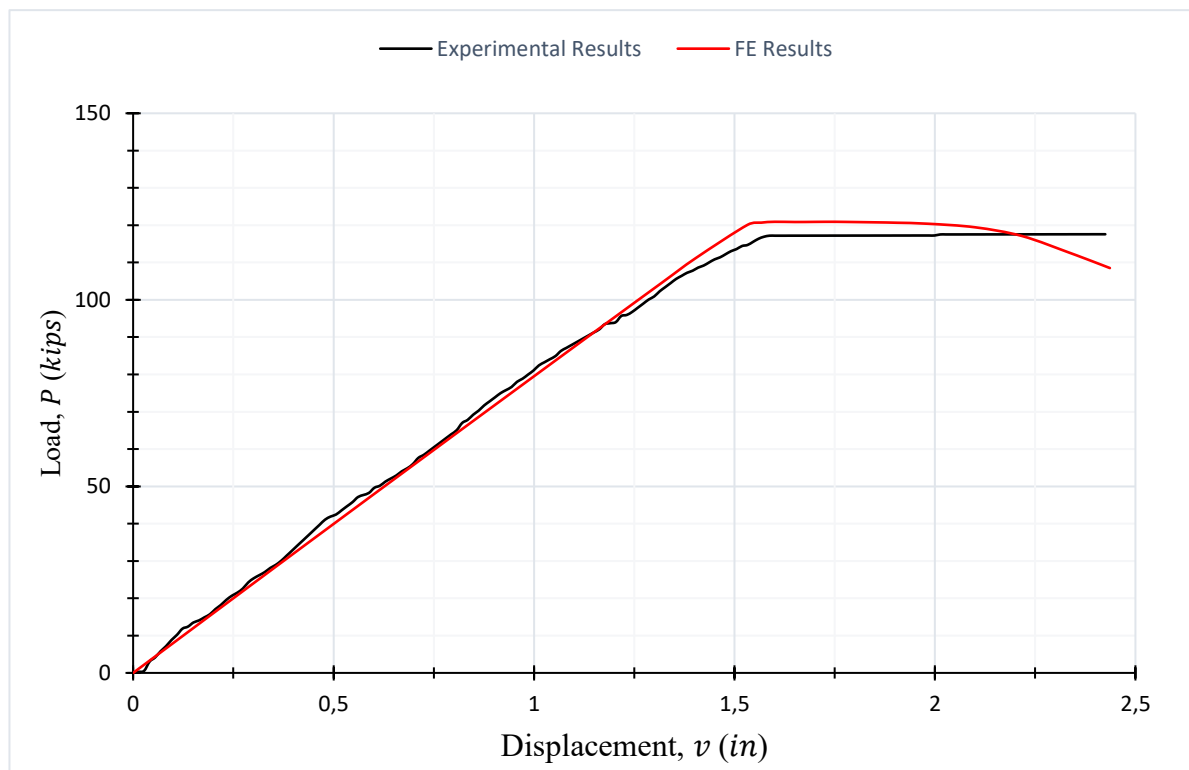
Figure 3.17. Experimental and FE graphical comparison

The FE results were found to almost perfectly coincide with the experimental results. An overall maximum deviation of 7.70% is found at $v = 2.44$ in. This overall maximum deviation occurs after the ultimate state. This part is not considered in this study as only realistic situations were dealt with here (situations before failure load). Thus, in the realistic range, a maximum deviation of 3.18% occurs at $v = 1.60$ in.

Imperfection tolerances during the erection of steel plate girders and geometrical nonlinearities
Master of Civil Engineering defended by SONNA DONKO Maël
NASPW Yaoundé 2019/2020

88

3.4.6.2. Ultimate load and maximum deflection

Experimental and FE results are presented in Table 3.18 and compared.

Table 3.18. Experimental and FE results comparison

Parameter	Experimental Result	FE Result	Deviation (%)
Ultimate load (kips)	118	120.92	**2.47**
Deflection at 100 kips (in)	1.20	1.26	**5.00**

The values obtained were seen to be very similar, with a deviation of 2.47% for the load and 5% for the deflection.

The FE results obtained were found to deviate from the experimental ones by not more than 10%. More so, in the realistic range, deviations of less than 5% were dealt with. Therefore, the FE modelling process was considered valid for subsequent GMNIA analysis.

Conclusion

These preliminary studies are the backbone of any successful FE parametric study. Thus, this chapter aimed to perform the verification of procedures described detailly in chapter 2 in order to conclude whether the FE modelling procedures described, again in chapter 2, will yield accurate parametric results. To conclude this, the chapter started with the selection of the Set 2 BCs that accurately models the behaviour of the flanges and stiffeners on the web confirmed by its 96.37%, 95.69%, 95.67%, 95.12% and 91.76% accuracy in modelling the behaviour during both linear buckling and GMNIA analyses. Also, the web plate was found to be excellently calibrated with a mesh density of $\frac{b}{s} = 40$, yielding a 99.74% convergence under every loading condition. After the web was well-calibrated, Basler's web plates of aspect ratios 0.75 and 1.5 were used to prove that the FE linear buckling procedures detailed in part are analytically valid, obtaining FE critical stress deviations of 2.56% and 0.75% from the analytical values of the 0.75 and 1.5 aspect ratio web plates respectively. The chapter then ended by a verification of the FE GMNIA procedures described in part 2.2.3.2 using Basler's T1 experiment on girder G4 and showing that the FE results deviated from the experimental ones by a maximum of 5% in realistic stress ranges. All this shows that the FE methods outlined in chapter 2 will always provide at least a 91.76% accuracy on the behaviour of real webs of plate girders.

Imperfection tolerances during the erection of steel plate girders and geometrical nonlinearities
Master of Civil Engineering defended by SONNA DONKO Maël
NASPW Yaoundé 2019/2020

89

CHAPTER 4. PARAMETRIC RESULTS AND INTERPRETATION

Introduction

After an accurate calibration and verification of the used Abaqus/CAE modelling methods for the web of plate girders, several webs with characteristics falling inside the verified range were selected to perform a thorough parametric study aimed at determining the effects of various influential parameters on the imperfection tolerance limits. To attain this objective, chapter 4 starts by describing the characteristics of both the ideal perfect and real imperfect webs selected for the study under various loading conditions during the erection phase of steel plate girders. This section is followed by the presentation of the selected webs' buckling stresses, ultimate strengths and tolerance limits provided by codes' analytical formulations. Next to that is the presentation of ideally perfect webs' FE eigenmodes and critical stresses then imperfect webs' FE ultimate strengths. The FE and analytical results known; they are then compared before looking into the effect of each influential parameter on the ultimate strength. Finally, when the effects of the parameters on the strength are known, regression analyses are performed to capture trends and thus derive equations that can explicitly be used to find both the ultimate strength and the tolerance limit as a function of the studied parameters. Also, the proposed tolerance limit equation and that given by the American and European codes are compared to check parameter dependency and a possible relaxation in the codes' tolerance limits which will be highly welcomed by steel plate girders' fabricators and erectors.

4.1. Presentation of webs

Von Mises stresses experienced by webs are found to always be below or at its yield strength. As such, an elastic perfectly plastic steel behaviour with no strain hardening was used in the course of this study as it is capable of perfectly describing the pre- and post-buckling behaviour of the webs until it reaches its ultimate strength. Thus, the most commonly found plate girder steel properties were used: $E = 206\,000$ MPa, $\nu = 0.3$ and $f_y = 355$ MPa. Most importantly, the parameters chosen for this study are aspect ratio, plate slenderness, stress ratio and initial imperfection amplitude as focus has been given to these by many researchers and they seem to influence the ultimate strength. The chosen ranges of each of these parameters reflect real-life occurrences of webs of plate girders. By applying the proposed strategy, the

Imperfection tolerances during the erection of steel plate girders and geometrical nonlinearities
Master of Civil Engineering defended by SONNA DONKO Maël
NASPW Yaoundé 2019/2020

90

webs to be studied are obtained by varying aspect ratio, plate slenderness ratio, stress ratio and initial imperfection amplitude.

4.1.1. Variation in aspect ratio

An initial web of plate girder with dimensions a = b = 1500 mm and a small initial thickness of t = 6 mm was selected.

Variation of dimensions to satisfy the selected aspect ratios of 1, 1.5 and 2 was performed. As such, 3 webs were obtained and given in Table 4.1.

Table 4.1. Webs of plate girders selection through variation in aspect ratio

ID	b (mm)	a (mm)	$\alpha = \dfrac{a}{b}$
P1	1500	1500	1
P2	1500	2250	1.5
P3	1500	3000	2

4.1.2. Variation in slenderness ratio

Variation of the thickness was done to satisfy the selected slenderness ratio range of $[\beta_{cr}, 250]$ as stated in part 2.2.1.1. This gives equations (4.1) and (4.2).

$$\beta_{cr} = \sqrt{k_\sigma \cdot \frac{\pi^2}{12(1 - v^2)} \cdot \frac{E}{f_y}} = \sqrt{23.9 \cdot \frac{\pi^2}{12(1 - 0.3^2)} \cdot \frac{206\,000}{355}} \qquad (4.1)$$

$$\Rightarrow \beta_{cr} = 111.96 \Rightarrow \beta \in [111.96, 250] \qquad (4.2)$$

As such, the values of 125, 150, 187.5 and 250 were used to obtain thicknesses a, b, c and d with values of 6, 8, 10, and 12 mm respectively as shown in Table 4.2. This gives a total of 12 webs.

Imperfection tolerances during the erection of steel plate girders and geometrical nonlinearities
Master of Civil Engineering defended by SONNA DONKO Maël
NASPW Yaoundé 2019/2020

91

Table 4.2. Webs of plate girders selection through variation in slenderness ratio

ID	b (mm)	a (mm)	t (mm)	$\alpha = \dfrac{a}{b}$	$\beta = \dfrac{b}{t}$
P1a	1500	1500	6	1	250
P1b	1500	1500	8	1	187.5
P1c	1500	1500	10	1	150
P1d	1500	1500	12	1	125
P2a	1500	2250	6	1.5	250
P2b	1500	2250	8	1.5	187.5
P2c	1500	2250	10	1.5	150
P2d	1500	2250	12	1.5	125
P3a	1500	3000	6	2	250
P3b	1500	3000	8	2	187.5
P3c	1500	3000	10	2	150
P3d	1500	3000	12	2	125

4.1.3. Variation in stress ratio (loading condition)

Also, the 3 different loading conditions of pure compression ($\psi = 1$), pure bending($\psi = -1$) and eccentric compression ($\psi = -0.5$) were applied to the webs. Thus, this yielded a total of 36 webs to be studied.

4.1.4. Variation in initial imperfection amplitude

As post-buckling cannot be studied on a perfect structure, 17 different imperfection amplitudes (as seen in Table 4.3) were applied on the 36 webs to study their behaviour as imperfection amplitude increases in the chosen range of $\left[\dfrac{b}{100\,000}, \dfrac{b}{10}\right]$. These imperfections have the shape of their corresponding eigenmodes. This led to a total of 612 models to be studied under post-buckling.

Imperfection tolerances during the erection of steel plate girders and geometrical nonlinearities
Master of Civil Engineering defended by SONNA DONKO Maël
NASPW Yaoundé 2019/2020

92

Table 4.3. Selection of imperfection amplitudes

Imperfection	Parameter, k	Amplitude, b/k (mm)
Imp_1	100000	0.015
Imp_2	10000	0.15
Imp_3	1000	1.5
Imp_4	500	3
Imp_5	300	5
Imp_6	200	7.5
Imp_7	150	10
Imp_8	125	12
Imp_9	100	15
Imp_{10}	80	18.75
Imp_{11}	60	25
Imp_{12}	50	30
Imp_{13}	40	37.5
Imp_{14}	30	50
Imp_{15}	20	75
Imp_{16}	15	100
Imp_{17}	10	150

In summary, 36 linear buckling analyses and 612 nonlinear GMNIA analyses are to be performed for a complete parametric study. The FE model of a loaded generic web with Set 2 boundary condition and mesh density of 40 is shown in Figure 4.1.
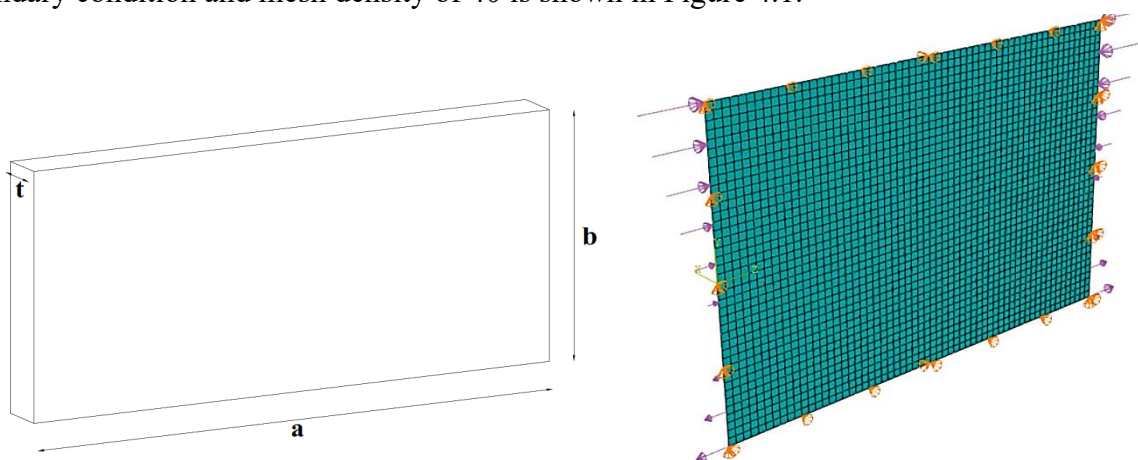
Figure 4.1. Geometry and FE model of a generic web of a plate girder

Imperfection tolerances during the erection of steel plate girders and geometrical nonlinearities
Master of Civil Engineering defended by SONNA DONKO Maël
NASPW Yaoundé 2019/2020
93

4.2. Analytical results

Analytical codes' formulations were detailly presented in part 2.2.2. In this section, the formulations given were implemented to obtain buckling stresses, ultimate strengths and imperfection tolerances of the 36 perfect webs of plate girders under study.

4.2.1. Buckling stress

Buckling stresses given by EC3-1-5 is found by applying equations detailed in part 2.2.2.1. Thus, the buckling stresses values are calculated and presented in Table 4.4.

Table 4.4. EC3-1-5 critical stress results

ID	$\alpha = \dfrac{a}{b}$	$\beta = \dfrac{b}{t}$	$\sigma_{cr.EC3}$ (N/mm^2)		
			Pure compression $\psi = 1$	Eccentric $\psi = -0.5$	Pure bending $\psi = -1$
P1a	1	250	11.92	39.92	71.14
P1b	1	187.5	21.18	70.97	126.47
P1c	1	150	33.10	110.88	197.60
P1d	1	125	47.66	159.67	284.55
P2a	1.5	250	11.92	39.92	71.14
P2b	1.5	187.5	21.18	70.97	126.47
P2c	1.5	150	33.10	110.88	197.60
P2d	1.5	125	47.66	159.67	284.55
P3a	2	250	11.92	39.92	71.14
P3b	2	187.5	21.18	70.97	126.47
P3c	2	150	33.10	110.88	197.60
P3d	2	125	47.66	159.67	284.55

Imperfection tolerances during the erection of steel plate girders and geometrical nonlinearities
Master of Civil Engineering defended by SONNA DONKO Maël
NASPW Yaoundé 2019/2020
94

4.2.2. Ultimate strength

The EC3-1-5's ultimate strength is gotten by applying the equations detailed in part 2.2.2.2, Appendix 1 gives the detailed calculation results for every loading condition. Table 4.5 summarises the ultimate strengths obtained for the 3 loading conditions.

Table 4.5. Summary of EC3-1-5 analytical ultimate strength values

ID	$\alpha = \dfrac{a}{b}$	$\beta = \dfrac{b}{t}$	$f_{u.EC3}$ (N/mm^2)		
			Pure compression $\psi = 1$	Eccentric $\psi = -0.5$	Pure bending $\psi = -1$
P1a	1	250	62.42	159.17	180.76
P1b	1	187.5	82.06	193.59	222.62
P1c	1	150	101.12	224.03	261.43
P1d	1	125	119.59	251.37	297.89
P2a	1.5	250	62.42	159.17	180.76
P2b	1.5	187.5	82.06	193.59	222.62
P2c	1.5	150	101.12	224.03	261.43
P2d	1.5	125	119.59	251.37	297.89
P3a	2	250	62.42	159.17	180.76
P3b	2	187.5	82.06	193.59	222.62
P3c	2	150	101.12	224.03	261.43
P3d	2	125	119.59	251.37	297.89

4.2.3. Imperfection tolerance limits

4.2.3.1. American specification results

The American Welding Society through code AWS D1.1/D1.1M:2010 provides that steel girders with a depth of web, D, and no intermediate stiffeners have a maximum allowable variation from the flatness of webs given by $D/150$. This value is independent of the aspect ratio, the slenderness ratio and even of the stress ratio. In this study, D = b = 1500 mm, thus, $\text{Tolerance limit} = \text{Imp}_{AWS\ D1.1/D1.1M} = 10$ mm.

Imperfection tolerances during the erection of steel plate girders and geometrical nonlinearities
Master of Civil Engineering defended by SONNA DONKO Maël
NASPW Yaoundé 2019/2020

95

4.2.3.2. European specification results

Eurocode provides essential tolerance limits for webs of plated structural elements through EN 1090-2 as stated in part 2.2.2.3. This tolerance limit is independent of the aspect ratio and the stress ratio but depends on the slenderness ratio. The values are computed and given in Table 4.6.

Table 4.6. EN 1090-2 tolerance limits on imperfection amplitudes

ID	$\alpha = \dfrac{a}{b}$	$\beta = \dfrac{b}{t}$	$Imp_{EN\ 1090-2}$ (mm)
P1a	1	250	18.75
P1b	1	187.5	17.58
P1c	1	150	14.06
P1d	1	125	12
P2a	1.5	250	18.75
P2b	1.5	187.5	17.58
P2c	1.5	150	14.06
P2d	1.5	125	12
P3a	2	250	18.75
P3b	2	187.5	17.58
P3c	2	150	14.06
P3d	2	125	12

4.3. FE results

As preliminary studies were performed successfully and the FE formulations for linear buckling and GMNIA analyses were confirmed, the formulations previously detailed in part 2.2.3.2 were implemented to obtain: buckling modes and buckling stresses of the 36 perfect webs of plate girders and; ultimate strengths of the 612 imperfect webs for subsequent comparison with the analytical results.

4.3.1. Buckling stress

The webs of the plates are modelled using the verified FE modelling methods in Abaqus/CAE and launched through a buckle step to obtain the eigenmodes and eigenvalues that will be used to calculate the buckling stress, then used in subsequent GMNIA analyses. The

Imperfection tolerances during the erection of steel plate girders and geometrical nonlinearities
Master of Civil Engineering defended by SONNA DONKO Maël
NASPW Yaoundé 2019/2020
96

eigenmode obtained for each of the 36 plates is given in Table 4.7. Each mode represents the mode of 4 webs with varying thicknesses (plates a,b, c and d).

Table 4.7. Eigenmodes of the webs under study

Loading	Web Plates P1	Web Plates P2	Web Plates P3
$\psi = 1$			
$\psi = -0.5$			
$\psi = -1$			

Imperfection tolerances during the erection of steel plate girders and geometrical nonlinearities
Master of Civil Engineering defended by SONNA DONKO Maël
NASPW Yaoundé 2019/2020

97
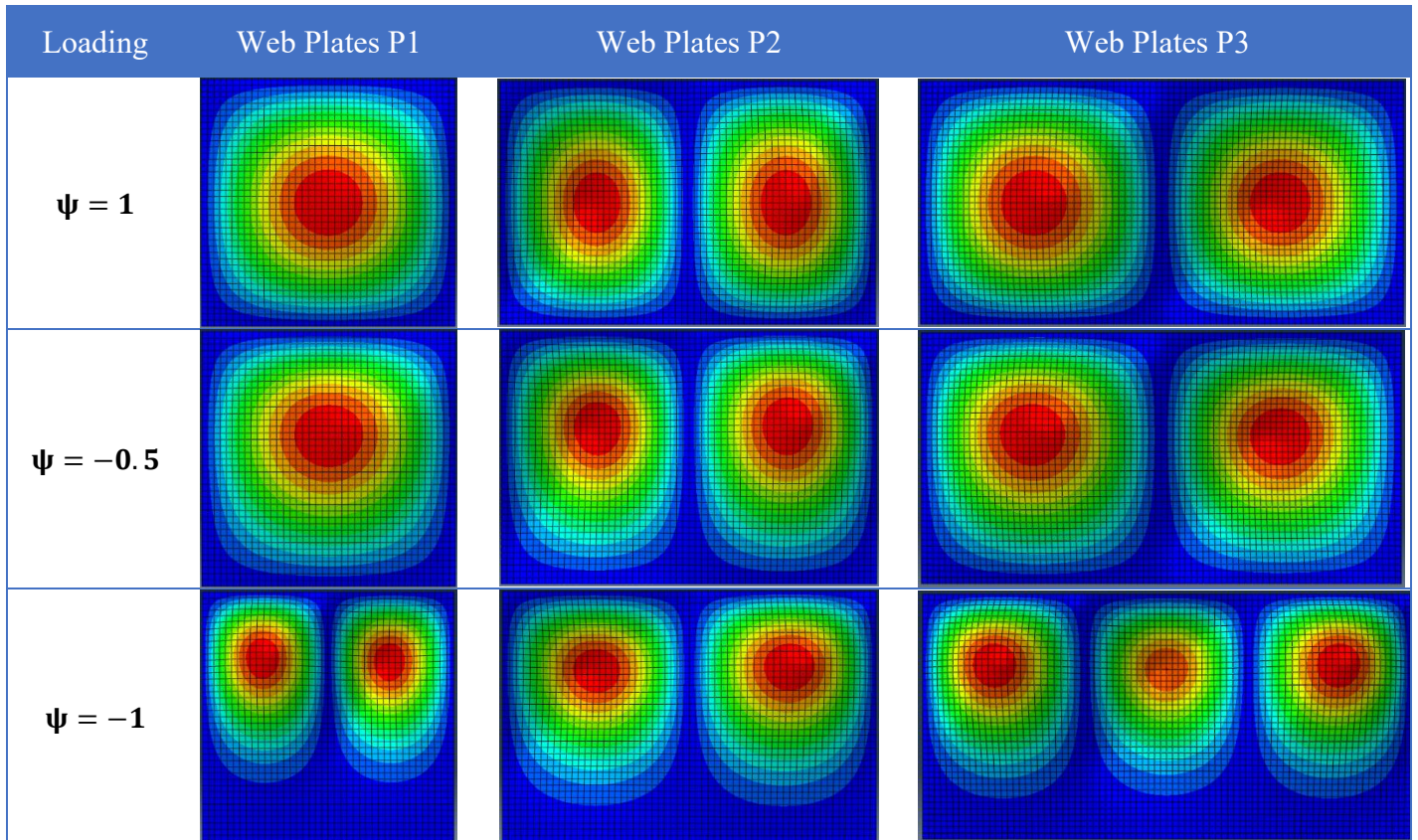
Table 4.8 summarises the buckling stress, of the 36 webs, calculated by dividing the eigenvalues, obtained from Abaqus/CAE linear buckle step, by the web's thickness.

Table 4.8. FE critical stress results

ID	$\alpha = \dfrac{a}{b}$	$\beta = \dfrac{b}{t}$	$\sigma_{cr.FE}$ (N/mm^2)		
			Pure compression $\psi = 1$	Eccentric $\psi = -0.5$	Pure bending $\psi = -1$
P1a	1	250	11.34	38.61	73.78
P1b	1	187.5	20.14	68.59	131.03
P1c	1	150	31.43	107.05	204.46
P1d	1	125	45.21	153.98	293.99
P2a	1.5	250	12.49	39.71	70.58
P2b	1.5	187.5	22.19	70.54	125.38
P2c	1.5	150	34.64	110.11	195.69
P2d	1.5	125	49.83	158.39	281.46
P3a	2	250	11.62	39.42	70.17
P3b	2	187.5	20.65	70.04	124.64
P3c	2	150	32.23	109.34	194.54
P3d	2	125	46.37	157.30	279.82

Imperfection tolerances during the erection of steel plate girders and geometrical nonlinearities
Master of Civil Engineering defended by SONNA DONKO Maël
NASPW Yaoundé 2019/2020

98

4.3.2. Ultimate strength

After going through a Static Riks step, the ultimate strength results were calculated as stated in part 2.2.3.2. 36 results computed at the lowest imperfection amplitude are given in Table 4.9.

Table 4.9. FE ultimate strength results of practically perfect web

ID	$\alpha = \dfrac{a}{b}$	$\beta = \dfrac{b}{t}$	$f_{u.FE}$ at Imp_1 (N/mm^2)		
			Pure compression $\psi = 1$	Eccentric $\psi = -0.5$	Pure bending $\psi = -1$
P1a	1	250	57.26	127.42	173.39
P1b	1	187.5	74.71	169.40	227.98
P1c	1	150	92.41	211.96	278.07
P1d	1	125	110.76	258.68	332.21
P2a	1.5	250	59.70	129.44	171.52
P2b	1.5	187.5	77.66	171.40	226.93
P2c	1.5	150	95.60	213.61	287.66
P2d	1.5	125	113.12	253.43	340.56
P3a	2	250	58.81	128.51	171.91
P3b	2	187.5	76.18	170.89	225.59
P3c	2	150	94.12	214.31	284.03
P3d	2	125	112.68	257.97	335.78

Imperfection tolerances during the erection of steel plate girders and geometrical nonlinearities
Master of Civil Engineering defended by SONNA DONKO Maël
NASPW Yaoundé 2019/2020

99

4.3.3. Ratio of ultimate strength to critical stress

The ratio between the ultimate stress and critical stress was calculated and a plot against slenderness ratio is presented in Figure 4.2.
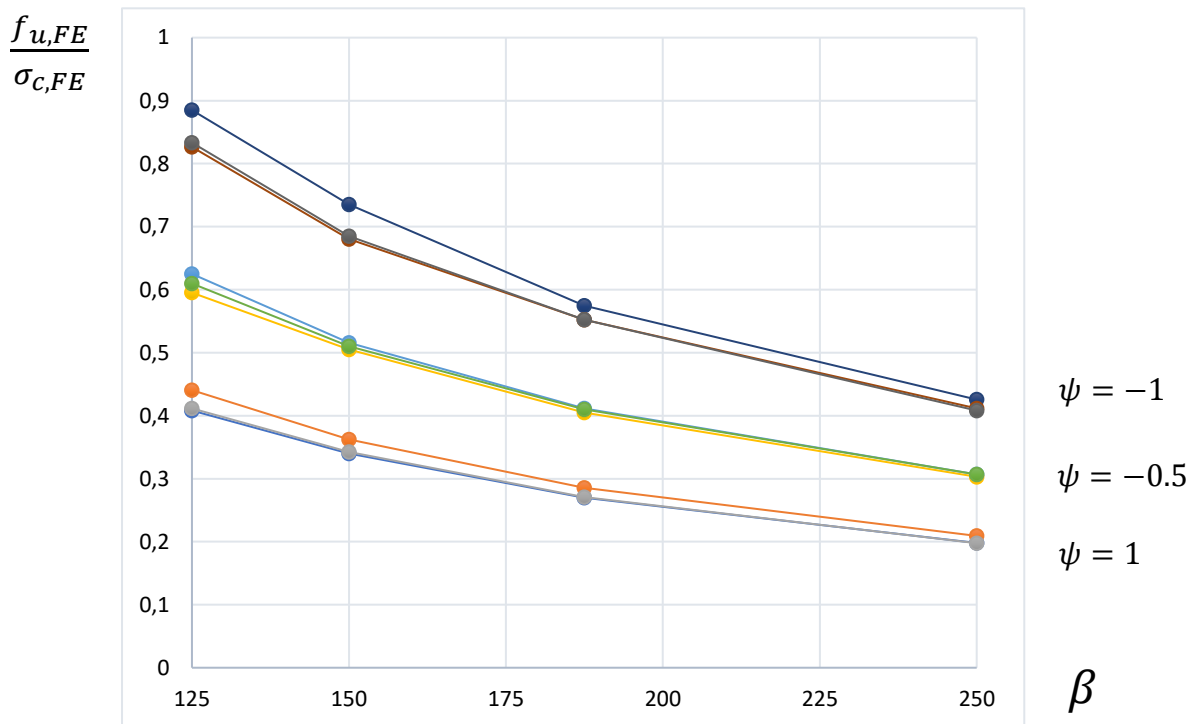
Figure 4.2. Ratio of ultimate strength to critical stress against slenderness ratio graph

This graph shows that, as the slenderness ratio increases the named ratio decreases, thus more slender webs possess higher post-buckling strength reserves. This, irrespective of the loading condition. Also, as the loading condition changes from pure bending ($\psi = -1$) to pure compression ($\psi = 1$), the ratio decreases and the post-buckling reserve increases. As such, very slender webs subjected to pure compression possess a high post-buckling reserve. It is also observed that a change in aspect ratio has little to no effect on the stated ratio as a set of 3 curves are always seen to be quite superimposed for each stress ratio.

Imperfection tolerances during the erection of steel plate girders and geometrical nonlinearities
Master of Civil Engineering defended by SONNA DONKO Maël
NASPW Yaoundé 2019/2020

100

4.4. Results comparison

After the presentation of the code's analytical and FE buckling stresses of the 36 perfect webs, and ultimate strengths of the 612 imperfect webs, a detailed comparison of the results obtained was done, starting with the buckling stresses then the ultimate strengths.

4.4.1. Buckling stress comparison

EC3-1-5 and FE critical stresses are summarised in Table 4.10 and the deviation is calculated. It is found that the maximum deviation between these values is 5.43%, thus showing that EC3-1-5 accurately defines the critical stress of the web of plate girders ($< 10\%$).

Also, these results show that the FE model used for these analyses can be adequately used for other research studies on the critical stress of the web of plate girders.

Table 4.10. EC3-1-5 vs FE critical stress comparison

ID	$\alpha = \dfrac{a}{b}$	$\beta = \dfrac{b}{t}$	Pure compression $\psi = 1$			Eccentric $\psi = -0.5$			Pure bending $\psi = -1$		
			$\sigma_{cr.EC3}$	$\sigma_{cr.FE}$	$\Delta\sigma_{cr}\%$	$\sigma_{cr.EC3}$	$\sigma_{cr.FE}$	$\Delta\sigma_{cr}\%$	$\sigma_{cr.EC3}$	$\sigma_{cr.FE}$	$\Delta\sigma_{cr}\%$
P1a	1	250	11.92	11.34	**5.09**	39.92	38.61	**3.38**	71.14	73.78	**3.59**
P1b	1	187.5	21.18	20.14	**5.19**	70.97	68.59	**3.47**	126.47	131.03	**3.48**
P1c	1	150	33.10	31.43	**5.30**	110.88	107.05	**3.58**	197.60	204.46	**3.35**
P1d	1	125	47.66	45.21	**5.43**	159.67	153.98	**3.70**	284.55	293.99	**3.21**
P2a	1.5	250	11.92	12.49	**4.60**	39.92	39.71	**0.53**	71.14	70.58	**0.79**
P2b	1.5	187.5	21.18	22.19	**4.52**	70.97	70.54	**0.61**	126.47	125.38	**0.87**
P2c	1.5	150	33.10	34.64	**4.44**	110.88	110.11	**0.70**	197.60	195.69	**0.98**
P2d	1.5	125	47.66	49.83	**4.35**	159.67	158.39	**0.81**	284.55	281.46	**1.10**
P3a	2	250	11.92	11.62	**2.53**	39.92	39.42	**1.26**	71.14	70.17	**1.38**
P3b	2	187.5	21.18	20.65	**2.60**	70.97	70.04	**1.33**	126.47	124.64	**1.47**
P3c	2	150	33.10	32.23	**2.69**	110.88	109.34	**1.41**	197.60	194.54	**1.58**
P3d	2	125	47.66	46.37	**2.79**	159.67	157.30	**1.51**	284.55	279.82	**1.69**

These results are also represented as a ratio form in Figure 4.3 where it is noticed that the analytical results given by EC3-1-5 are almost always non-conservative.

Imperfection tolerances during the erection of steel plate girders and geometrical nonlinearities
Master of Civil Engineering defended by SONNA DONKO Maël
NASPW Yaoundé 2019/2020

101
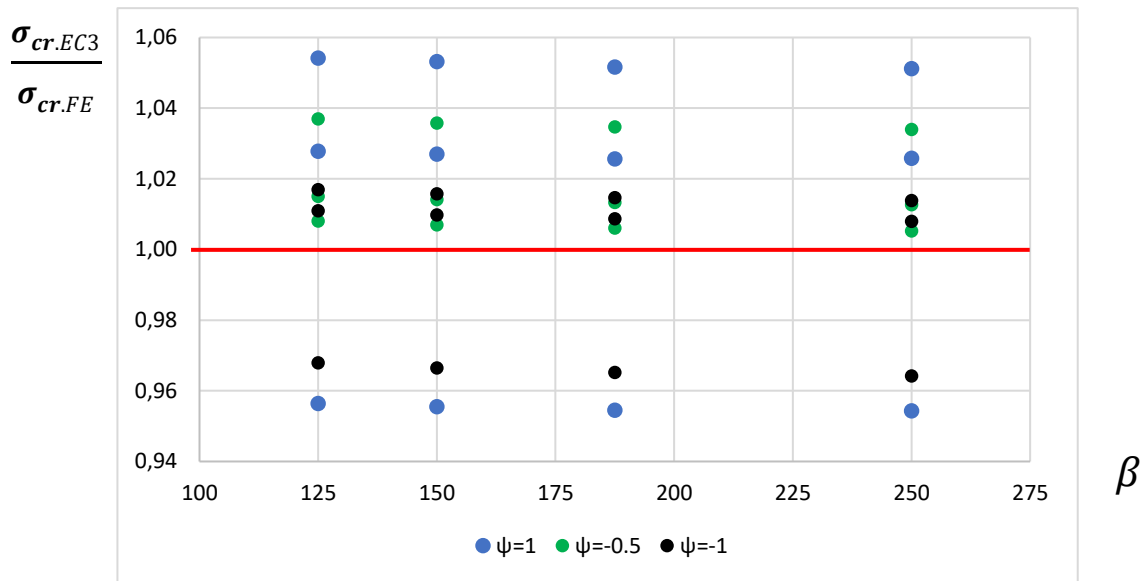
Figure 4.3. Ratio of EC3-1-5 to FE critical stress against slenderness ratio graph

4.4.2. Ultimate strength comparison

4.4.2.1. Strength at least imperfection

Here, the ultimate strength computed from EC3-1-5 and the FE results considering an imperfection amplitude of $\text{Imp}_1 = 0.015$ mm were summarised and compared in Table 4.11.

Table 4.11. Analytical EC3-1-5 vs FE ultimate strength at least imperfection comparison

ID	$\alpha = \dfrac{a}{b}$	$\beta = \dfrac{b}{t}$	Pure compression $\psi = 1$			Eccentric $\psi = -0.5$			Pure bending $\psi = -1$		
			$f_{u.EC3}$	$f_{u.FE}$	$\Delta f_u\%$	$f_{u.EC3}$	$f_{u.FE}$	$\Delta f_u\%$	$f_{u.EC3}$	$f_{u.FE}$	$\Delta f_u\%$
P1a	1	250	62.42	57.26	**9.01**	159.17	127.42	**24.91**	180.76	173.39	**4.25**
P1b	1	187.5	82.06	74.71	**9.83**	193.59	169.40	**14.28**	222.62	227.98	**2.35**
P1c	1	150	101.12	92.41	**9.42**	224.03	211.96	**5.69**	261.43	278.07	**5.98**
P1d	1	125	119.59	110.76	**7.97**	251.37	258.68	**2.82**	297.89	332.21	**10.33**
P2a	1.5	250	62.42	59.70	**4.55**	159.17	129.44	**22.96**	180.76	171.52	**5.39**
P2b	1.5	187.5	82.06	77.66	**5.67**	193.59	171.40	**12.94**	222.62	226.93	**1.90**
P2c	1.5	150	101.12	95.60	**5.77**	224.03	213.61	**4.88**	261.43	287.66	**9.12**
P2d	1.5	125	119.59	113.12	**5.73**	251.37	253.43	**0.81**	297.89	340.56	**12.53**
P3a	2	250	62.42	58.81	**6.14**	159.17	128.51	**23.85**	180.76	171.91	**5.15**
P3b	2	187.5	82.06	76.18	**7.71**	193.59	170.89	**13.29**	222.62	225.59	**1.32**
P3c	2	150	101.12	94.12	**7.44**	224.03	214.31	**4.54**	261.43	284.03	**7.96**
P3d	2	125	119.59	112.68	**6.13**	251.37	257.97	**2.56**	297.89	335.78	**11.29**

Imperfection tolerances during the erection of steel plate girders and geometrical nonlinearities
Master of Civil Engineering defended by SONNA DONKO Maël
NASPW Yaoundé 2019/2020

102

Results show that the FE ultimate strength results deviate a lot from the EC3-1-5 analytical results with a maximum deviation of up to 24.91%. This occurs in slender plates when $\psi = -0.5$ and -1.

However, high deviations in slender plates are normal as many tests presented in Nishino et. al (1967), Dwight et. al (1968), Fukumoto and Itoh (1984) showed that Winter's function (used in EC3-1-5) tends to overestimate the ultimate resistance of slender plates. This occurs because Winter's equation was derived from his experiments on cold-formed plates different from the hot-rolled plates that make up steel plate girders

Also, the stocky plates' strength deviations can be explained by the fact that the slenderness ratio is getting closer to the critical slenderness value of $\beta_{cr} = 111.96$.

Figure 4.4 tends to confirm that for all plates, apart from those subjected to pure bending, Eurocode's ultimate strength formulation is overestimated.
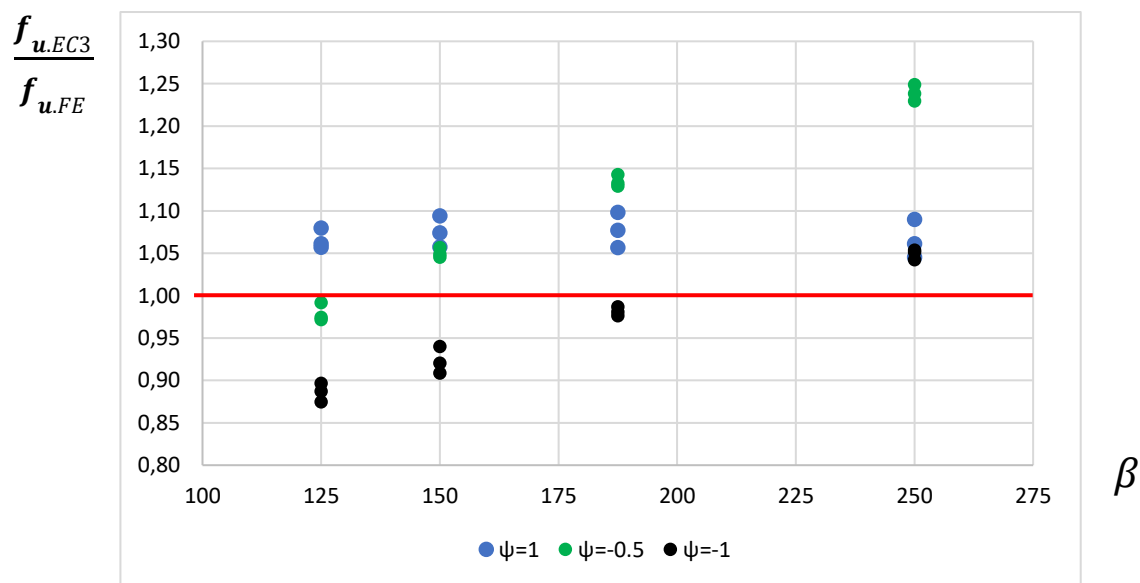
Figure 4.4. Ratio of EC3-1-5 to FE ultimate strength against slenderness ratio graph

Imperfection tolerances during the erection of steel plate girders and geometrical nonlinearities
Master of Civil Engineering defended by SONNA DONKO Maël
NASPW Yaoundé 2019/2020
103

4.4.2.2. Strength at the tolerance limit

Here, the aim was to find the difference in strength between Eurocode's analytical formulation and the FE strength at Eurocode's imperfection tolerance limit. Thus, besides the analytical values, Table 4.12 presents the values of FE ultimate strength found with the initial imperfection limit that corresponds to the tolerance limit values calculated in 4.2.2.

Table 4.12. Analytical EC3-1-5 vs FE ultimate strength at tolerance limit comparison

ID	$\alpha = \dfrac{a}{b}$	$\beta = \dfrac{b}{t}$	Pure compression $\psi = 1$			Eccentric $\psi = -0.5$			Pure bending $\psi = -1$		
			$f_{u.EC3}$	$f_{u.FE}$	$\Delta f_u\%$	$f_{u.EC3}$	$f_{u.FE}$	$\Delta f_u\%$	$f_{u.EC3}$	$f_{u.FE}$	$\Delta f_u\%$
P1a	1	250	62.42	56.24	**10.99**	159.17	122.79	**29.63**	180.76	150.52	**20.09**
P1b	1	187.5	82.06	72.70	**12.87**	193.59	159.12	**21.66**	222.62	187.37	**18.81**
P1c	1	150	101.12	89.90	**12.48**	224.03	201.25	**11.32**	261.43	222.86	**17.31**
P1d	1	125	119.59	108.05	**10.68**	251.37	237.12	**6.01**	297.89	258.71	**15.14**
P2a	1.5	250	62.42	57.70	**8.17**	159.17	120.71	**31.86**	180.76	159.52	**13.32**
P2b	1.5	187.5	82.06	73.88	**11.06**	193.59	156.59	**23.63**	222.62	203.11	**9.60**
P2c	1.5	150	101.12	89.72	**12.71**	224.03	193.79	**15.60**	261.43	250.48	**4.37**
P2d	1.5	125	119.59	108.13	**10.60**	251.37	228.08	**10.21**	297.89	287.09	**3.76**
P3a	2	250	62.42	57.64	**8.28**	159.17	123.00	**29.41**	180.76	157.17	**15.01**
P3b	2	187.5	82.06	74.12	**10.71**	193.59	161.08	**20.18**	222.62	200.66	**10.94**
P3c	2	150	101.12	91.54	**10.46**	224.03	201.19	**11.35**	261.43	241.23	**8.37**
P3d	2	125	119.59	109.90	**8.82**	251.37	240.67	**4.45**	297.89	277.02	**7.53**

Eurocode's analytical strength results are found to be around 20% more than the FE ultimate strength at Eurocode's tolerance limit. This result proves that either the tolerance limit is too large or the analytical provision is overestimated. The second option is more feasible as the tolerance limit will be proven to be instead too strict.

Imperfection tolerances during the erection of steel plate girders and geometrical nonlinearities
Master of Civil Engineering defended by SONNA DONKO Maël
NASPW Yaoundé 2019/2020

104

4.5. Proposed equations

This section provides the effects of the aspect ratio, slenderness ratio, stress ratio and initial imperfection amplitude on the ultimate strength of the webs of plate girders, then with the help of the known effects, regression hypotheses are defined and the derived ultimate strength and tolerance limit equations are presented.

4.5.1. Effect of parameters

Having obtained the ultimate strength values of 612 imperfect webs, the effect of every parameter was studied. The results obtained were presented on a logarithmic scale, which best suits its behaviour, 3D graphs are drawn using Graph Expert Professional (Hyams, 2014). The effects of initial imperfection amplitude (amplitude parameter, k) are implicitly represented.

4.5.1.1. Effect of aspect ratio

The 3D graph of Figure 4.5 summarises the results obtained for all the 612 imperfect webs and it was found that a change in aspect ratio does not have a significant influence on the ultimate strength of the web of plate girders as the curves are superimposed. This happens no matter the initial imperfection amplitude.
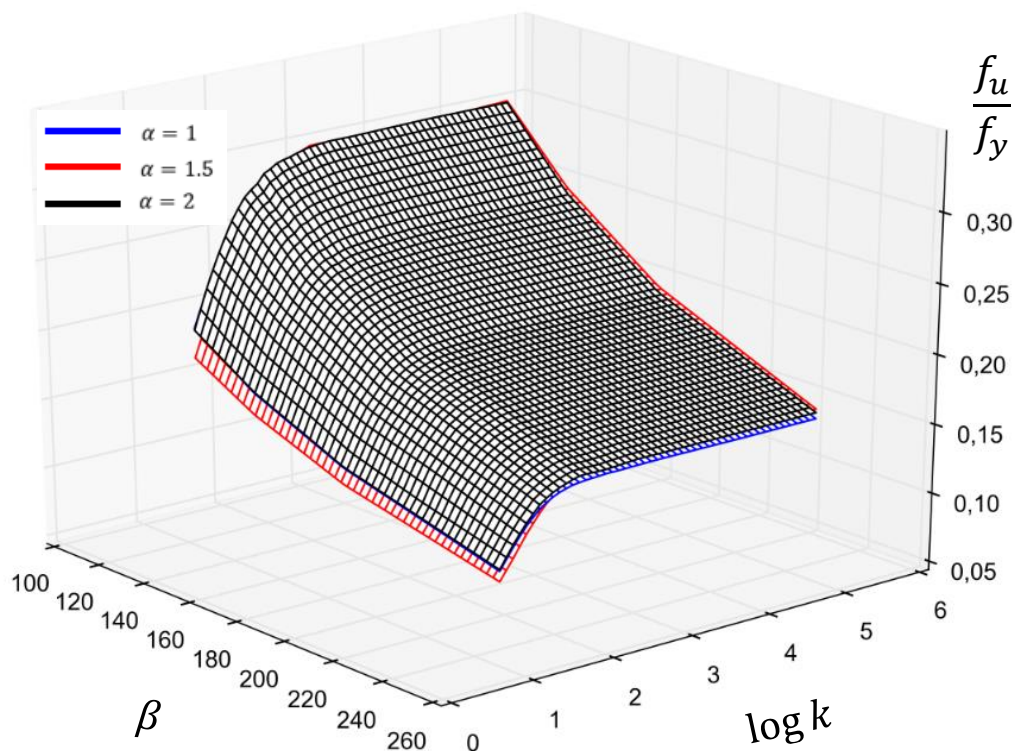
Figure 4.5. 3D graphical summary of the effect of aspect ratio

Imperfection tolerances during the erection of steel plate girders and geometrical nonlinearities
Master of Civil Engineering defended by SONNA DONKO Maël
NASPW Yaoundé 2019/2020
105

4.5.1.2. Effect of slenderness ratio

Here, it was realised that an increase in the slenderness ratio leads to a decrease in the ultimate strength of the plate, no matter the imperfection amplitude. Also, it was noticed that for every loading condition, the rate at which the strength decreases is increased as the slenderness ratio decreases. The graph in Figure 4.6 summarises the behaviour of the webs, with different aspect ratios and slenderness ratios, as initial imperfection amplitude decreases.

It was again noticed that aspect ratio has no reasonable influence and that the strength increases as the slenderness ratio decreases.
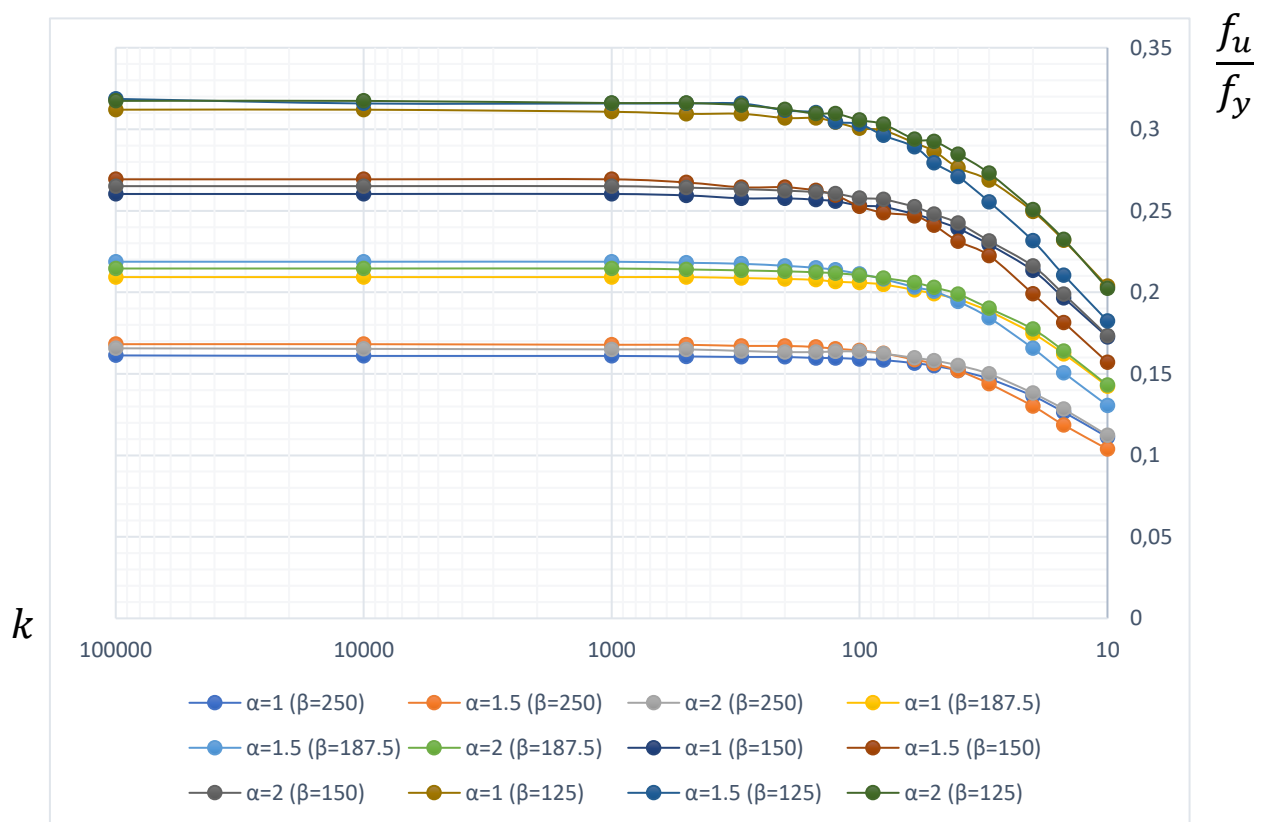
Figure 4.6. Effect of slenderness ratio on the drop in ultimate strength for all aspect ratios during pure compression

The 3D graph of Figure 4.7 summarises the results obtained for all the 612 webs and confirms that the slenderness ratio has an inverse effect on the ultimate strength.

Imperfection tolerances during the erection of steel plate girders and geometrical nonlinearities
Master of Civil Engineering defended by SONNA DONKO Maël
NASPW Yaoundé 2019/2020

106
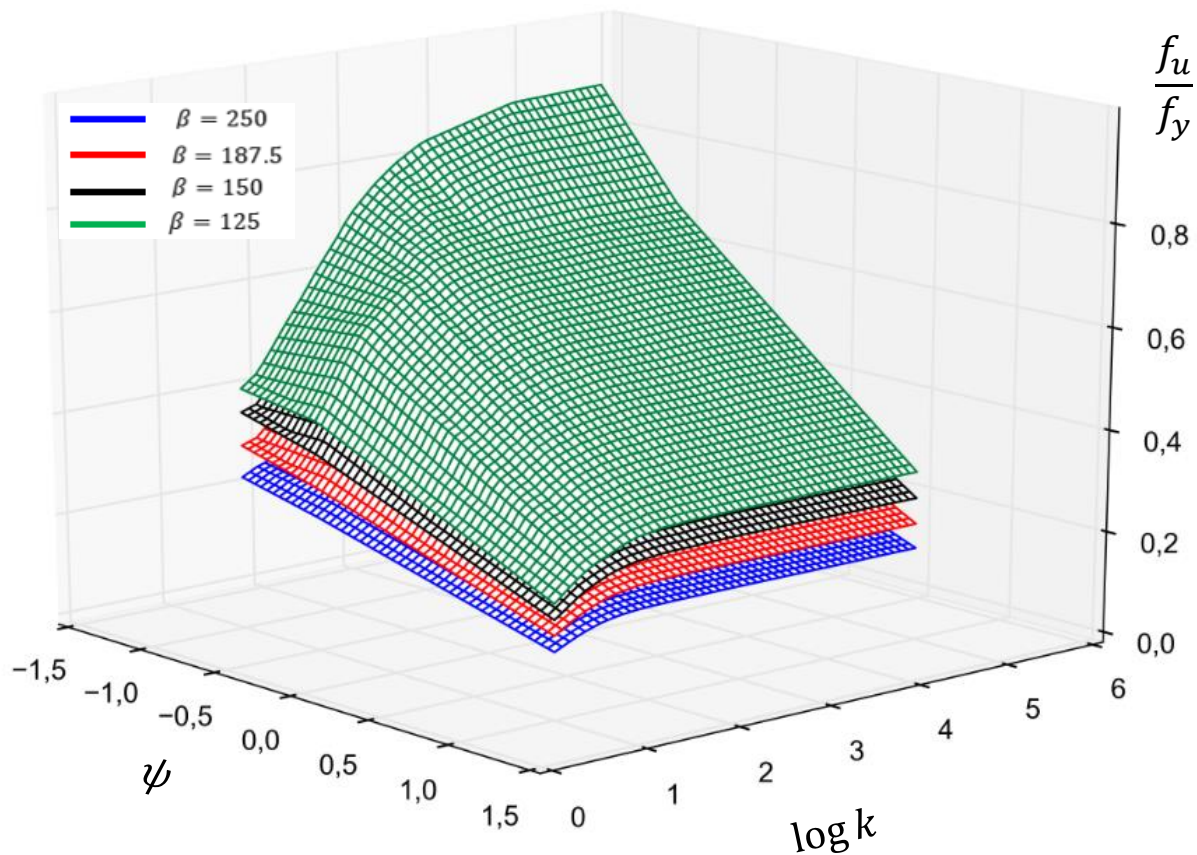
Figure 4.7. 3D graphical summary of the effect of slenderness ratio

4.5.1.3. Effect of stress ratio

As loading changes from pure compression ($\psi = 1$) to pure bending ($\psi = -1$), it was well noticed that the strength of the plate increases. Also, for webs subjected to more bending, the post-buckling reserve tends to increase faster as the slenderness ratio increases. This is noticed, in Figure 4.9, by the fact that ultimate strength tends to occur at yield strength. Figure 4.9 shows the results obtained for all the 12 square webs under all the 3 loading conditions.

The curves seen close to each other are those representing varying aspect ratios. Thus, it is realised that the aspect ratio still has little to no effect on ultimate strength.

The 3D graph of Figure 4.8 summarises the results obtained for all the 612 webs under study and confirms that the stress ratio has an inverse relationship with the ultimate strength.

Imperfection tolerances during the erection of steel plate girders and geometrical nonlinearities   107
Master of Civil Engineering defended by SONNA DONKO Maël
NASPW Yaoundé 2019/2020
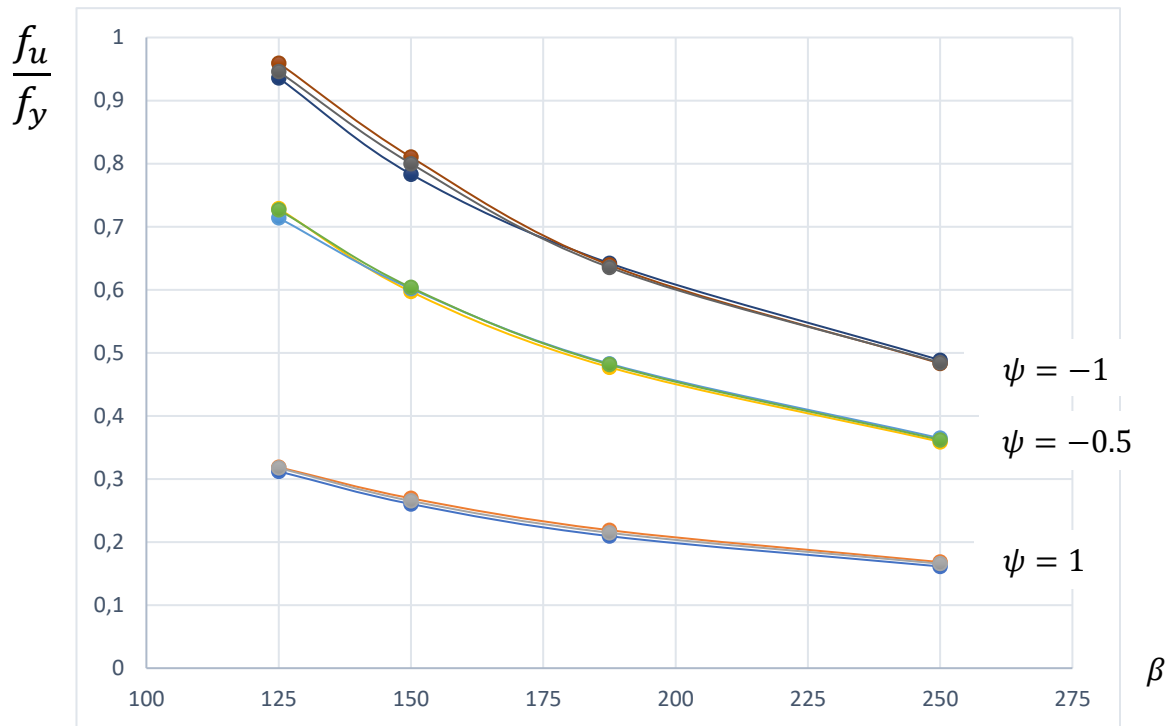
Figure 4.9. Effect of stress ratio on the drop in ultimate strength for all the plates at lowest initial imperfection amplitude
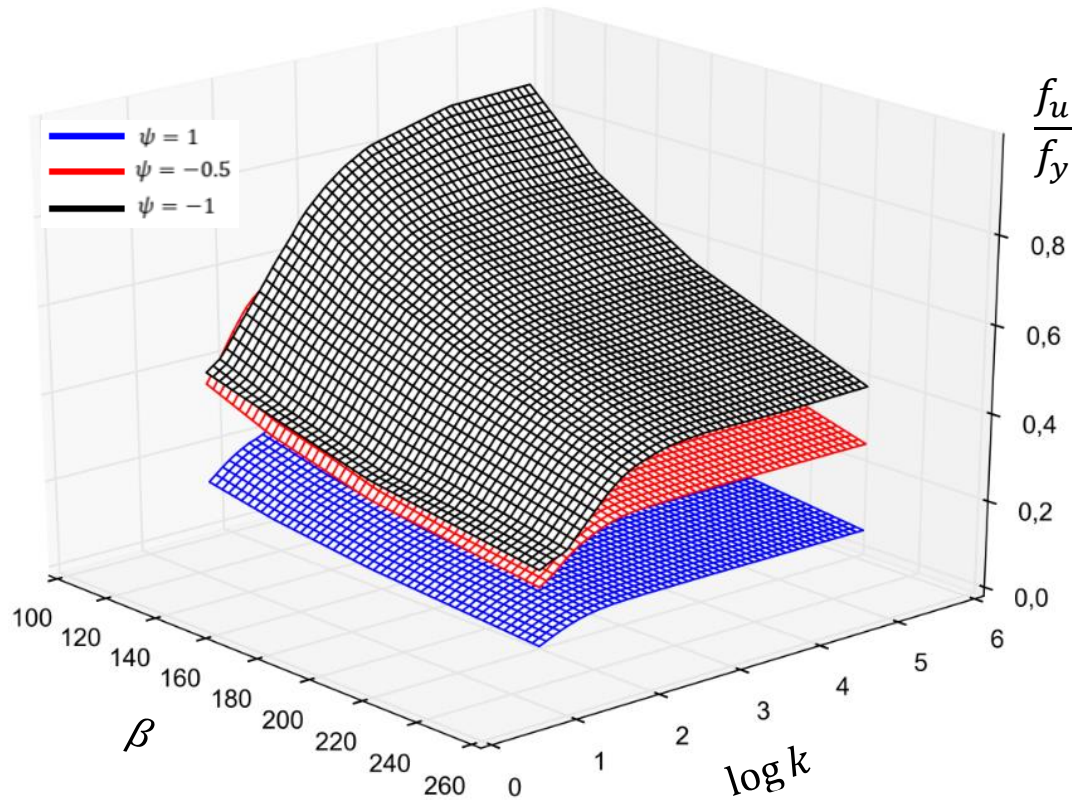
Figure 4.8. 3D graphical summary of the effect of stress ratio

Imperfection tolerances during the erection of steel plate girders and geometrical nonlinearities
Master of Civil Engineering defended by SONNA DONKO Maël
NASPW Yaoundé 2019/2020

108

4.5.2. Proposed ultimate strength equation

FE ultimate strengths were computed for 612 imperfect webs and the results obtained went through thorough parametric studies, trends were noticed in the graphs obtained and thus a possibility was seen to set up, through a regression study, an ultimate strength equation as a function of the parameters studied. This was done by defining a regression study hypothesis, deriving the equation and then verifying it.

4.5.2.1. Regression hypothesis

It was hypothesised, after a parametric study, that the aspect ratio does not have a significant influence on the ultimate strength of the web of plate girders, on the other hand, slenderness ratio and initial imperfection amplitude have inverse relationships for every loading condition. Furthermore, varying the loading condition also has an inverse relationship with the strength. As such, using regression analysis, an equation is derived to describe precisely the influence of these parameters on the ultimate strength of the web plate.

4.5.2.2. Equation derivation

Here, a multiple nonlinear regression analysis technique was used to study the effect of loading condition (stress ratio), slenderness ratio and initial imperfection amplitude on the strength.

A first analysis is done on Curve Expert Professional (Hyams, 2018) to determine the appropriate relationship between the parameters. The form obtained is given by equation (4.3).

$$\frac{f_u}{f_y}(\psi, \beta, \delta) = \frac{a + b \cdot \psi + c \cdot \beta + d \cdot \delta}{1 + e \cdot \psi + f \cdot \beta + g \cdot \delta} \qquad (4.3)$$

where: a, b, c, d, e, f and g are constants to be determined.

The equation is then used to obtain precise values of the constants. The values are obtained with correlation coefficients of determination, $R^2 = 99.32\%$ and $R = 99.66\%$ and shown in Appendix 2. These results show excellent conformity between the derived equation and the FE nonlinear results. Then, equation (4.4) is obtained as:

$$\frac{f_u}{f_y}(\psi, \beta, \delta) = \frac{1,57982 - 0,468445 \cdot \psi - 0,00193765 \cdot \beta + 0,00232979 \cdot \delta}{1 + 0,358912 \cdot \psi + 0,0109572 \cdot \beta + 0,0214963 \cdot \delta} \qquad (4.4)$$

Imperfection tolerances during the erection of steel plate girders and geometrical nonlinearities
Master of Civil Engineering defended by SONNA DONKO Maël
NASPW Yaoundé 2019/2020
109

The last step consisted of manually refining the constants to reduce errors between the FE results and the results obtained from the equation. This was done keeping in mind the 95% confidence interval obtained and presented in Table 4.13.

Table 4.13. Range of 95% confidence interval for all the constants

Constant	Value	Range (95% confidence)	
		Lower limit	Upper limit
a	1.579830	1.32	1.84
b	-0.468448	-0.59	-0.35
c	-0.001938	-0.0022	-0.0017
d	0.002330	0.001	0.003
e	0.358910	0.29	0.43
f	0.010957	0.0074	0.014
g	0.021496	0.02	0.03

The final equation was then given in equation (4.5)

$$\forall\ \alpha \in [1, 2],$$

$$\forall\ \beta \in [125, 250],$$

$$\forall\ \delta \in \left[\frac{b}{100\ 000}, \frac{b}{20}\right] \text{ and}$$

$$\forall\ \psi \in [-1, 1]$$

$$\frac{f_u}{f_y}(\psi, \beta, \delta) = \frac{1{,}54 - 0{,}445 \cdot \psi - 0{,}002 \cdot \beta + 0{,}0024\ \cdot \delta}{1 + 0{,}3 \cdot \psi + 0{,}0108 \cdot \beta + 0{,}024 \cdot \delta} \tag{4.5}$$

4.5.2.3. Equation verification

To verify the equation derived, a web model, different from the ones used in the analyses, was selected from the range of study. This web had properties given in equation (4.6).

$$\begin{cases} a = b = 1200 \text{ mm} \\ t = 6 \text{ mm} \end{cases} \Longrightarrow \begin{cases} \alpha = 1 \\ \beta = 200 \end{cases} \tag{4.6}$$

The chosen web of plate girder is subjected to an eccentric compression with stress ratio $\psi = 0.5$. It is modelled using the verified FE modelling procedure. The FE results obtained and the results given by the derived formula are presented in Table 4.14 and compared.

Imperfection tolerances during the erection of steel plate girders and geometrical nonlinearities
Master of Civil Engineering defended by SONNA DONKO Maël
NASPW Yaoundé 2019/2020
110

Table 4.14. Deviation of the proposed equation from the FE results

Imperfection	k	$\delta = \dfrac{b}{k}$ (mm)	$\dfrac{f_{u,FE}}{f_y}$	$\dfrac{f_{u,Equation}}{f_y}$	$\Delta \dfrac{f_u}{f_y}$
Imp_1	100000	0.012	0.253	0.277	9.69
Imp_2	10000	0.12	0.253	0.277	9.69
Imp_3	1000	1.2	0.253	0.276	9.09
Imp_4	500	2.4	0.252	0.274	8.78
Imp_5	300	4	0.251	0.272	8.29
Imp_6	200	6	0.249	0.270	8.19
Imp_7	150	8	0.250	0.267	6.97
Imp_8	125	9.6	0.250	0.266	6.25
Imp_9	100	12	0.248	0.263	6.03
Imp_{10}	80	15	0.246	0.260	5.59
Imp_{11}	60	20	0.242	0.255	5.23
Imp_{12}	50	24	0.239	0.251	5.09
Imp_{13}	40	30	0.233	0.246	5.17
Imp_{14}	30	40	0.226	0.237	5.26
Imp_{15}	20	60	0.208	0.223	7.65

The results obtained here show a maximum deviation of 9.69%. Thus, this confirms the reliability of the derived equation on the range of the parameters studied.

4.5.3. Proposed tolerance limit

Tolerance limits on imperfections in the web of plate girders are given by specific codes. Past studies have shown that these limits are usually strict and conservative. Also, these limits are found not to be completely inclusive. A normalised drop in strength was used to derive a less conservative and more inclusive parameter-wise equation for tolerance limit. To do this, a regression study hypothesis was defined followed by an equation derivation and verification.

4.5.3.1. Regression hypothesis

After obtaining a verified ultimate strength equation that is a function of loading condition (stress ratio), slenderness ratio and imperfection amplitude, it is then understood that tolerance limit on the web's initial imperfection amplitude is a function of both stress ratio and

Imperfection tolerances during the erection of steel plate girders and geometrical nonlinearities
Master of Civil Engineering defended by SONNA DONKO Maël
NASPW Yaoundé 2019/2020
111

slenderness ratio as opposed to that given by EN 1090-2 and AWS D1.1/D1.1M. As such, a study is conducted to find an equation that explicitly demonstrates the effect of both loading condition and slenderness ratio on the tolerance limit.

4.5.3.2. Equation derivation

To achieve this, the following procedure was executed: identify the tolerance limits proposed by international codes and research papers; determine the drop in ultimate strength of a web with the aforementioned proposed tolerance limit as imperfection amplitude using the derived strength equation, the drop is calculated from the supposed perfect web with minimum imperfection amplitude $\delta = Imp_1$; determine the most appropriate curve that perfectly describes this drop and obtain its equation which will be a function of both loading condition and slenderness ratio.

a) Research works' tolerance limits

Added to AWS D1.1/D1.1M and EN 1090-2 tolerance limits calculated in part 4.2.3, some researchers (Rangelov, 1992; Sadovský & Baláž, 1996) also proposed theoretical strength-based approach tolerances on initial imperfection amplitudes of the web of plate girders. These limits are given in equation (4.7).

$$\text{Tolerance limits} = \begin{cases} \text{Imp}_{\text{Rangelov}} = \dfrac{b^2}{30\,000 \cdot t} \\ \text{Imp}_{\text{Sadovský}} = \dfrac{b^2}{15\,000 \cdot t} \end{cases} \quad \text{for } \; b/t \geq 120 \qquad (4.7)$$

b) Maximum drop in FE ultimate strength at tolerance limits

The equation of drop in FE strength was gotten from the derived strength equation. This drop in strength was given by equation (4.8) as:

$$\begin{cases} \Delta f_u(\psi, \beta, \delta) = \dfrac{f_u(\psi, \beta, \delta = Imp_1) - f_u(\psi, \beta, \delta)}{f_u(\psi, \beta, \delta = Imp_1)} \cdot 100 \\ \Rightarrow \Delta f_u(\psi, \beta, Imp_i)\% = 1 - \dfrac{f_u(\psi, \beta, Imp_i)}{f_u(\psi, \beta, Imp_1)} \\ \Rightarrow \Delta f_u(\psi, \beta, Imp_i)\% = 1 - \dfrac{g(\psi, \beta, Imp_i)}{g(\psi, \beta, Imp_1)} \end{cases} \qquad (4.8)$$

where $g(\delta) = \dfrac{f_u}{f_y}(\delta)$

Imperfection tolerances during the erection of steel plate girders and geometrical nonlinearities
Master of Civil Engineering defended by SONNA DONKO Maël
NASPW Yaoundé 2019/2020

112

This drop in strength was plotted for each set of tolerance limit as seen in Figure 4.10.
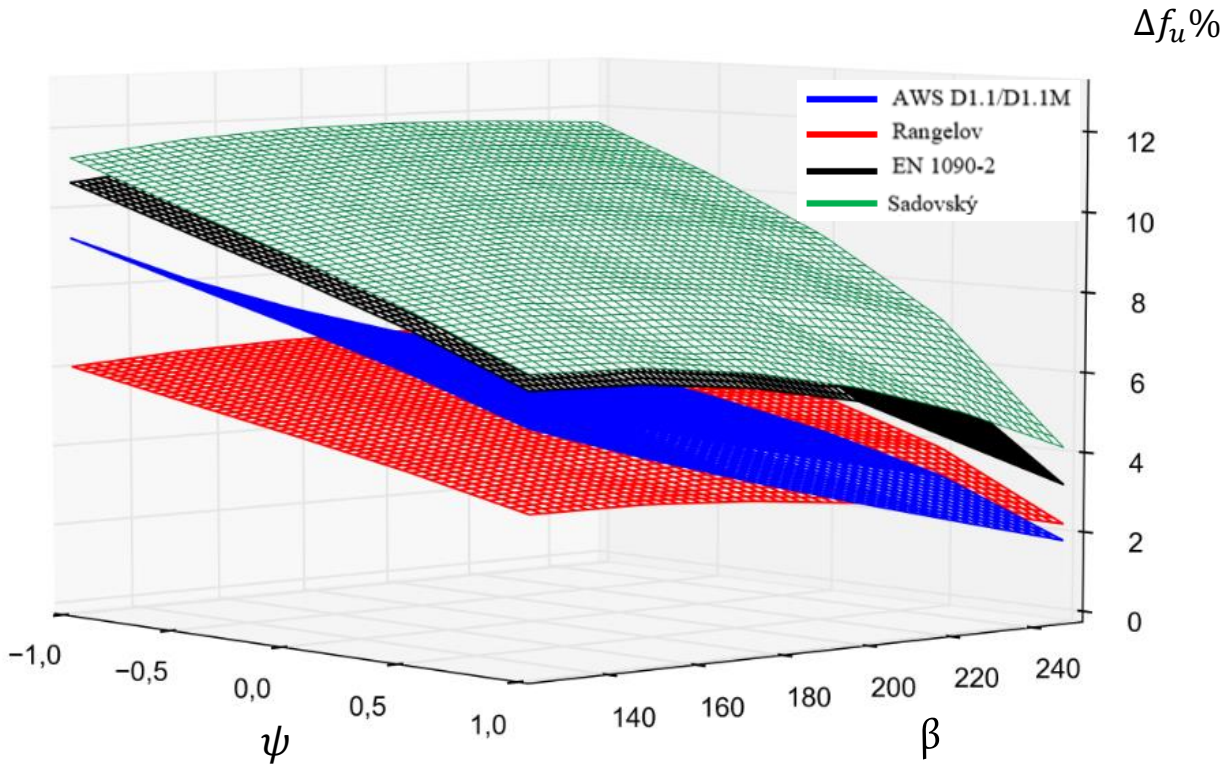
Figure 4.10. 3D graphical representation of the drop in strength at given tolerance limits

It was then realised that the tolerance limit given by AWS D1.1/D1.1M and that given by Rangelov are too conservative with strength reduction as low as 2%. Also, it was realised that the EN 1090-2 tolerance limit, with a maximum drop of 11.15%, has an appropriate drop and is a conservative form of the limit given by Sadovský.

c) Tolerance determination

The maximum drop in the strength of 11.15% was then fixed as a normalised drop for the range of values of the study. Thus, the imperfection amplitude that corresponds to this normalised fixed drop was determined.

From equation (4.8), equations (4.9) to (4.13) were obtained.

$$\Delta f_u \% = 1 - \frac{g(\delta = Imp_i)}{g(\delta = Imp_1)} \tag{4.9}$$

and

$$g(\psi, \beta, \delta) = \frac{f_u}{f_y}(\psi, \beta, \delta) = \frac{1{,}54 - 0{,}445 \cdot \psi - 0{,}002 \cdot \beta + 0{,}0024 \cdot \delta}{1 + 0{,}3 \cdot \psi + 0{,}0108 \cdot \beta + 0{,}024 \cdot \delta} \tag{4.10}$$

Imperfection tolerances during the erection of steel plate girders and geometrical nonlinearities
Master of Civil Engineering defended by SONNA DONKO Maël
NASPW Yaoundé 2019/2020

113

yielding,

$$g(\psi, \beta, Imp_i) = (1 - \Delta f_u\%)g(\psi, \beta, \delta = Imp_1) \tag{4.11}$$

$$\Rightarrow Imp_i = \frac{(1 + 0,3 \cdot \psi + 0,0108 \cdot \beta) \cdot (1 - \Delta f_u\%) \cdot g(\psi, \beta, Imp_1) - (1,54 - 0,445 \cdot \psi - 0,002 \cdot \beta)}{0,0024 - 0,024 \cdot (1 - \Delta f_u\%) \cdot g(\psi, \beta, Imp_1)} \tag{4.12}$$

where: $\Delta f_u = 11.15\%$

$$\Rightarrow Imp_i = \frac{0.9 \cdot (1 + 0,3 \cdot \psi + 0,0108 \cdot \beta) \cdot g(\psi, \beta, Imp_1) - (1,54 - 0,445 \cdot \psi - 0,002 \cdot \beta)}{0,0024 - 0,0216 \cdot g(\psi, \beta, Imp_1)} \tag{4.13}$$

This equation was represented on the graph of Figure 4.11. Also, the tolerances given by AWS D1.1/D1.1M and EN 1090-2 were plotted for comparison.

The results obtained show that the initial imperfection amplitude obtained at a fixed global drop in the strength of 11.15% was always higher than AWS D1.1/D1.1M and EN 1090-2 tolerance limits.

As already stated in b), AWS D1.1/D1.1M tolerance was found to be too conservative. It was also noted that, for the normalised drop in strength, EN 1090-2 tolerance limit was found to be slightly conservative at low slenderness ratio values during pure bending loading. This is seen on the graph as both the proposed tolerance limit and EN 1090-2 limit are tangent to each other. As the slenderness ratio becomes more than 200 and the stress ratio increases, the limit given by EN 1090-2 becomes more and more conservative. Therefore, for a normalised drop in strength, the tolerance limits proposed by both codes can be relaxed.

d) Derivation

From the graph of Figure 4.11, a simplified equation can be derived which explicitly describes the proposed tolerance limit as a function of stress ratio and slenderness limit.

The equation was derived by using a multiple nonlinear regression analysis technique employed in Curve Expert Professional (Hyams, 2018). This yielded equation (4.14).

$$\text{Proposed Tolerance Limit} = Imp_{Proposed} = a \cdot [(b \cdot \psi + c)^2 + (d \cdot \beta + e)^2] \tag{4.14}$$

where: $a = 0.000224, b = 80.23, c = 184.218, d = 0.948$ and $e = 81.67$

These values of the constants obtained had correlation coefficients of determination, $R^2 = 98.41\%$ and $R = 99.20\%$ and are shown in Appendix 3. These results

Imperfection tolerances during the erection of steel plate girders and geometrical nonlinearities
Master of Civil Engineering defended by SONNA DONKO Maël
NASPW Yaoundé 2019/2020

114

showed good conformity between the derived equation and the proposed tolerance curve of Figure 4.11.
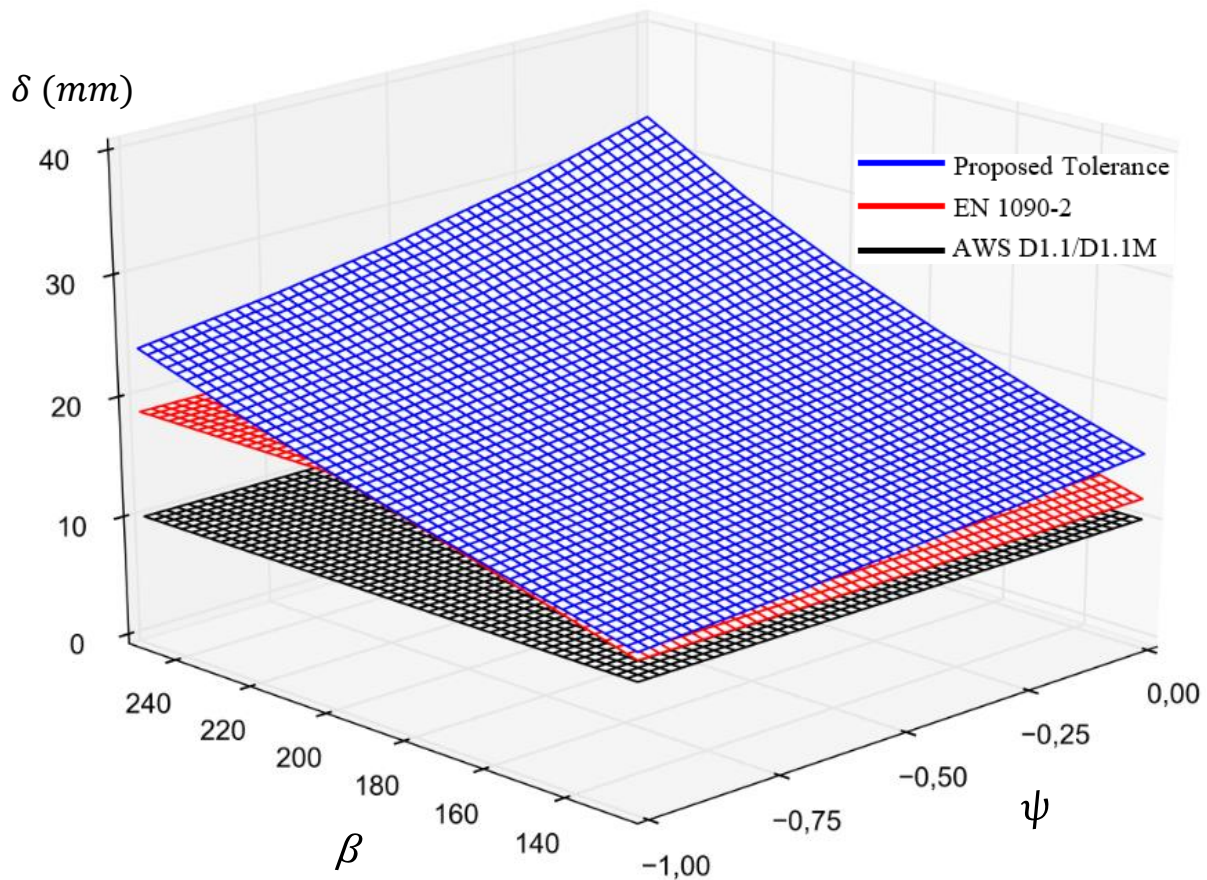
Figure 4.11. Comparison between the proposed tolerance limit and codes specification limits

The next step was to manually refine the constants obtained to bring out a more practical equation. In this case, the refined constants are such that equation (4.14) yields equation (4.15).

$$\forall\ \psi \in [-1, 0]$$

$$\forall\ \beta \in [125, 250]$$

$$\text{Proposed Tolerance Limit} = \frac{(80 \cdot \psi + 185)^2 + (\beta + 75)^2}{4500} \qquad (4.15)$$

For the web under study of depth 1500 mm and for real-life bridge engineering plate girders during the erection phase ($\psi \in [-1, 0[$ and $\beta \in [125, 250]$), Table 4.15 shows that the derived and proposed tolerance limit equation provides an EN 1090-2 tolerance relaxation of up to 40% in less slender webs and 60% in more slender webs. Compared to AWS D1.1/D1.1M, there is a possible relaxation of around 80% in less slender webs and close to 200% in more slender webs.

Imperfection tolerances during the erection of steel plate girders and geometrical nonlinearities
Master of Civil Engineering defended by SONNA DONKO Maël
NASPW Yaoundé 2019/2020
115

These relaxation percentages strongly depend on the loading condition (stress ratio) as the stated percentages tend to reduce when the loading tends to be more of pure bending (experienced in doubly symmetric plate girders).

Therefore, the codes' tolerance limit of singly symmetric plate girders (eccentric loading) with thin webs (high slenderness ratio) is strict and should be relaxed.

In contrast to the tolerance limit given by EN 1090-2 and AWS D1.1/D1.1M, the proposed tolerance limit with a normalised drop of 11.15% is a function of both the loading condition (stress ratio) and the slenderness ratio.

Imperfection tolerances during the erection of steel plate girders and geometrical nonlinearities
Master of Civil Engineering defended by SONNA DONKO Maël
NASPW Yaoundé 2019/2020

116

Table 4.15. Deviation of the proposed tolerance limit to the codes provisions limits

Stress ratio ψ	Slenderness ratio β = b/t	Proposed Limit (mm)	EN 1090-2 Limit (mm)	Deviation (%)	AWS Limit (mm)	Deviation (%)
-1	125	11.34	11.72	3.24	10	13.39
-1	150	13.70	14.06	2.58	10	37.00
-1	175	16.34	16.41	0.41	10	63.39
-1	200	19.26	18.75	2.70	10	92.56
-1	225	22.45	18.75	19.73	10	124.50
-1	250	25.92	18.75	38.25	10	159.22
-0.75	125	12.36	11.72	5.48	10	23.61
-0.75	150	14.72	14.06	4.69	10	47.22
-0.75	175	17.36	16.41	5.82	10	73.61
-0.75	200	20.28	18.75	8.15	10	102.78
-0.75	225	23.47	18.75	25.19	10	134.72
-0.75	250	26.94	18.75	43.70	10	169.44
-0.5	125	13.56	11.72	15.72	10	35.61
-0.5	150	15.92	14.06	13.22	10	59.22
-0.5	175	18.56	16.41	13.13	10	85.61
-0.5	200	21.48	18.75	14.55	10	114.78
-0.5	225	24.67	18.75	31.59	10	146.72
-0.5	250	28.14	18.75	50.10	10	181.44
-0.25	125	14.94	11.72	27.48	10	49.39
-0.25	150	17.30	14.06	23.02	10	73.00
-0.25	175	19.94	16.41	21.53	10	99.39
-0.25	200	22.86	18.75	21.90	10	128.56
-0.25	225	26.05	18.75	38.93	10	160.50
-0.25	250	29.52	18.75	57.45	10	195.22
0	125	16.49	11.72	40.75	10	64.94
0	150	18.86	14.06	34.08	10	88.56
0	175	21.49	16.41	31.01	10	114.94
0	200	24.41	18.75	30.19	10	144.11
0	225	27.61	18.75	47.23	10	176.06
0	250	31.08	18.75	65.75	10	210.78

Imperfection tolerances during the erection of steel plate girders and geometrical nonlinearities
Master of Civil Engineering defended by SONNA DONKO Maël
NASPW Yaoundé 2019/2020

117

4.5.3.3.   Equation verification

To verify the equation derived, a web model, different from the ones used in the analyses, was selected from the range of study. This web had properties given in equation (4.16).

$$\begin{cases} a = b = 1200 \text{ mm} \\ \quad\quad t = 6 \text{ mm} \end{cases} \implies \begin{cases} \alpha = 1 \\ \beta = 200 \end{cases} \tag{4.16}$$

The chosen web of plate girder is subjected to an eccentric compression with stress ratio $\psi = -0.5$. It is modelled using the verified FE modelling procedure with an imperfection amplitude equal to 21.48 mm (obtained from the derived tolerance limit equation). The FE results obtained (146.51 N/mm^2) with this imperfection is compared to the results obtained (157.97 N/mm^2) from the supposed perfect structure (imperfection of 0.012 mm). The drop in strength at the given tolerance limit is found to be 7.25%. This percentage is in perfect agreement with the normalised maximum drop of 11.15%. Thus, this confirms the reliability of the derived equation on the range of the parameters studied.

Imperfection tolerances during the erection of steel plate girders and geometrical nonlinearities
Master of Civil Engineering defended by SONNA DONKO Maël
NASPW Yaoundé 2019/2020

118

Conclusion

The parametric study, varying aspect ratio, slenderness ratio, stress ratio and imperfection amplitudes yielded 36 ideal perfect webs and 612 real imperfect webs. EC3-1-5 was used to calculate the buckling stress of the 36 perfect webs for comparison with the FE buckling stress values of the same webs. The results obtained showed that the FE model used for linear buckling analyses can be adequately used for other research studies on the critical stress of the web of plate girders as a maximum deviation of only 5.43% was encountered. These results also show that EC3-1-5 analytical results are almost always non-conservative with respect to the FE results and both methods could be used interchangeably. Studying the ratio of ultimate strength to critical stress values, it is realised that thin webs possess high post-buckling strength reserves than thick webs. Comparing the FE ultimate strengths of 36 imperfect webs with initial imperfection amplitudes of 0.015mm or EN 1090-2 tolerance limit and EC3-1-5 analytical ultimate strength results, Fukumoto's findings on Winter's function (used in EC3-1-5) overestimating the ultimate strength of slender plates were reaffirmed with a deviation of up to 24.91%. Investigating the effects of the parameters on the ultimate strength, it was realised that aspect ratio does not influence the ultimate strength of the web of plate girders, whereas, slenderness ratio, stress ratio and initial imperfection amplitude all have inverse relationships with the ultimate strength. Thus, an ultimate strength equation was derived from the 612 imperfect webs of plate girders. As opposed to codes' provisions, this equation is also a function of initial imperfection amplitude. By fixing a normalised drop in the strength of 11.15% then using the ultimate strength equation derived, corresponding imperfection amplitudes and thus tolerance limits were obtained. A proposed equation for the tolerance limit was derived and it was shown that tolerance limits are a function of both the stress ratio and slenderness ratio as opposed to that given by AWS D1.1/D1.1M and EN 1090-2. Also, it was noticed that EN 1090-2 tolerance limit can be relaxed by 40% in less slender webs and 60% in more slender webs compared to AWS D1.1/D1.1M which can be relaxed to around 80% in less slender webs and close to 200% in more slender webs of monosymmetric plate girders.

Imperfection tolerances during the erection of steel plate girders and geometrical nonlinearities
Master of Civil Engineering defended by SONNA DONKO Maël
NASPW Yaoundé 2019/2020

119

GENERAL CONCLUSION

In order to investigate the effects of web aspect ratio, slenderness ratio, stress ratio and initial imperfection amplitude on the ultimate strength of I-shaped steel plate girders subjected to local web-bend buckling and their effect on web imperfection tolerance limit, a parametric study was performed. 36 perfect webs and 612 imperfect webs were modelled and analysed using Abaqus/CAE FE linear buckling and GMNIA analyses. Prior to the parametric study, preliminary studies, based on analytical and experimental findings, were done to verify the FE modelling procedures adopted. After investigating the FE GMNIA results, it was found that thin webs possess a higher post-buckling reserve strength than thick webs. Backed by Fukumoto's findings, the analytical ultimate strength results provided by the European code were found to be overestimated by 24.91% with respect to the FE results. This overestimation could lead to a sudden failure of a plate girder during its erection phase. The length of the web was found not to affect its ultimate strength provided it is maintained within the limits of this study (aspect ratio ranging from 1 to 2). A decrease in the web's thickness (increase in slenderness ratio) reduces the web's ultimate strength. Furthermore, a move from the use of bisymmetric to the use of monosymmetric plate girders (increase in stress ratio) implies a reduction in the ultimate strength. Also, a regression analysis was done to propose an ultimate strength then a tolerance limit equation based on the fact that strength reduction is equal to the maximum reduction provided by the American and European codes (11.15%). It was then noticed that, for monosymmetric plate girders, the European tolerance limit can be relaxed by 40% in less slender webs and 60% in more slender webs compared to the American limit which can be relaxed to around 80% in less slender webs and close to 200% in more slender webs. The relaxed tolerance limit equation will be highly welcomed by fabricators as it will help to reduce costly web straightening operations. To erectors, the equations will serve as an on-site tool to easily compute the ultimate strength and imperfection limit of webs of plate girders. Also, both the calibrated web boundary condition and mesh density of 40, will ease the FE modelling of researchers and designers working on similar FE linear buckling and GMNIA analyses. As perspectives, further numerical studies should be performed to study the influence of both patch and shear loadings on the proposed equations. Experimental studies are also recommended to confirm, under a more global behaviour, the proposed equations.

Imperfection tolerances during the erection of steel plate girders and geometrical nonlinearities
Master of Civil Engineering defended by SONNA DONKO Maël
NASPW Yaoundé 2019/2020

120

BIBLIOGRAPHY

ABAQUS. (2014). Abaqus 6.14. *Abaqus 6.14 Analysis User's Guide*, 14.

Alinia, M. M., Gheitasi, A., & Shakiba, M. (2011). Postbuckling and ultimate state of stresses in steel plate girders. *Thin-Walled Structures*, *49*(4), 455–464. https://doi.org/10.1016/j.tws.2010.12.008

AutoDesk Inc. (2017). *How to Perform a Mesh Convergence Study | Simulation Mechanical | Autodesk Knowledge Network*. https://knowledge.autodesk.com/support/simulation-mechanical/learn-explore/caas/sfdcarticles/sfdcarticles/How-to-Perform-a-Mesh-Convergence-Study.html

AWS D1.1/D1.1M:2010. (2010).

Basler, K., Yen, B. T., Mueller, J. A., & Thurlimann, B. (1960). Web buckling tests on welded plate girders. In *Fritz Engineering Laboratory, Lehigh University*.

Basler, Konrad, Bung-Tseng, Y., Mueller, J. A., & Thürlimann, B. (1960). Web buckling tests on welded plate girders - Overall introduction and Part 1 The test girders. *Fritz Engineering Laboratory, Lehigh University*, *165*(No. 251-11).

Beg, D., Kuhlmann, U., Davaine, L., & Braun, B. (2011). *Design of Plated Structures_ Eurocode 3_ Design of Steel Structures, Part 1-5 - Design of Plated Structures, First Edition*.

Clarin, M. (2007). *Plate Buckling Resistance - Patch Loading of Longitudinally Stiffened Webs and Local Buckling*.

Di Pietro, L., Di Virgilio, F., & Pantano, E. (2012). Residual Stresses in Steel Members: A Review of available Analytical Expressions. *The Eletronic Library*, *34*(1), 1–5.

Ellobody, E. (2014). *Finite Element Analysis and Design of Steel and Steel-Concrete Composite Bridges* (1st ed.). Butterworth-Heinemann.

EN 1090-2:2018 (E). (2018).

EN 1993-1-5:2006 (E) (Vol. 1, Issue 2005). (2011).

Fukumoto, Y., & Itoh, Y. (1984). *Basic From Strength Test of Steel Plates*. *1*(344).

Imperfection tolerances during the erection of steel plate girders and geometrical nonlinearities
Master of Civil Engineering defended by SONNA DONKO Maël
NASPW Yaoundé 2019/2020
121

Galishnikova, V., Dunaiski, P., & Pahl, P. J. (2009). Geometrically Non-linear Analysis of Plane Trusses and Frames. In *Non-Linear Finite Element Analysis of Solids and Structures*. https://doi.org/10.1002/9781118375938.ch3

Ghadami, A., & Broujerdian, V. (2019). Shear behavior of steel plate girders considering variations in geometrical properties. *Journal of Constructional Steel Research*, *153*, 567–577. https://doi.org/10.1016/j.jcsr.2018.11.009

Gorenc, B., Tinyou, R., & Syam, A. (2012). *Steel Designers' Handbook*.

Graciano, C., Casanova, E., & Martínez, J. (2011). Imperfection sensitivity of plate girder webs subjected to patch loading. *Journal of Constructional Steel Research*, *67*(7), 1128–1133. https://doi.org/10.1016/j.jcsr.2011.02.006

Hayward, B. A., Sadler, N., & Tordoff, D. (2002). *A Practical Approach to Design for Efficient Fabrication and Construction* (Issue 34).

Helwig, T., Reagan, H., Zhang, Y., Espinoza, O., & Mercan, B. (2015). *Fabricated Plate Tolerances for Steel Bridges*.

Hyams, D. G. (2014). *GraphExpert professional documentation. Release 1.1.3*.

Hyams, D. G. (2018). CurveExpert Professional Documentation. *Hyams Development*, 213. https://bit.ly/2UBpckG

Jayanta, S. (2016). *Local buckling and section classification*. 1–8. http://www.steel-insdag.org/TeachingMaterial/Chapter8.pdf

Kala, J., Škaloud, M., Melcher, J., & Kala, Z. (2010). Imperfections in steel plated structures and their impact on ultimate strength. *Proceedings of SDSS' Rio 2010: International Colloquium Stability and Ductility of Steel Structures*, *2*, 779–785.

Kassem, M. R. (1989). *THE BEHAVIOUR AND DESIGN OF TRANSVERSE WEB STIFFENERS IN BRIDGE GIRDERS*.

Loorits, K., & Mekaniikka, R. (1995). Classification of Cross Sections for steel beams in Different Design Codes. *Rakenteiden Mekaniikka*, *28*(1), 19–33.

Maiorana, E., Pellegrino, C., & Modena, C. (2009). Imperfections in steel girder webs with and without perforations under patch loading. *Journal of Constructional Steel Research*,

Imperfection tolerances during the erection of steel plate girders and geometrical nonlinearities
Master of Civil Engineering defended by SONNA DONKO Maël
NASPW Yaoundé 2019/2020

122

65(5), 1121–1129. https://doi.org/10.1016/j.jcsr.2008.10.007

Massonet, C. (1980). Tolerances in steel plated structures. *IABSE Surveys*.

McAnallen, L. E., Padilla-Llano, D. A., Zhao, X., Moen, C. D., Schafer, B. W., & Eatherton, M. R. (2014). Initial geometric imperfection measurement and characterization of cold-formed steel C-section structural members with 3D non-contact measurement techniques. *Structural Stability Research Council Annual Stability Conference 2014, SSRC 2014*, 566–590.

McGuire, W., Gallagher, R. H., & Ziemian, R. D. (1999). *Matrix Structural Analysis, With MASTAN2* (p. 480). http://books.google.com/books/about/Matrix_Structural_Analysis_With_MASTAN2.html?id=_I4AAAACAAJ&pgis=1

Obinna, U. (2020). *Imperfection Analysis of Structures With Solved Examples - Structville*. https://structville.com/2017/11/imperfection-analysis-of-structures-with-solved-examples.html

Pham, N. H., Pham, C. H., & Rasmussen, K. J. R. (2018). Incorporation of measured geometric imperfections into finite element models for cold-rolled aluminium sections. *Lecture Notes in Civil Engineering*, *8*, 161–171. https://doi.org/10.1007/978-981-10-6713-6_15

Przemieniecki, J. S. (1968). *Theory of Matrix Structural Analysis*.

Radio Museum. (2016). https://www.radiomuseum.org/museum/cam/pont-allemand-d-edea-bruecke-von-edea-edea/.html

Rangelov, N. (1992). A theoretical approach to the limiting of initial imperfections in steel plates. *Der Stahlbau*, *61*(5), 151–156.

Ritter, K. (2000). *Nonlinear problems*. 213–225. https://doi.org/10.1007/bfb0103942

Rossini, N. S., Dassisti, M., Benyounis, K. Y., & Olabi, A. G. (2012). Methods of measuring residual stresses in components. *Materials and Design*, *35*, 572–588. https://doi.org/10.1016/j.matdes.2011.08.022

Sadovský, Z., & Baláž, I. (1996). Tolerances of initial deflections of steel plates and strength of I cross-section in compression and bending. *Journal of Constructional Steel Research*,

Imperfection tolerances during the erection of steel plate girders and geometrical nonlinearities
Master of Civil Engineering defended by SONNA DONKO Maël
NASPW Yaoundé 2019/2020

123

38(3), 219–238. https://doi.org/10.1016/0143-974X(96)00020-X

Salman, J. C., & Johnson, E. J. (1996). *Steel structures design & behaviour*.

Schafer, B. W. (1996). *Scholars ' Mine Geometric Imperfections and Residual Stresses for Use in the Analytical Modeling of Cold-formed Steel Members*.

Shin, D. K., Cho, E. Y., & Kim, K. (2013). Ultimate flexural strengths of plate girders subjected to web local buckling. *International Journal of Steel Structures*, *13*(2), 291–303. https://doi.org/10.1007/s13296-013-2008-3

Steel Construction. (2015). *Steel material properties - Steelconstruction.info*. https://www.steelconstruction.info/Steel_material_properties%0Ahttp://www.steelconstruction.info/Steel_material_properties%0Ahttps://www.steelconstruction.info/Steel_material_properties%0Ahttp://www.steelconstruction.info/Steel_material_properties

Structures, C. (2021). *Poutres soudées assemblées (WWF)*. https://www.canamstructures.com/fr/produits/plaques-soudees/#gallery-1-2

T. Segui, W. (2013). Steel Design. In *Journal of Chemical Information and Modeling* (Vol. 53, Issue 9).

Techniques of superstructure construction. (2014).

Tetougueni, C. D., Maiorana, E., Zampieri, P., & Pellegrino, C. (2019). Plate girders behaviour under in-plane loading: A review. *Engineering Failure Analysis*, *95*(August 2018), 332–358. https://doi.org/10.1016/j.engfailanal.2018.09.021

Timoshenko, S. P., Gere, J. M., & Prager, W. (1962). Theory of Elastic Stability, Second Edition. In *Journal of Applied Mechanics* (Vol. 29, Issue 1, pp. 220–221). https://doi.org/10.1115/1.3636481

Vasios, N. (2015). Nonlinear Analysis of Structures. *NASA Contractor Reports*.

Wood, R. D. (1997). Analysis of geometrically nonlinear structures. In *Advances in Engineering Software* (Vol. 28, Issue 1). https://doi.org/10.1016/s0965-9978(96)00037-3

Ziemian, R. D., & Wiley, J. (2010). Guide To Stability Design Criteria for Metal Structures. In *Sixth Edition*.

Imperfection tolerances during the erection of steel plate girders and geometrical nonlinearities
Master of Civil Engineering defended by SONNA DONKO Maël
NASPW Yaoundé 2019/2020

124

APPENDICES

Appendix 1. EC3-1-5 ultimate strength calculations

This part presents EC3-1-5 analytical ultimate strength parameter calculations under pure compression, $\psi = 1$. Here,

$$\begin{cases} y_{eff,G} = y_{\Delta A} = 0 \text{ mm} \\ e = 750 \text{ mm} \\ y_{sup} = y_{eff} = 750 \text{ mm} \end{cases}$$

ID	α	β	$\bar{\lambda}_p$	ρ	b_{eff} (mm)	b_{e1} (mm)	b_{e2} (mm)	A (mm^2)	I (mm^4)	A_{eff} (mm^2)	I_{eff} (mm^4)	f_u/f_y	f_u (MPa)
P1a	1	250	5.46	0.18	263.74	131.87	131.87	9.00E+03	1.69E+09	1.58E+03	7.43E+08	0.18	62.42
P1b	1	187.5	4.09	0.23	346.73	173.36	173.36	1.20E+04	2.25E+09	2.77E+03	1.23E+09	0.23	82.06
P1c	1	150	3.27	0.28	427.26	213.63	213.63	1.50E+04	2.81E+09	4.27E+03	1.78E+09	0.28	101.12
P1d	1	125	2.73	0.34	505.32	252.66	252.66	1.80E+04	3.38E+09	6.06E+03	2.39E+09	0.34	119.59
P2a	1.5	250	5.46	0.18	263.74	131.87	131.87	9.00E+03	1.69E+09	1.58E+03	7.43E+08	0.18	62.42
P2b	1.5	187.5	4.09	0.23	346.73	173.36	173.36	1.20E+04	2.25E+09	2.77E+03	1.23E+09	0.23	82.06
P2c	1.5	150	3.27	0.28	427.26	213.63	213.63	1.50E+04	2.81E+09	4.27E+03	1.78E+09	0.28	101.12
P2d	1.5	125	2.73	0.34	505.32	252.66	252.66	1.80E+04	3.38E+09	6.06E+03	2.39E+09	0.34	119.59
P3a	2	250	5.46	0.18	263.74	131.87	131.87	9.00E+03	1.69E+09	1.58E+03	7.43E+08	0.18	62.42
P3b	2	187.5	4.09	0.23	346.73	173.36	173.36	1.20E+04	2.25E+09	2.77E+03	1.23E+09	0.23	82.06
P3c	2	150	3.27	0.28	427.26	213.63	213.63	1.50E+04	2.81E+09	4.27E+03	1.78E+09	0.28	101.12
P3d	2	125	2.73	0.34	505.32	252.66	252.66	1.80E+04	3.38E+09	6.06E+03	2.39E+09	0.34	119.59

Imperfection tolerances during the erection of steel plate girders and geometrical nonlinearities
Master of Civil Engineering defended by SONNA DONKO Maël
NASPW Yaoundé 2019/2020

125

This part presents EC3-1-5 analytical ultimate strength parameter calculations under eccentric compression, $\psi = -0.5$. Here,

$$\begin{cases} e = 750 \text{ mm} \\ y_{sup} = 750 \text{ mm} \end{cases}$$

ID	α	β	$\bar{\lambda}_p$	ρ	b_{eff} (mm)	b_{e1} (mm)	b_{e2} (mm)	A (mm²)	I (mm⁴)
P1a	1	250	2.98	0.32	319.87	127.95	191.92	9.00E+03	1.69E+09
P1b	1	187.5	2.24	0.42	419.62	167.85	251.77	1.20E+04	2.25E+09
P1c	1	150	1.79	0.52	515.93	206.37	309.56	1.50E+04	2.81E+09
P1d	1	125	1.49	0.61	608.81	243.52	365.29	1.80E+04	3.38E+09
P2a	1.5	250	2.98	0.32	319.87	127.95	191.92	9.00E+03	1.69E+09
P2b	1.5	187.5	2.24	0.42	419.62	167.85	251.77	1.20E+04	2.25E+09
P2c	1.5	150	1.79	0.52	515.93	206.37	309.56	1.50E+04	2.81E+09
P2d	1.5	125	1.49	0.61	608.81	243.52	365.29	1.80E+04	3.38E+09
P3a	2	250	2.98	0.32	319.87	127.95	191.92	9.00E+03	1.69E+09
P3b	2	187.5	2.24	0.42	419.62	167.85	251.77	1.20E+04	2.25E+09
P3c	2	150	1.79	0.52	515.93	206.37	309.56	1.50E+04	2.81E+09
P3d	2	125	1.49	0.61	608.81	243.52	365.29	1.80E+04	3.38E+09

ID	$y_{eff,G}$ (mm)	$y_{\Delta A}$ (mm)	y_{eff} (mm)	A_{eff} (mm²)	I_{eff} (mm⁴)	f_u/f_y	f_u (MPa)
P1a	233.93	281.99	983.93	4.92E+03	9.37E+08	0.45	159.17
P1b	184.26	291.96	934.26	7.36E+03	1.47E+09	0.55	193.59
P1c	143.70	301.59	893.70	1.02E+04	2.07E+09	0.63	224.03
P1d	109.68	310.88	859.68	1.33E+04	2.70E+09	0.71	251.37
P2a	233.93	281.99	983.93	4.92E+03	9.37E+08	0.45	159.17
P2b	184.26	291.96	934.26	7.36E+03	1.47E+09	0.55	193.59
P2c	143.70	301.59	893.70	1.02E+04	2.07E+09	0.63	224.03
P2d	109.68	310.88	859.68	1.33E+04	2.70E+09	0.71	251.37
P3a	233.93	281.99	983.93	4.92E+03	9.37E+08	0.45	159.17
P3b	184.26	291.96	934.26	7.36E+03	1.47E+09	0.55	193.59
P3c	143.70	301.59	893.70	1.02E+04	2.07E+09	0.63	224.03
P3d	109.68	310.88	859.68	1.33E+04	2.70E+09	0.71	251.37

Imperfection tolerances during the erection of steel plate girders and geometrical nonlinearities
Master of Civil Engineering defended by SONNA DONKO Maël
NASPW Yaoundé 2019/2020
126

This part presents EC3-1-5 analytical ultimate strength parameter calculations under pure bending $\psi = -1$. Here, $y_{sup} = 750$ mm

ID	α	β	$\bar{\lambda}_p$	ρ	b_{eff} (mm)	b_{e1} (mm)	b_{e2} (mm)	A (mm²)	I (mm⁴)
P1a	1	250	2.23	0.43	319.20	127.68	191.52	9.00E+03	1.69E+09
P1b	1	187.5	1.68	0.56	418.26	167.30	250.95	1.20E+04	2.25E+09
P1c	1	150	1.34	0.68	513.64	205.45	308.18	1.50E+04	2.81E+09
P1d	1	125	1.12	0.81	605.34	242.14	363.21	1.80E+04	3.38E+09
P2a	1.5	250	2.23	0.43	319.20	127.68	191.52	9.00E+03	1.69E+09
P2b	1.5	187.5	1.68	0.56	418.26	167.30	250.95	1.20E+04	2.25E+09
P2c	1.5	150	1.34	0.68	513.64	205.45	308.18	1.50E+04	2.81E+09
P2d	1.5	125	1.12	0.81	605.34	242.14	363.21	1.80E+04	3.38E+09
P3a	2	250	2.23	0.43	319.20	127.68	191.52	9.00E+03	1.69E+09
P3b	2	187.5	1.68	0.56	418.26	167.30	250.95	1.20E+04	2.25E+09
P3c	2	150	1.34	0.68	513.64	205.45	308.18	1.50E+04	2.81E+09
P3d	2	125	1.12	0.81	605.34	242.14	363.21	1.80E+04	3.38E+09

ID	$y_{eff,G}$ (mm)	$y_{\Delta A}$ (mm)	y_{eff} (mm)	A_{eff} (mm²)	I_{eff} (mm⁴)	f_u/f_y	f_u (MPa)
P1a	163.95	406.92	913.95	6.42E+03	1.05E+09	0.51	180.76
P1b	118.36	416.83	868.36	9.35E+03	1.63E+09	0.63	222.62
P1c	79.75	426.36	829.75	1.26E+04	2.29E+09	0.74	261.43
P1d	46.49	435.53	796.49	1.63E+04	3.01E+09	0.84	297.89
P2a	163.95	406.92	913.95	6.42E+03	1.05E+09	0.51	180.76
P2b	118.36	416.83	868.36	9.35E+03	1.63E+09	0.63	222.62
P2c	79.75	426.36	829.75	1.26E+04	2.29E+09	0.74	261.43
P2d	46.49	435.53	796.49	1.63E+04	3.01E+09	0.84	297.89
P3a	163.95	406.92	913.95	6.42E+03	1.05E+09	0.51	180.76
P3b	118.36	416.83	868.36	9.35E+03	1.63E+09	0.63	222.62
P3c	79.75	426.36	829.75	1.26E+04	2.29E+09	0.74	261.43
P3d	46.49	435.53	796.49	1.63E+04	3.01E+09	0.84	297.89

Imperfection tolerances during the erection of steel plate girders and geometrical nonlinearities
Master of Civil Engineering defended by SONNA DONKO Maël
NASPW Yaoundé 2019/2020

127

Appendix 2. Regression parameters for ultimate strength equation derivation

Imperfection tolerances during the erection of steel plate girders and geometrical nonlinearities
Master of Civil Engineering defended by SONNA DONKO Maël
NASPW Yaoundé 2019/2020

128

Appendix 3. Regression parameters for tolerance limit equation derivation

CurveExpert Professional 2.7.3 - D:\School\ENSTP\MEng 5\Thesis\Work\Exercise\Parametric Analyses\Tol Limit Reg Analysis\Tol Prop Eqn Derivation.cxp

File Edit Data Calculate Tools Window Help

Model Information
Name: Paraboloid
Type: Regression

$$y = a((bx_1 + c)^2 + (dx_2 + e)^2)$$

Parameters

Name	Value
a	2,23732042005585 9E-04
b	8,02314148547065 0E-01
c	1,84217881986598 7E-02
d	9,47600071071663 9E-01
e	8,16742716828638 0E-01

Copy

Model Evaluation
Live   x= ---   y= ---   f(x) = ---

Result Detail Residuals Convergence PHist

Numeric Formatting: ● Normal ○ Fixed Point ○ Scientific ○ Engineering   6

Confidence level: 95

Overview

Name	Paraboloid
Kind	Regression
Family	Polynomial
Equation	y = a * ((b*x1 + c)^2 + (d*x2 + e)^2)
# of Indep. Vars	2
Weighting	Default
Standard Error	0.70242615 16414995
Correlation Coeff. (r)	0.992020
Coeff. of Determination (r^2)	0.984104515 7154444
DOF	25
AICC	-17.062547

Parameters

	Value	Std Err	Range (95% confidence)
a	0.000224	252.170557	-519.354760 to 519.355207
b	80.231415	45121158.129861	-92928684.481911 to 92928844.944741
c	184.217882	103625769.486914	-213421083.099143 to 213421451.534907
d	0.947600	533020.515684	-1097775.353860 to 1097777.249060
e	81.674272	45928286.261104	-94590994.542361 to 94591157.890904

Dataset: 30 x 3   3D   fr_FR

Export HTML   Print Report

OK

Imperfection tolerances during the erection of steel plate girders and geometrical nonlinearities
Master of Civil Engineering defended by SONNA DONKO Maël
NASPW Yaoundé 2019/2020
129